

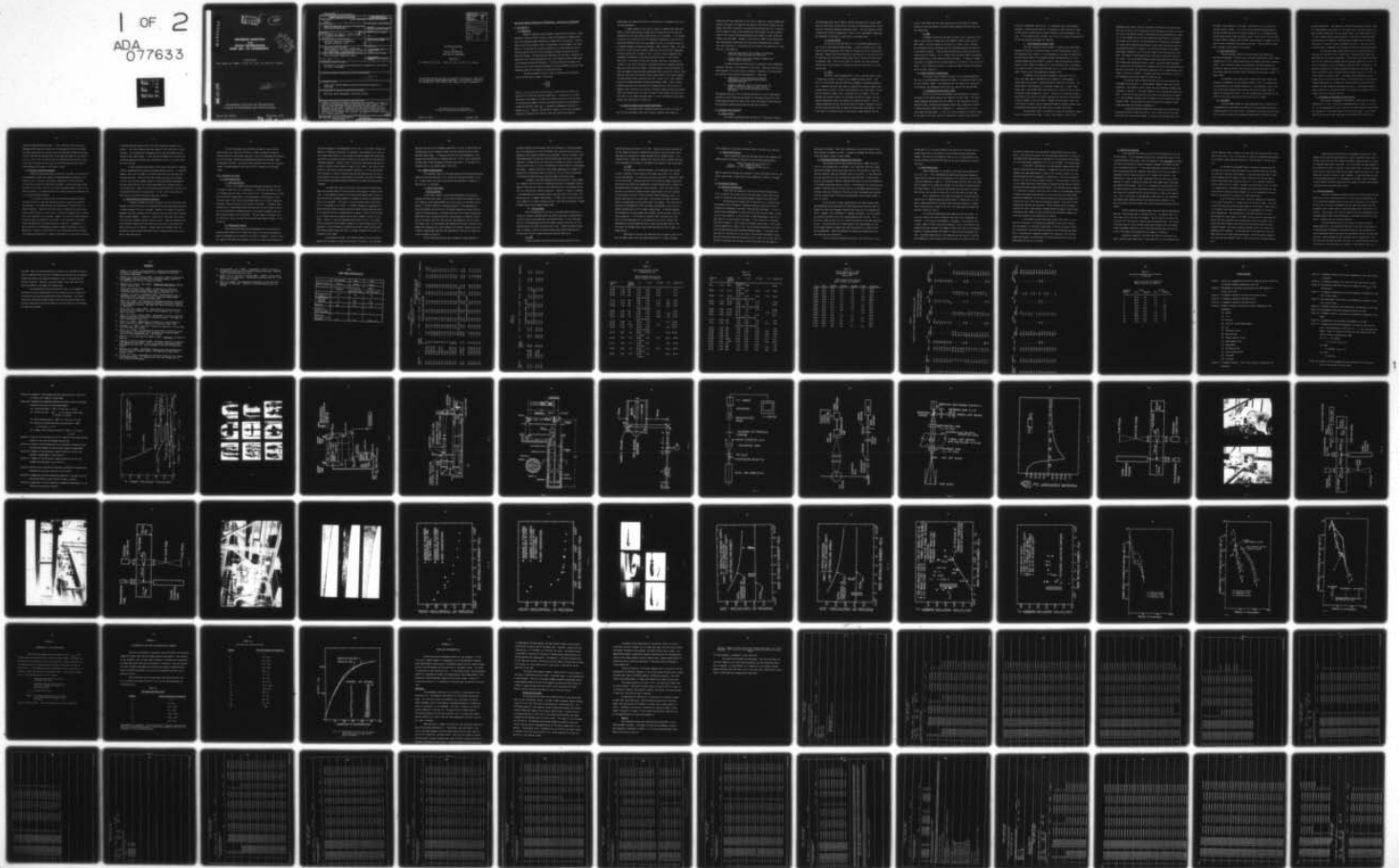
AD-A077 633

PENNSYLVANIA STATE UNIV UNIVERSITY PARK APPLIED RESE--ETC F/G 20/4
CAVITATION INCEPTION AND NUCLEI DISTRIBUTIONS JOINT ARL/CIT EXP--ETC(U)
SEP 79 E M GATES , M L BILLET , J KATZ N00014-79-C-6043

UNCLASSIFIED

NL

1 OF 2
ADA
077633



AD A 077633

LEVEL IV

12
P.S.

CAVITATION INCEPTION
and
NUCLEI DISTRIBUTIONS
JOINT ARL / CIT EXPERIMENTS

D D C
REF ID: A61115
DEC 5 1979
E

prepared by

E.M. Gates, M.L. Billet, J. Katz, K.K. Ooi, J.W. Holl, A.J. Acosta

JWC FILE COPY

This document has been approved
for public release and sale; its
distribution is unlimited.

CALIFORNIA INSTITUTE OF TECHNOLOGY
DIVISION OF ENGINEERING AND APPLIED SCIENCE

Report No. E244.1

September 1979

79 12 4 128

(9) Technical rept. 23 Jan 78 - Sep 79

UNCLASSIFIED

SECURITY CLASSIFICATION OF THIS PAGE (When Data Entered)

REPORT DOCUMENTATION PAGE		READ INSTRUCTIONS BEFORE COMPLETING FORM
1. REPORT NUMBER E244.1	2. GOVT ACCESSION NO.	3. RECIPIENT'S CATALOG NUMBER
4. TITLE (and Subtitle) CAVITATION INCEPTION AND NUCLEI DISTRIBUTIONS JOINT ARL/CIT EXPERIMENTS		5. TYPE OF REPORT & PERIOD COVERED Technical 1/23/78 - 9/79
6. AUTHOR(S) E.M. Gates, M.L. Billet, J. Katz, K.K. [unclear], J.W. Holl, A.J. Acosta		6. PERFORMING ORG. REPORT NUMBER E244.1
9. PERFORMING ORGANIZATION NAME AND ADDRESS California Institute of Technology Pasadena, California 91125		8. CONTRACT OR GRANT NUMBER(s) S78-1
11. CONTROLLING OFFICE NAME AND ADDRESS Applied Research Laboratory, Pennsylvania State University, P.O. Box 30, State College Pa. 16801 (Prof. J. William Holl)		10. PROGRAM ELEMENT, PROJECT, TASK AREA & WORK UNIT NUMBERS 11 Sep 79
14. MONITORING AGENCY NAME & ADDRESS (if different from Controlling Office) Naval Sea System Command (Code 63R31)		12. REPORT DATE September 1979
15. NO0014-79-C-6043		13. NUMBER OF PAGES 100
16. DISTRIBUTION STATEMENT (of this Report) Distribution is unlimited and reproduction is permitted for any purpose of the U.S. Government.		15. SECURITY CLASS. (of this report) Unclassified
17. DISTRIBUTION STATEMENT (of the abstract entered in Block 20, if different from Report) 12/103		15a. DECLASSIFICATION/DOWNGRADING SCHEDULE
18. SUPPLEMENTARY NOTES Joint effort Applied Research Laboratory/California Institute of Technology		
19. KEY WORDS (Continue on reverse side if necessary and identify by block number) Cavitation, Nuclei Measurement, Cavitation Scaling		
20. ABSTRACT (Continue on reverse side if necessary and identify by block number) A number of cavitation inception experiments have been made on a series of identical non-separating bodies in three different water tunnels. Measure- ments of nuclei were made by light scattering in three tunnels and by holography in one tunnel. These point out that particulates were present. Schlieren observations of transition were also made to compare the flow within each of the tunnels and to evaluate the connection between transition and cavitation inception.		

Accession For	
NTIS GRA&I	<input checked="" type="checkbox"/>
DDC TAB	<input type="checkbox"/>
Unannounced	<input type="checkbox"/>
Justification _____	
By _____	
Distribution/ _____	
Availability Codes	
Dist.	Avail and/or special
A	

CAVITATION INCEPTION
and
NUCLEI DISTRIBUTIONS
JOINT ARL/CIT EXPERIMENTS

prepared by

E.M. Gates, M.L. Billet, J. Katz, K.K. Ooi, J.W. Holl, A.J. Acosta

This work was carried out under the auspices of sub-contract number S78-1 and the Naval Sea System Command Code 63R31. Distribution is unlimited and reproduction is permitted for any purpose of the U.S. Government.

California Institute of Technology
Division of Engineering and Applied Science

CAVITATION INCEPTION AND NUCLEI DISTRIBUTIONS - JOINT ARL/CIT EXPERIMENTS

1. Introduction

A. Background

Hydraulic machines (such as pumps, propellers and turbines), valves hydrofoils and any hydraulic device in which the dynamically reduced pressure falls below the vapor pressure are susceptible to cavitation. The presence of cavitation causes a loss in performance, erosion damage, and noise; hence, it is desirable to be able to predict for a given device the set of operating conditions which form the boundary between cavitating and non-cavitating states. The difficulties associated with testing or observing in operation a full scale prototype has led to the extensive use of model testing to determine cavitation behavior. To then extrapolate the model test results to full scale requires knowledge of scaling parameters and laws which adequately describe the behavior of cavitating flows.

The main parameter currently used to characterize a cavitating flow is the cavitation number (σ) given by:

$$\sigma = \frac{P_{\infty} - P_v}{\frac{1}{2} \rho V_{\infty}^2}$$

where P_{∞} , P_v , ρ , V_{∞} are the liquid pressure, vapor pressure, density and velocity at infinity and the bulk temperature. The value of σ at which cavitation first appears is called the inception value (σ_i) and the value of the cavitation number at which a cavitating condition is suppressed is called the desinent value (σ_d). A hysteresis phenomenon exists and in general $\sigma_d \geq \sigma_i$. However, the cavitation number is not the only parameter required to determine the inception index and despite considerable

experimental and theoretical efforts a complete set of parameters has still not been determined.

A major reason for the lack of success in determining these parameters is that there has been a great deal of confusion over the lack of reproducibility of test results from one facility to another. In an attempt to clarify this situation, the ITTC sponsored a comparative test series in which many different facilities were asked to carry out cavitation tests on a standard headform (Lindgren and Johnsson, 1966; Johnsson, 1969). The wide variation in not only the inception index but also the physical appearance of the cavitation (as is shown in Figs. 1 and 2) strongly suggested that fundamental differences in the flow conditions existed in the various facilities. As a result of the ITTC findings, there was a resurgence of interest in the area of cavitation inception and several important developments have since occurred, namely: the development of accurate methods to count and measure freestream gas bubbles and particulates (e.g. Keller, 1972; Peterson, 1972) and the discovery that viscous effects like laminar separation and boundary layer transition can play a major role in the inception process on streamlined bodies (Arakeri and Acosta, 1976). There is ample evidence that both the distribution of freestream nuclei and the type of boundary layer transition can strongly influence inception (Gates and Acosta, 1978), but the monitoring of either or both of these factors during cavitation tests is not common and hence there is little information on how these factors vary from facility to facility.

B. Specific Objectives of Present Experiments

In the present work a comparative test series much like that of the ITTC was undertaken except that a special emphasis was placed on

monitoring the flow conditions at the time of inception. Hence although the scale of the tests with regard to the number of facilities involved (3) was modest, the effort to monitor flow conditions was ambitious; for in addition to the inception index, nuclei populations were counted, schlieren observations of the viscous flow were obtained and an attempt to count cavitation "events" was also made. Further, in one facility (LTWT) nuclei populations were simultaneously measured by two techniques (holography and a counter like that of Keller's). By monitoring the different flow conditions in each facility it was hoped to

1. determine more clearly the influence of freestream nuclei on travelling bubble cavitation and
2. further observe the relation between inception and boundary layer transition.

The above objectives relate mainly to determining the fundamental processes involved in the inception of cavitation. There were also several other purposes of the study which, although as important as the ones above, are related to more practical considerations. These were:

1. comparison of nuclei distributions obtained simultaneously by holography and by Keller's scattering technique.
2. attempt to base the "call" of inception upon the number of cavitation events per unit time by employing a light scattering technique to count the events.

The purposes here were first to develop confidence in nuclei measurements obtained by either technique and second to investigate the possibilities of developing an arbitrary "event rate" which would define travelling bubble cavitation inception which could be applied universally.

II. Equipment and Procedures

A. Water Tunnels

The present experiments were carried out in three water tunnels:

the High Speed Water Tunnel (HSWT), the Low Turbulence Water Tunnel (LTWT) both of which are at the California Institute of Technology and the 12-inch tunnel at the Applied Research Laboratory (ARL). The main features of each of these facilities are summarized in Table 1 and a few comments regarding the treatment of the water in each facility are made below.

1. 12-inch Tunnel

The circuit of the ARL facility is illustrated schematically in Fig. 3 and is described by Lehman (1959). It has no resorber, but it does have an effective deaerator with which air contents as low as 2 ppm can be obtained. Normally cavitation testing in the facility is carried out at low air contents, but during the present tests the air content was held at approximately 7 ppm. Even at this "high" air content very few freestream bubbles were visible except at inception at the low velocities (i.e. less than 30 fps).

2. LTWT

The LTWT is shown schematically in Fig. 4 and the tunnel circuit is described in detail in Vanoni, et al (1950) and Gates (1977). From Fig. 4 it can be seen that the LTWT has no resorber or separate deaerator. Air is removed from the tunnel water by reducing the pressure above a free surface while the water is slowly recirculated by the tunnel pump — a minimum air content of about 7 ppm is attainable by this method. Since the maximum test section velocity is only about 25 feet per second, low test section pressures (≈ 2 psia) are required to produce cavitation. The low pressure combined with the "relatively high air content" produces a flow in the test section which tends to have many large freestream bubbles. Also, since there is no effective way to continuously remove bubbles from the

circuit, after each test the tunnel water must be circulated for several minutes to allow the bubbles to collect and be removed from the circuit by the vacuum pump.

3. HSWT

A schematic drawing of the HSWT is given in Fig. 5 and the circuit details can be found in Knapp, Daily and Hammitt (1970) or more recently Ward (1976). The main feature of the facility is that it has a resorber for microbubble control and hence very few freestream bubbles are observed in the working section. Like the LTWT the HSWT has no effective system for reducing the air content. Air is removed from the tunnel water by producing super-cavitation on a test model and the sting mount. At regular intervals the tunnel is stopped and the free gas bubbles are allowed to rise and are removed. In this fashion a minimum air content of about 9 ppm may be attained after one day's operation.

B. Nuclei Counters - Descriptions

Two optical nuclei counters were used in the present experiments. The first is the holographic type and the second is a scattering type similar to that of Keller (1972). The scattering unit was used at all three facilities whereas the holography counter was only used at the LTWT and HSWT.

1. Holographic Nuclei Counter (HNC)

Nuclei distributions were deduced from holograms of a volume of the water in the working section just ahead of the test model. The experimental apparatus and method for this counter is much the same as used by Peterson (1972), Feldberg and Shlemenson (1973) and is described in detail in Gates and Bacon (1978) and in Appendix III. Essentially it is a two step image forming process. In the first step a hologram of a sample volume of the water in the test section is recorded on a special high resolution

film by a "holocamera" (see Fig. 6). In the second step, the developed hologram is reconstructed (see Fig. 7) producing a three dimensional image of the original volume which can then be probed at the investigator's leisure. In the present tests a volume 1 cm X 1 cm X 2.5 cm near the centerline of the test section was chosen for sampling.

2. Light Scattering Counter (LSC)

The light scattering nuclei counter is based on the relationship between the radius of a scattering center (R) and the scattered intensity. The scattered light intensity is also dependent on the angle of observation, the polarization angle of the scattered beam, the wavelength (λ) of the scattering beam and the refraction indices of the various mediums involved. However, Keller (1972) has shown that if the scattered light is collected at an angle of 90° to the scattering beam there is a unique relationship between intensity and a non-dimensional parameter $2\pi R/\lambda$.

A schematic of the scattering counter is provided in Fig. 8. First, the laser beam is expanded and collimated by a beam expander. A square aperture is used to isolate the central portion of the beam. The square beam is then focused by a long focal length lens. A small focal length lens is positioned after the focal point of the first lens so that a collimated scattering beam will result. The size of the scattering beam is determined by the size of the square aperture and the ratio of the effective focal lengths of the two lenses. Between the two lenses, there is a filter which is used to insure a scattering beam of constant intensity and an aperture positioned at the focal point to reduce reflections.

The scattered light is collected by a lens and focused by a second lens on a photomultiplier tube. A slot is positioned in front of the

photomultiplier tube to restrict the amount of scattered light collected. The size of the slot can be adjusted so that the measuring volume is cubical. The size of the control volume is determined from two considerations, namely, (1) the probability of only one scattering center being in the measuring volume at any time and (2) the characteristic dimension of the measuring volume which should be approximately three times the maximum radius of the scattering center of interest. The scattering volume in the present experiments presented a 0.76 X 0.38 mm window to the flow and was 0.76 mm deep. The output of the photomultiplier tube due to scattered light will be a pulse. This pulse goes through a signal conditioner which filters the high frequencies and adjusts the D.C. level. The pulse height processor now accepts the conditioned pulse, assesses the size of each detected pulse, and sorts the pulses into selectable categories until a predetermined total number of pulses is achieved. A display then gives the number of pulses in each category and the total amount of counting time.

During the tests at the 12-inch ARL facility the processor was programmed to divide the $0 \rightarrow \sim 35$ micrometer diameter range into 15 size categories. The number of nuclei larger than 35 micrometers diameter were indicated in channel 16. The total number of nuclei counted per sample was 1000. During the Caltech tests the size range investigated was increased to $3 \rightarrow 50$ micrometers diameter and the number of nuclei counted per sample reduced to 250. The calibration curves giving particle diameter versus signal amplitude are provided in Appendix II.

It was previously mentioned that the scattering volume had the dimensions 0.76 mm X 0.38 mm X 0.76 mm. This is only true for the LTWT which has flat test section windows. At both the 12-inch ARL tunnel and

the HSWT it was necessary to introduce a correction for the curvature of the test section windows. This correction was determined experimentally and for the HSWT was found to be about 30 percent i.e., the sample volume was 30 percent smaller than previously stated. Since the 12-inch ARL facility has a smaller diameter than the HSWT, the correction is greater for this facility and is estimated to be about 35 percent. These corrections have been included in the reduction of the data.

C. Flow Visualization

Thermal boundary layers on the test models were observed by schlieren photography. The particular schlieren configuration used is shown schematically in Fig. 9 and is essentially the same as that used by Arakeri (1973). Also following Arakeri, the prerequisite density gradient was produced by heating the body with internal cartridge type electric heaters. The system components and experimental technique are described in detail in Gates (1977).

At the HSWT and the ARL 12-inch tunnels correction lenses were necessary to compensate for the window curvature. Also, the windows did not have optically flat outside surfaces so it was necessary to put a thin film of glycerine between the correction lens and the tunnel window to reduce the "orange peel" effect. No such problems were encountered at the LTWT as it has flat, good quality glass test section windows.

D. Test Models

The test model chosen for these experiments has a contour which is generated by the potential flow solution to a distributed source disk oriented normally to a uniform flow. By adjusting the source disk distribution a series of bodies can be generated each having a different minimum

pressure coefficient. The models are called Schiebe bodies (Schiebe, 1972). This model geometry was chosen for the reason that it has been shown not to have a laminar separation (van der Meulen, 1976). The significance of this is that a streamlined non-separating body typically has travelling bubble type cavitation at inception. Besides being a common type of cavitation that occurs in practice, travelling bubble cavitation is the only type of cavitation that is amenable to the concept of event or occurrence counting.

Two stainless steel Schiebe bodies with a minimum pressure coefficient of -0.75 and "final" diameters of 1.0125 and 2.025 inches were fabricated for the present experiments. The contour and pressure distribution for this particular Schiebe body are provided graphically in Fig. 10 and the information is also presented in tabulated form in Appendix I. No quantitative measure of surface roughness was made, but each model was highly polished (a highly polished surface typically has a 0.1×10^{-6} m rms finish, Beckwith and Buck, 1961). The models were supported by a one-bladed sting in the 12-inch ARL tunnel, a two-bladed sting in the LTWT and a three-bladed sting in the HSWT with the nose being at least three and normally six body diameters upstream of the sting. Misalignment from the tunnel centerline in the LTWT and HSWT is estimated to be about 0.2° but is unknown for the 12-inch ARL facility.

E. Arrangement of Equipment at Each Facility

The physical arrangement of equipment at each facility is shown schematically in Figs. 11, 13 and 15 photographically in Figs. 12, 14 and 16. In the foregrounds of Figs. 14 and 16 the light source (an argon laser) and the special filters and lenses of the LSC may be seen. In all three facilities the conditioned laser beam was reflected 90° into the test

section through the bottom window. In Fig. 12(b) the receiving optics, photomultiplier tube and a portion of the processor of the LSC are shown. The light sources and collimating lens of the schlieren system can be seen in Fig. 12(a) and the focusing lens, knife edge and camera box are shown in Fig. 16. Only in Fig. 14 can any part of the HNC be seen and that is the mirror which reflects the ruby laser pulse 90° through the test section. The holography film holder is not shown in place.

F. Cavitation Testing Procedures

Before any experiments were carried out, the water in each facility was deaerated to reduce the number of freestream bubbles produced in the tunnel circuit. This was of particular importance in the LTWT and ARL 12-inch tunnel neither of which have a resorber. During the present tests the total air content in the 12-inch tunnel was approximately 7 ppm, in the LTWT 7-9 ppm and in the HSWT 9-10 ppm (air content levels were measured with a van Slyke blood gas analyzer).

In a typical cavitation test the following procedure was used. The water velocity in the test section was set at a specified value and kept constant. The tunnel pressure was then gradually lowered until inception occurred. Ideally at the occurrence of inception the tunnel pressures, tunnel velocity, a nuclei count, a schlieren photograph and a cavitation event rate were to be recorded. However, this was not always possible. During the tests in the ARL-12 inch tunnel it was found that the stroboscope interfered with the receiving optics of the LSC. Consequently, it was not possible to simultaneously observe inception and obtain a nuclei population. Instead, in this facility, the following method was followed: five separate observations of inception were made at a given tunnel velocity.

An average was then taken of the five tunnel pressures recorded at inception. The tunnel pressure was then reduced to this value and a "count" obtained. This procedure was repeated twice so that two counts were obtained at each tunnel speed. In the LTWT and the HSWT this difficulty was avoided by masking the strobe light sufficiently so that it did not interfere with the LSC.

In both the HSWT and the ARL-12 inch tunnel the point of inception could be approached very gradually with good pressure control. In the LTWT, however, due to the low head on the tunnel pump during an inception test the pump cavitates. Each test then had to take less than forty seconds since by that time the abundant supply of cavitation bubbles generated at the pump would reach the test section and dramatically change the free-stream conditions. Hence the tunnel pressure was reduced very rapidly until the presence of cavitation was observed. In the 12-inch tunnel and the HSWT values of cavitation desinence were also recorded.

F. Determination of Cavitation Inception

A standard procedure has been to observe the test body under stroboscopic lighting and to say that inception occurs when macroscopic cavities or bubbles become visible on the model. However, this method is observer-dependent and there has been a shift towards using cavitation event counters free of human judgment. Inception is then said to occur when the "cavitation event rate" reaches a certain arbitrary value. There are problems with event counters though, which relate mainly to the type of cavitation that occurs and also to its location. Further, what the threshold level for detecting an event and what the event rate at inception should be are also open to much questioning.

During the present work an effort was made to use an optical event counter much like that of Keller's (1972) to determine inception. Certain practical difficulties arose and it had to be abandoned and throughout all the tests inception was determined by observing the model under stroboscopic lighting. To maintain some consistent definition of inception, though, the same observers were used to "call" inception at each water tunnel.

III. Presentation of Data

A. Visual Observations

1. Schlieren Results

In Fig. 17 an example schlieren photograph obtained on the two inch model in each facility is presented. In each case the model is seen in silhouette and the flow is from right to left. The magnification is such that the surface length shown in the photographs is approximately 10 mm. As can be seen in this figure, the Schiebe model has no laminar separation and hence transition occurs on the surface of the body. To present these observations in a more quantitative way that point on the surface at which the first noticeable disturbance occurs in the laminar boundary layer has been called the position of transition. The arc length to diameter ratio at transition, $(S/D)_t$, has been plotted versus body Reynolds number in Figs. 18 and 19.

2. Photographic Results

Also during these tests 35 mm photographs of the cavitation at inception were taken to first record the type of cavitation and second to obtain an estimate of the location on the body of inception. Several different types of cavitation were observed to occur at inception and examples of

each are presented in the photographs of Fig. 20. In Fig. 20(a) "travelling bubble" or "Knappian" cavitation is presented. Here bubbles on or close to the surface grow rapidly as they approach and pass through the minimum pressure point on the body and then collapse as they continue into the region of increasing pressure. Another type of "travelling" cavitation which was observed in the ARL 12-inch tunnel is shown in Fig. 20(b). This type of cavitation will be called "travelling patch" cavitation. In this case a patch (the term patch is used to indicate that what was observed was not just a large bubble) of cavitation would appear on the model and give the impression of moving downstream along the surface of the model and then quickly disappear.

The remaining types of cavitation that occurred on the Schiebe body were attached forms of cavitation which could appear in several fashions. In one sequence a patch of cavitation would appear remain fixed in position and then disappear perhaps to reappear at another circumferential position on the model. This type is called "transient patch" cavitation and is illustrated in Fig. 20(c). In another sequence an attached cavity would form that unlike the patch type had a smooth leading edge and covered at least half of the circumference of the model — this will be referred to as a steady partially attached cavity and an example is given in Fig. 20(d). Finally, it was also observed (particularly on the 1-inch model) that the cavitation could suddenly appear as a steady attached cavity that completely circled the model circumference and had a smooth leading edge. This type has been called just that — a steady, attached cavity and is illustrated in Fig. 20(e).

As mentioned previously, the second purpose of the 35 mm photography was to attempt to locate the position of inception. This has been

done and the results are presented graphically in Figs. 21 and 22 were the estimated position of inception $(S/D)_i$ has been plotted versus the body Reynolds number (Re_D) . In reducing the data from the photographs it was assumed that the position of inception was the further point upstream on the body when travelling bubble cavitation occurred or, in the case of an attached cavity, the leading edge of the cavity.

B. Inception Observations

The inception index (σ_i) has been plotted versus the body Reynolds number for the two-inch body in Fig. 23 and for the one-inch model in Fig. 24. In each figure the type of cavitation that occurred at inception in each facility is indicated.

1. ARL-12 inch Tunnel

(a) Two-inch Body

At the lowest velocity tested (30 feet/second) the following sequence of events took place: as the tunnel pressure was gradually lowered a "popping" sound became audible but no cavitation on the model was observed. A further reduction in pressure resulted in the appearance of travelling bubble type cavitation, the bubbles appearing to grow from the region of minimum pressure. Continued lowering of the tunnel pressure produced more travelling bubble cavitation and eventually a transient "patch" type of cavitation (see Fig. 20) occurred simultaneously with the travelling bubble type. As the pressure was lowered even further, the patch type became more prevalent until quite suddenly an attached, steady cavity with a laminar leading edge (see Fig. 20) appeared and there was no longer any travelling bubble cavitation.

As the freestream velocity was increased, the same sequence of

cavitation events occurred except that the difference in pressure between the first appearance of travelling bubble type inception and the first appearance of the steady attached cavity decreased. Further increases in the freestream velocity caused the transient patch type cavitation to be more prevalent at inception and with continuing increases in velocity the patch type cavitation was in its turn replaced and at velocities of 55 feet/second and higher, inception occurred as the sudden appearance of a steady, attached cavity which would cover a portion of, or all of the circumference of the body and there were no travelling bubble cavitation events.

In general, when the attached cavitation occurred it would appear very suddenly over the entire circumference and have a transparent leading edge far upstream very similar to that associated with the attached cavitation on a body having a laminar separation. However, in several instances it was observed that an attached, patch cavitation would first appear "far" downstream with a "jagged" leading edge. It would then (without any deliberate reduction in tunnel pressure) quickly "jump" upstream forming a steady, attached cavity with a smooth leading edge.

(b) One-inch Model

With the exception of the tests at 30 feet/second inception occurred as a steady, attached patch which would then grow circumferentially to form a cavity which completely encircled the body. At the freestream velocity of 30 feet/second travelling bubble inception occurred, but this data was taken just after the tunnel was filled. Travelling bubble events were, in general, rare on the one-inch body even though freestream conditions were similar to those during the two-inch body tests.

2. LTWT

Travelling bubble type cavitation was always observed on both

test bodies during the tests in the LTWT. Lowering the tunnel pressure below the inception pressure produced profuse bubble cavitation which would eventually be replaced by a steady attached cavity supercavitation. The inception data is shown as a shaded area since an error in zeroing the pressure transducers only allows an estimate of the inception index to be made.

3. HSWT

The cavitation inception behavior in the HSWT was much the same as that in the ARL 12-inch tunnel at the higher velocities (i.e. greater than 50 feet/second). If cavitation tests were carried out immediately after filling the tunnel, inception would be of the travelling bubble type which would then very quickly be replaced by a steady attached cavity without any deliberate effort to reduce the tunnel pressure. After the tunnel water had been circulated for several minutes (approximately the time required for one complete circuit) travelling bubble events became very rare. Inception then occurred in several ways. One sequence of events was that a steady, attached patch of cavitation would first appear. This patch would then grow circumferentially until the model was completely encircled by a steady, attached cavity with a smooth leading edge. In another sequence the attached cavity would appear very suddenly without any patch type cavitation appearing. A third type of inception that occurred first took place with the appearance of an unsteady patch cavitation located "far" downstream on the test model and have a rough leading edge (see Fig. 20). This patch (or patches) would rapidly move upstream to form a steady, attached cavity.

Cavitation on the one inch model was much the same as that on the two inch model except that the sudden appearance of a steady, attached

cavity appears to be the more prevalent type of cavitation at inception.

C. Nuclei Distributions

Nuclei populations obtained from each counter were reduced to a number density distribution function by the following approximation:

$$N \left(\frac{R_1 + R_2}{2} \right) = \frac{\text{number of nuclei per unit volume with radii between } R_1 \text{ and } R_2}{(R_2 - R_1)}$$

Some of these distributions are presented in Figs. 25, 26 and 27 and all the nuclei counts taken in each facility are summarized in Tables II through VI.

V. Discussion of Results

A. Schlieren Observations

There were two reasons for making the schlieren observations: first, to monitor the viscous flow on the test body in each facility and second, to determine the relationship between inception and transition.

By observing the viscous flow in each facility it could be determined whether any differences in cavitation behavior could be partly attributed to differences in the basic flow past the test model. In Fig. 17 some schlieren photographs of transition on the two inch test model in each facility are presented. As can be seen in these photographs, transition in each facility is qualitatively the same, i.e. the transition is attached and occurs through the amplification of boundary layer waves. A more quantitative comparison is made in Figs. 18 and 19 where the position of transition has been plotted versus the body Reynolds number. It can easily be seen that all the data fall on one curve. The excellent agreement in both the qualitative and quantitative descriptions of transition in each facility lead one to conclude that the basic viscous flow about the test models in

each case is the same. Hence, any differences in cavitation behavior must be attributed to another variable. A comparison between the present observations and theory is made in Gates (1979).

B. Relationship between Inception and Transition

During some previous tests (Gates and Acosta, 1978) carried out with a 2-inch Schiebe body in the HSWT it was found that there was a good correlation between the pressure coefficient at the position of transition and the inception index for attached forms of cavitation. It was hoped that by using the schlieren flow visualization technique that it would be possible to simultaneously observe inception and transition and hence determine if the above speculation had any validity. Unfortunately, for some practical reasons it was not possible to carry out this simultaneous observation and instead, transition information from the schlieren photographs was combined with the inception data from the 35 mm photographs and has been plotted in Figs. 21 and 22.

As can be seen in these figures most of the data clusters somewhat downstream of the position of minimum pressure and certainly does not support any correlation between inception and transition for attached cavitation. However, this information is somewhat misleading. For the attached cavitation the position of the leading edge has been plotted. This is not where inception occurs for this type of cavitation as has been described earlier. The actual position is downstream of the leading edge, but the cavity moves forward so rapidly that the true position of inception could not be determined. Hence the observations regarding attached cavitation and transition are inconclusive.

As for the travelling bubble cavitation, the implication is very

strong that it is in no way related to the position of transition but is rather controlled by the location of the minimum pressure coefficient. However, the value of the inception index is not only determined by the minimum pressure coefficient but also by the nuclei population as we will see later.

C. Nuclei Populations

Nuclei populations in the ARL-12 inch tunnel were measured with the L.S.C. only. A few representative populations have been reduced to number density functions and are presented in Fig. 25 and all the distributions are summarized in Table II. As can be seen from the table, the nuclei density appears to be relatively constant for the range of velocities and pressures covered. From this one might deduce that the nuclei are mainly particulates, but as shall be seen this is not believed to be the case.

Nuclei populations in the HSWT were measured using both optical counters but on separate occasions approximately 11 months apart in time. Again a sample population from each counter has been reduced to a number density function and is shown in Fig. 26. The counts have also been summarized in Table III and IV.

The following observations were made with the LSC counter: at any given velocity the nuclei population was found to be independent of pressure. If the velocity was gradually increased, it was observed that a large number of small nuclei were produced. Also, if the velocity and pressure were held constant, the number of small particles (>10 micrometers diameter) increased whereas the number of large particles decreased with time. From these observations it was deduced that the nuclei in the HSWT are predominantly particulates which are believed to be particles of rust

and chips of paint which are continuously being removed from the tunnel walls. This conclusion agrees with the holography observations in which so few bubbles were observed that no estimate of a distribution could be made, i.e. the distribution presented in Fig. 26 for the HSWT is for particulates.

In the LTWT it was possible to simultaneously measure nuclei populations using both optical counters. A comparison of some distributions deduced from these measurements is made in Fig. 27 and in Table V all the available populations are compared in tabular form. The limited range of velocity and lack of precise pressure control in the LTWT made it difficult to vary tunnel conditions significantly to deduce from the LSC the relative populations of particulates and gas bubbles. From the HNC results, however, it is possible to classify the nuclei and in Table VI the holography results of Table V have been presented again but with the particulate and bubble populations separated. No distinction between particulate and bubble populations for nuclei less than 20 micrometers diameter is possible as background noise destroys the resolution. Nuclei between 20-50 micrometers diameter are mainly particulates, between 50-100 micrometers there are approximately equal numbers of each and above 100 micrometers diameter the nuclei are believed to be essentially all bubbles.

It can readily be seen from these results that there is a substantial difference in the populations measured by each nuclei counter. This discrepancy is discussed in more detail in Billet and Gates (1979), but no conclusion that could definitely explain the difference was drawn. This is a particularly important problem to be resolved if any reliable comparison between the performance of various cavitation facilities and measurement devices are to be made.

D. Nuclei and Inception

First consider the results for the 2-inch Schiebe body in the ARL 12-inch tunnel. As the freestream velocity was increased two trends in the inception behavior were noted. One, the inception index decreased and second, the type of cavitation at inception gradually changed from travelling bubble to attached cavitation. If the nuclei population remained constant, it would be expected that the inception index should rise since the number of encounters between model and nuclei will increase with velocity. The speculation is that at the higher freestream velocities the static tunnel pressure is high at inception and hence one might expect fewer freestream gas bubbles to be present. And, if it is assumed that particulates do not influence inception, then a decreasing inception index would be expected. The trend to an attached form of cavitation tends to support this speculation. For, it was found in the HSWT where there were very few freestream gas bubbles that attached forms of cavitation occurred whereas in the extremely bubbly flow of the LTWT only travelling bubble cavitation was observed.

Further supporting evidence comes from the inception observations upon the 1-inch Schiebe body in the ARL facility. The smaller model will "see" fewer nuclei than the 2-inch model. The main type of cavitation observed on the 1-inch body at inception was the attached type. The implication being that at a given velocity there may be enough nuclei to produce travelling bubble inception on the 2-inch model whereas there are too few on the 1-inch model and attached cavities appear at inception.

Cavitation inception in the LTWT was always of the travelling bubble type and even though there is some question as to the absolute value

of the inception index it tends to be lower than the values observed in the ARL 12-inch tunnel. This is surprising in that the LSC measured approximately an order of magnitude more nuclei/cc in the LTWT than in the ARL facility.

In the HSWT only attached forms of cavitation occurred and surprisingly for a given freestream velocity the inception index was the same for both the 1-inch and 2-inch bodies. (It may be noted here that if cavitation depends upon the number of nuclei "swept out" by the body that a smaller body should have a smaller value of σ_i for a constant concentration of nuclei per unit volume.) Further, as can be seen in Fig. 23, there is a suggestion of a correlation between the pressure coefficient at transition and the inception index although, this is not supported by observations of the position of transition in the present tests.

In all three facilities then, there are substantial differences in the type of cavitation at inception and the inception index. Since the viscous flow past each model has been shown to be the same in each facility it is apparent that these discrepancies are a consequence of different nuclei populations. The observations in the HSWT indicate first that particulates (at least those in the HSWT) are not sites for nucleation and second that when extremely few freestream gas bubbles are present that a simple explanation based on cavitation event encounters cannot be used. Instead it appears that some interaction between nuclei and transition is responsible for inception. At the other end of the spectrum in the LTWT where there are very many freestream bubbles, travelling bubble inception will occur and the inception index is then controlled by the bubble population.

These cavitation observations are somewhat inconclusive. Even though the LSC measures approximately an order of magnitude fewer nuclei in the ARL tunnel than the LTWT, travelling bubble inception occurs at a higher inception index than in the LTWT. Yet at the same time there appears to be a scarcity of nuclei in the ARL 12-inch water tunnel so that an attached cavity forms on the 2-inch model at the higher velocities and on the 1-inch model over the entire velocity range. (However, it may be pointed out that if the attached cavitation is a consequence of surface relative roughness we would expect the smaller body to be the rougher and hence that attached cavitation would form more readily then.)

VI. Concluding Remarks

From the introductory remarks it should be recalled that the main objectives of this investigation were to further pursue the questions of the relationships between transition and nuclei populations with inception. To carry out this work a non-separating test model was chosen under the assumption that it would exhibit travelling bubble type cavitation at inception. Surprisingly, this type of inception was only predominant in the extremely bubbly flow of the LTWT whereas in the HSWT and the ARL-12 inch tunnel attached forms of inception occurred.

Schlieren observations of the viscous flow about the model demonstrated that it was unaltered from facility to facility and hence it is believed that differences in cavitation behavior are attributable to nuclei populations and in particular the gas bubble fraction of these populations. Hence although the LSC indicates that the populations in the ARL tunnel and the HSWT are about the same, it is speculated that the bubble fraction of the distribution is smaller in the resorber facility i.e.

the HSWT. When very few gas bubbles are present as in the HSWT the cavitation at inception tends to be of the attached type and the lack of diameter effect here implies the concept of encounter rates is not applicable to defining inception. Whereas in extremely bubbly flows like that of the LTWT the encounter rate seems to be appropriate.

The consequence of these observations then is to re-emphasize the need for accurate measurements of nuclei populations and in particular to be able to distinguish between particulates and bubbles. The rather significant difference between counters must then be resolved before any reliable comparison of cavitation behavior from one facility or environment to another may be made.

REFERENCES

1. Arakeri, V.H. (1973). Viscous effects in inception and development of cavitation on axi-symmetric bodies, Ph.D. dissertation, California Institute of Technology.
2. Arakeri, V.H. and A.J. Acosta (1976). Cavitation inception observations on axisymmetric bodies at supercritical Reynolds numbers, Journal of Ship Research, Vol. 20, No. 1, March, pp. 40-50.
3. Beckwith, T.G. and N.I. Buck (1961). Mechanical Measurements, Addison-Wesley, Reading, Mass.
4. Billet, M.L. and E.M. Gates (1979). A comparison of two optical techniques for measuring cavitation nuclei. Submitted to A.S.M.E. Cavitation Symp. at the Winter Annual Meeting, New York, N.Y.
5. Feldberg, L.A. and K.T. Shlemenson (1973). The holographic study of cavitation nuclei. Discussion to Proc. IUTAM Symp. on Non-Steady Flow of Water at High Speeds, Leningrad, USSR.
6. Gates, E.M. (1977). The influence of freestream turbulence, freestream nuclei populations and a drag-reducing polymer on cavitation inception on two axisymmetric bodies. Eng. Rept. No. 183-2, California Institute of Technology.
7. Gates, E.M. and J. Bacon (1978). Determination of cavitation nuclei distributions by holography. Journal of Ship Research, Vol. 22, No. 1, March, pp. 29-31.
8. Gates, E.M. and A.J. Acosta (1978). Some effects of several freestream factors on cavitation inception on axisymmetric bodies. 12th Symp. on Naval Hydrodynamics, Wash., D.C.
9. Gates, E.M. (1979). Observations of transition on some axisymmetric bodies submitted to IUTAM. Symposium on Transition, Sept. 1979.
10. Johnsson, C.A. (1969). Cavitation inception on head forms, further tests 12th ITTC, Rome, pp. 381-392.
11. Keller, A.P. (1972). The influence of the cavitation nucleus on cavitation inception, investigated with a scattered light counting method. Journal of Basic Engineering, Dec., pp. 917-925.
12. Knapp, R.T., J.W. Daily and F.G. Hammitt (1970). Cavitation, Mc-Graw-Hill New York.
13. Lindgren, H. and C.A. Johnsson (1966). Cavitation inception on headforms ITTC comparative experiments. Pub. of the Swedish State Shipbuilding Experimental Tank, No. 58. (Also presented at the 11th ITTC meeting in Tokyo.)
14. Peterson, F.B. (1972). Hydrodynamic cavitation and some considerations of the influence of free gas content. 9th Symposium on Naval Hydrodynamics, Paris.
15. Schiebe, F.R. (1972). Measurement of cavitation susceptibility of water using standard bodies. St. Anthony Falls. Hyd. Lab. Project Rep. No. 118, University of Minnesota.

16. van der Meulen, J.H.J. (1976). A holographic study of cavitation on axisymmetric bodies and the influence of polymer additives. Doctoral Thesis, Netherlands Ship Model Basin.
17. Vanoni, V.A., E. Hsu and R.W. Davies (1950). Dynamics of particulate matter in fluid suspensions. Hydrodynamics Laboratory Rep. No. 71.1a, Calif. Inst. of Tech.
18. Ward, T.M. (1976). The hydrodynamics laboratory at the California Institute of Technology. Journal of Fluids Engineering, Dec., pp. 740-748.

TABLE I

WATER TUNNEL CHARACTERISTICS

	12-inch ARL	HSWT	LTWT
Type of Circuit	Closed	Closed	Closed
Working Section	Cylindrical 12-inch diameter	Cylindrical 14-inch dia. 48-inches long	Square 12 inch X 12 inch 96 inch long
Maximum Velocity (fps)	80	100	25
Pressure Range: Min(atm) Max(atm)	0 4	0.1 7.5	0.1 1.0
Resorber	No	Yes	No
Typical Air Content during tests mole/mole	4	9	7
Freestream Turbulence Level (percent)	0.15	0.2	0.05 → 3.6

Table 11

Nuclei Distributions in ARL 12 inch Tunnel
as Measured by LSC

Velocity fps	σ	Volume Sampled cc	1-3	3-6.5	6.5-10	10-12.5	12.5-16	16-19	19-21.5	> 21.5	Cumulative
Following Data Taken 2/28/78											
30.3	0.53-0.65	263	2.51	0.34	0.33	0.22	0.14	0.06	0.03	0.17	3.80
30.3	0.73-0.79	395	1.52	0.32	0.25	0.13	0.10	0.05	0.03	0.13	2.53
35.5	0.68-0.70	71	10.25	1.21	1.27	0.65	0.25	0.14	0.08	0.23	14.1
35.5	0.64-0.69	55	13.85	1.60	1.25	0.76	0.27	0.11	0.09	0.24	18.2
40.2	0.63	58	13.88	0.98	1.09	0.62	0.38	0.07	0.02	0.21	17.2
40.2	0.60-0.63	67	12.00	0.87	1.01	0.42	0.37	0.12	0.03	0.10	14.9
45.3	0.56-0.57	82	9.77	0.72	0.65	0.48	0.33	0.11	0.04	0.11	12.2
45.3	0.56	70	11.24	0.91	1.07	0.46	0.27	0.11	0.07	0.14	14.3
50.4	0.54	71	11.54	0.86	0.62	0.42	0.32	0.10	0.08	0.14	14.1
50.4	0.51-0.53	82	10.22	0.63	0.62	0.23	0.28	0.06	0.05	0.10	12.2
55.3	0.50-0.51	383	2.23	0.15	0.11	0.04	0.03	0.01	0.01	0.03	2.6
55.3	0.50-0.51	373	2.31	0.13	0.12	0.03	0.04	0.02	0.01	0.02	2.7
Above two counts noted as suspect in original data book.											
60.4	0.50-0.51	31	24.94	2.65	2.06	0.87	0.87	0.29	0.03	0.55	32.3
60.4	0.51-0.53	25	30.96	2.96	3.04	1.28	0.96	0.16	0.04	0.60	40.0
Following Data Taken 3/2/78											
29.1	0.73-0.76	89	7.57	0.80	0.27	0.38	0.21	0.45	0.38	1.17	11.2
28.6	0.78-0.80	62	11.06	1.05	0.44	0.66	0.47	0.56	0.47	1.42	16.1
36.0	0.57-0.60	84	8.02	0.69	0.18	0.42	0.33	0.52	0.30	1.44	11.9
36.1	0.59-0.61	84	8.44	0.70	0.29	0.30	0.42	0.40	0.48	0.88	11.9
39.9	0.59-0.60	103	6.79	0.55	0.26	0.37	0.16	0.31	0.43	0.84	9.7

Table 11
continued

Velocity fps	σ	Volume Sampled cc	1-3	3-6.5	6.5-10	10.12.5	12.5-16	16-19	19-21.6	> 21.5	Cumulative
45.3	0.43-0.49	336	2.09	0.18	0.07	0.11	0.08	0.13	0.10	0.21	3.0
45.3	0.46-0.48	330	2.14	0.19	0.06	0.10	0.10	0.11	0.09	0.24	3.0
50.4	0.44-0.46	200	3.84	0.27	0.10	0.11	0.11	0.17	0.11	0.31	5.0
55.3	0.47-0.48	201	3.67	0.33	0.12	0.12	0.06	0.14	0.11	0.40	5.0
60.5	0.42	277	2.63	0.20	0.07	0.10	0.07	0.13	0.09	0.32	3.6

Following Data Taken 3/3/78

Tunnel stopped and opened to clean model

TABLE III

Nuclei Distributions in HSWT
as Measured by LSC

Velocity fps	σ	Volume Sampled cc	Nuclei Distribution (no./cc) Nuclei Diameter (micrometers)				Cumulative
			< 11	11-21.5	21.5-50	> 50	
20.83	4.75	224	3.60	0.64	0.06	-	4.46
20.76	0.96	244	3.60	0.24	0.08	-	4.10
20.78	4.77	222	4.16	0.28	0.06	-	4.50
Rest 10 minutes							
31.14	2.12	154	5.88	0.28	0.10	0.24	6.50
31.25	0.43	304	2.84	0.40	0.04	0.02	3.30
31.28	2.10	234	4.12	0.36	0.12	0.02	4.62
Rest 10 minutes							
46.82	0.94	164	4.58	0.60	0.04	-	5.22
46.72	0.51	66	12.78	0.54	0.18	1.64	15.14
46.93	0.94	56	13.42	0.92	0.08	2.34	17.84
Rest 10 minutes							
62.70	0.66	21	44.20	1.34	-	2.10	47.64
62.82	0.54	22.2	43.24	1.62	0.18	-	45.04
62.76	0.66	13.2	76.66	0.90	-	0.60	78.16
Rest 10 minutes							
62.76	0.66	12.2	63.60	0.66	-	17.70	81.96
1 minute							
62.76	0.66	13.4	62.98	0.60	0.30	10.74	74.62
1 minute							
62.76	0.66	14.4	65.56	0.84	-	3.06	69.46
6 minutes							
62.76	0.66	14.4	67.50	1.12	0.28	0.56	69.46
2 minutes							
62.76	0.66	15.6	62.56	1.02	-	0.52	64.10
1 minute							

Table III
continued

Velocity fps	σ	Volume Sampled cc	< 11	11-21.5	21.5-50	> 50	Cumulative
62.3	0.41	20.0	5 minutes 49.20	0.80	-	-	50.00
62.93	0.41	21.16	5 minutes 45.94	0.94	0.18	0.18	47.24
62.93	0.41	16.70	5 minutes 57.72	0.72	0.48	0.72	59.64
Run 10 minutes at Atmos. Press.							
30.60	2.20	57.40	16.24	1.04	0.14	-	17.42
30.60	0.45	49.28	18.66	1.46	0.16	-	20.30
Tunnel Rest for 30 minutes							
46.68	0.94	43.78	21.66	1.10	0.10	-	22.86
46.90	0.49	31.54	29.16	1.14	-	1.40	31.70
46.91	0.93	33.20	29.16	0.72	0.24	-	30.12
Tunnel Rested Overnight							
31.62	0.93	292	2.94	0.32	0.16	-	3.42
31.62	0.93	310	2.52	0.56	0.12	0.02	3.22
Cavitation Testing Starts							
31.23	0.27	236	3.46	0.64	0.14	-	4.24
30.89	0.25	272	3.00	0.48	0.18	0.02	3.68
41.79	0.36	272	3.14	0.44	0.08	0.02	3.68
52.60	0.45	284	3.12	0.14	0.04	0.22	3.52
62.28	0.47	109.12	8.32	0.62	0.10	0.10	9.14
63.04	0.60	53.56	10.76	0.82	0.14	6.94	18.66
30.49	0.41	724	1.10	0.22	0.06	-	1.38
41.32	0.33	608	1.24	0.36	0.04	0.02	1.66
52.56	0.45	230	3.62	0.16	0.04	0.54	4.36

Table IV
Nuclei Populations in HSWT
as Measured by Holography
(Katz 1978)

Nuclei Distribution (no./cc)
Nuclei Diameter (micrometers)

σ	< 40	40-100	100-150	150-200	> 200	Cumulative
0.238	40.4	16.8	4.0	0.4	0.8	62.40
0.257	44.4	8.8	3.6	2.8	1.2	60.80
0.223	32.0	14.0	5.6	1.6	2.0	55.2
0.230	26.8	7.2	1.2	0.4	0.4	36.0
0.410	35.6	15.2	6.4	1.6	0.8	58.8
0.469	42.0	21.2	2.4	0.4	-	66.0
0.433	41.2	14.4	5.6	1.6	0.4	63.2
0.431	24.4	8.4	2.0	0.4	0.4	35.6
0.464	30.0	11.2	2.8	1.6	0.8	46.4
0.615	14.0	4.4	-	-	0.4	18.8
0.647	38.0	14.8	2.0	1.2	-	56.0
0.610	26.0	14.8	3.2	1.2	0.4	45.6
0.613	37.6	14.8	3.6	0.8	0.4	57.2
0.727	28.4	6.4	0.8	-	-	35.6
0.737	27.2	8.8	2.4	0.4	0.4	39.2

TABLE V

Comparison of Nuclei Measurements Obtained in LTWT

Nuclei Distribution (number/cc)
Nuclei Diameter (micrometers)

Hologram Number	Velocity fps	σ (est)	< 20			20-50			>50			Cumulative Hplo. Light Scattering
			Holo.	Light Scattering	Holo.	Light Scattering	Holo.	Light Scattering	Holo.	Light Scattering		
1	23.5	0.46	224	-	82.8	-	8.0	-	315	-		
4	23.3	0.42	338	-	126	-	7.2	-	471	-		
5	23.3	0.39	266	-	126	-	2.4	-	394	-		
6	23.3	0.38	294	-	116	-	1.2	-	411	-		
7	23.5	0.39	285	-	84	-	2.8	-	372	-		
8	23.4	0.40	239	-	79	-	2.8	-	318	-		
9	23.5	0.39	308	-	110	-	44	-	422	-		
12	4.5	35.78	-	82.80	-	3.52	-	-	-	87.8		
13	4.5	35.34	-	76.20	-	4.22	-	-	-	81.0		
14	4.5	32.92	-	81.0	-	4.96	-	-	-	88.4		
15	4.2	25.49	-	61.0	-	3.96	-	-	-	66.0		
16	4.2	25.83	221	82.0	39	4.6	1.2	1.0	261	88.0		
17	20.4	3.19	290	208.0	116	4.2	3.2	0.8	409	212.0		
18	20.2	3.28	-	139.4	-	0.56	-	-	-	140.0		
19	20.1	2.13	-	193.6	-	7.22	-	-	-	202.0		
20	20.1	1.99	-	172.0	-	2.10	-	-	-	175.6		
21	20.0	1.42	-	486.8	-	2.68	-	-	-	490.0		
22	20.1	1.41	-	494.0	-	12.24	-	-	-	510.0		
23	22.5	0.45	-	133.2	-	0.54	-	-	-	136.0		
24	22.6	0.47	308	126.0	106	3.6	1.6	0.6	416	128.0		
25	22.2	0.47	312	172.0	81	2.8	1.6	-	394	176.0		

Hologram Number	Velocity Fps	σ (est.)	< 20		20-50		>50		Cumulative Light Scattering
			Holo.	Light Scattering	Holo.	Light Scattering	Holo.	Light Scattering	
26	22.6	0.48	-	134.0	-	2.74	-	-	136.8
27	22.6	0.51	-	144.0	-	1.8	-	0.6	146.0
28	22.7	0.50	-	145.4	-	3.0	-	0.6	149.0
29	22.7	0.47	-	136.2	-	2.8	-	-	139.0
30	18.5	0.60	-	178.8	-	6.0	-	1.4	186.2
31	20.7	0.44	-	146.2	-	-	-	0.6	146.8
33	20.9	0.52	-	65.	-	1.6	-	-	66.6
34	20.3	0.54	204	166.0	66	0.6	2.8	0.6	168.0
35	21.6	0.51	242	146.0	64	1.6	4.4	-	148.0
36	21.0	0.51	-	174.8	-	5.0	-	0.8	180.0
37	20.9	0.48	-	156.2	-	3.2	-	0.6	160.0
38	23.1	0.45	-	150.4	-	2.4	-	-	152.8
39	23.5	0.43	-	166.2	-	0.6	-	-	166.8
40	23.3	0.47	-	174.4	-	0.7	-	0.7	175.8

Table VI
Particulate and Bubble Distributions
in the LTWT

Nuclei Distribution (number/cc)
Nuclei Diameter (micrometers)

Hologram Number	20-50		50-100	
	Part.	Bubbles	Part.	Bubbles
1	82.0	0.8	8.0	-
4	124.8	1.2	6.0	1.2
5	122.4	3.2	2.4	-
6	113.6	2.4	0.4	0.8
7	70.0	14.4	-	2.8
8	69.2	10.0	1.2	1.6
9	104.0	6.0	0.4	4.0
17	98.0	17.6	0.4	2.8
24	92.8	12.8	0.4	1.2
25	70.0	10.8	0.4	1.2

FIGURE CAPTIONS

Figure 1: Results of a comparative cavitation inception test on a modified ellipsoidal headform sponsored by the ITTC.

Figure 2: Photographs of incipient cavitation on the ITTC headform in various facilities.

Figure 3: A schematic drawing of the ARL 12-inch water tunnel.

Figure 4: A schematic drawing of the LTWT circuit.

Figure 5: A schematic drawing of the HSWT circuit.

Figure 6: Schematic drawing illustrating the main components of the holocamera.

- (a) etalon
- (b) iris
- (c) dye cell
- (d) ruby rod - flash lamp assembly
- (e) iris
- (f) dielectric mirror
- (g) beam splitter
- (h) neutral density filter
- (i) beam expander lens
- (j) 25μ pinhole
- (k) collimating lens
- (l) front surface mirror
- (m) pin diode
- (n) film pack

Figure 7: A schematic representation of the system to reconstruct the holograms.

Figure 8: A schematic drawing of the basic components of the light scattering counter.

Figure 9: A schematic drawing of the schlieren flow visualization system.

Figure 10: The pressure coefficient versus arc length for the $C_{p_{min}} = -0.75$ Schiebe body.

Figure 11: A schematic representation of the arrangement of equipment at the ARL 12-inch tunnel.

Figure 12: Two photographs illustrating the arrangement of equipment at the ARL 12-inch tunnel.

Figure 13: A schematic drawing of the experimental configuration at the LTWT.

Figure 14: A photograph of the actual equipment used at the LTWT.

Figure 15: A schematic drawing illustrating the equipment arrangement at the HSWT.

Figure 16: A photograph of the equipment arrangement at the HSWT.

Figure 17: A sequence of schlieren photographs illustrating transition on the 2 inch Schiebe body in each facility. In each photograph the model is seen in silhouette with the flow from right to left and the arc length is approximately 10mm.

(a) ARL 12-inch tunnel

$$V = 35.1\text{fps} \quad S/D_t = 0.67$$

(b) HSWT

$$V = 30.0\text{fps} \quad S/D_t = 0.72$$

(c) LTWT

$$V = 20.7\text{fps}$$

Figure 18: A summary of the averaged schlieren observations of transition on the 2-inch diameter Schiebe model.

Figure 19: A summary of the averaged schlieren observations of transition on the one inch diameter Schiebe model.

Figure 20: A sequence of photographs showing the several types of incipient cavitation that occur on the Schiebe models.

(a) travelling bubble - LTWT, $V = 24.0$ fps, $\sigma = 0.53$

(b) travelling patch - ARL 12 inch tunnel and ARL model
 $V = 60$ fps, $\sigma = 0.365$

(c) patch type cavitation - HSWT, $V = 41.5$ fps, $\sigma = 0.43$

(d) partially attached and patch type cavitation - HSWT
 $V = 41.6$ fps, $\sigma = .40$

(e) steady, fully attached cavitation - HSWT, $V = 41.6$ fps
 $\sigma = 0.39$

Figure 21: A plot of the estimated position of inception versus body Reynolds number for the two inch diameter Schiebe body.

Figure 22: A graph of the estimated position of cavitation inception versus body Reynolds number for the one inch diameter Schiebe model.

Figure 23: A summary of the cavitation inception data for the two inch diameter Schiebe model in each facility.

Figure 24: A summary of the cavitation inception data for the one inch diameter Schiebe model in each facility.

Figure 25: Several nuclei distribution functions calculated from populations obtained with the LSC in the ARL 12-inch tunnel.

Figure 26: A comparison of nuclei populations measured in the HSWT with the LSC and the HNC at a time interval of about 11 months.

Figure 27: A comparison of nuclei populations measured simultaneously in the LTWT by the two optical counters.

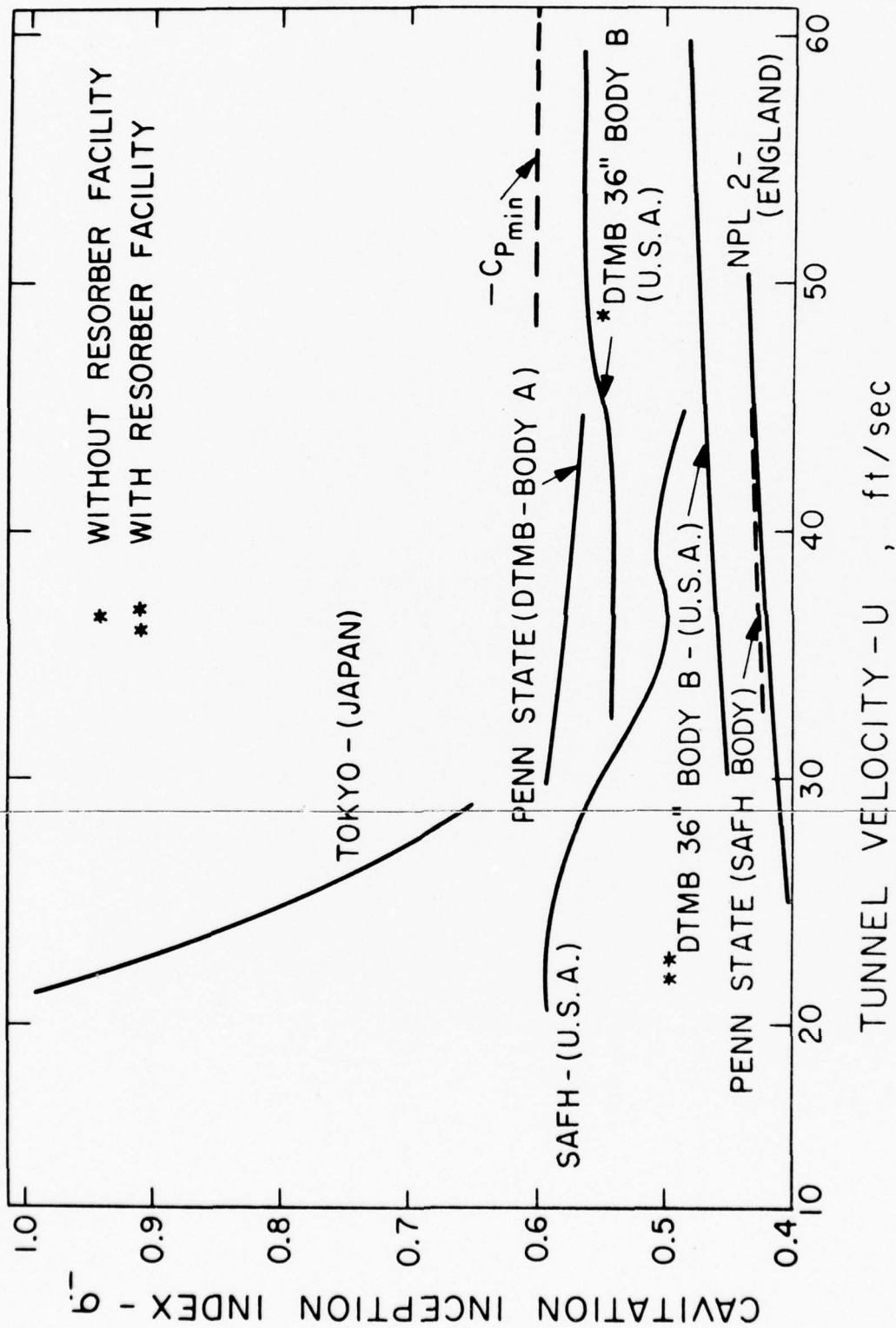


Fig.1

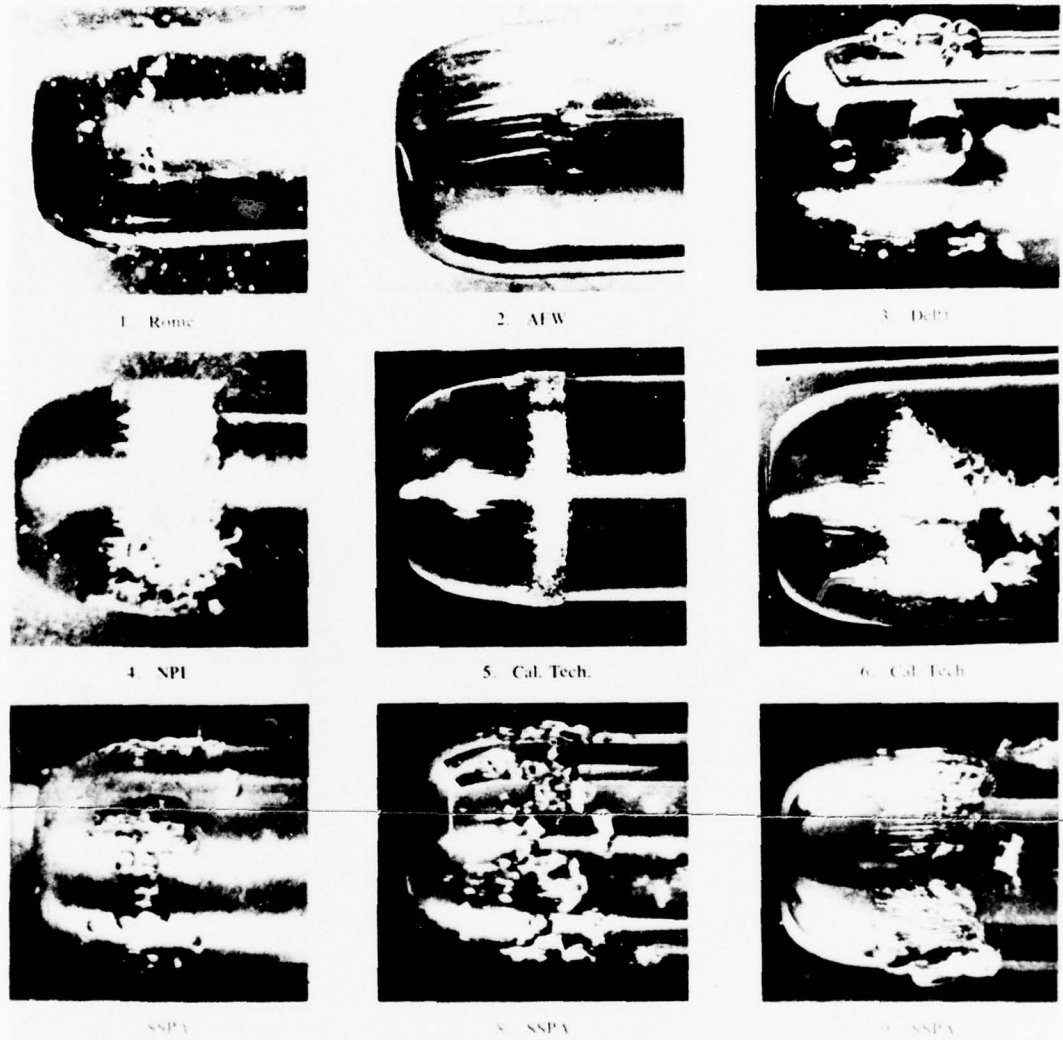


Fig. 2

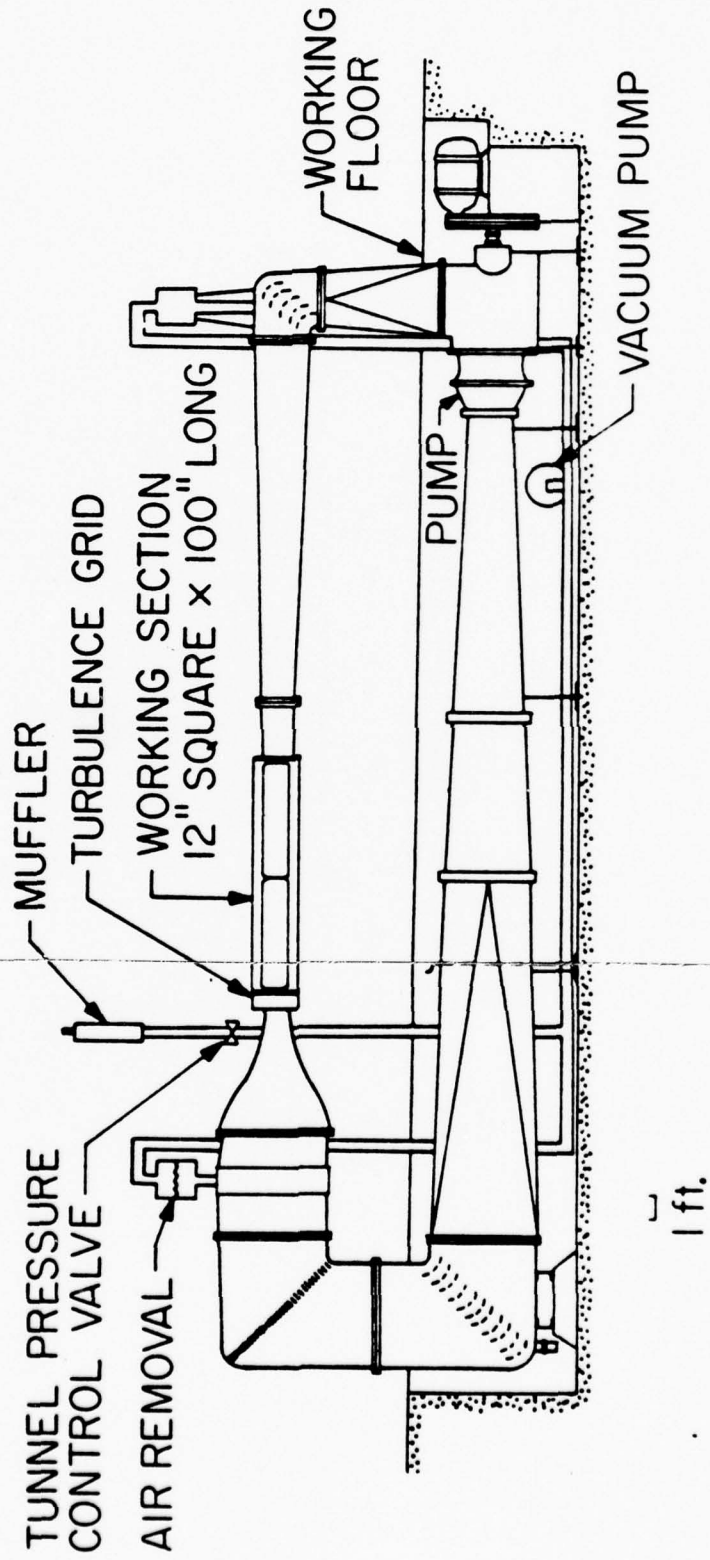


Fig. 4

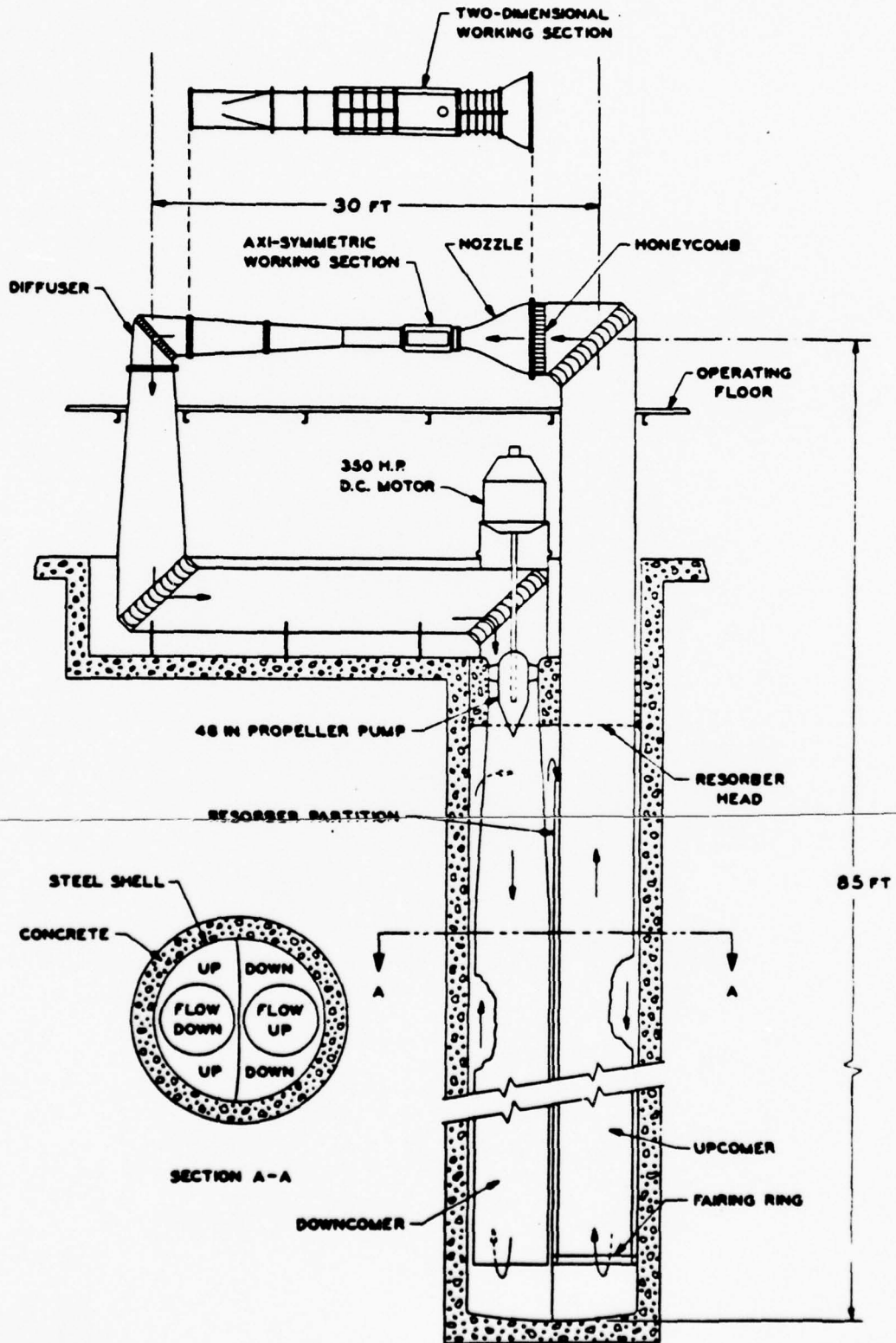


Fig. 5

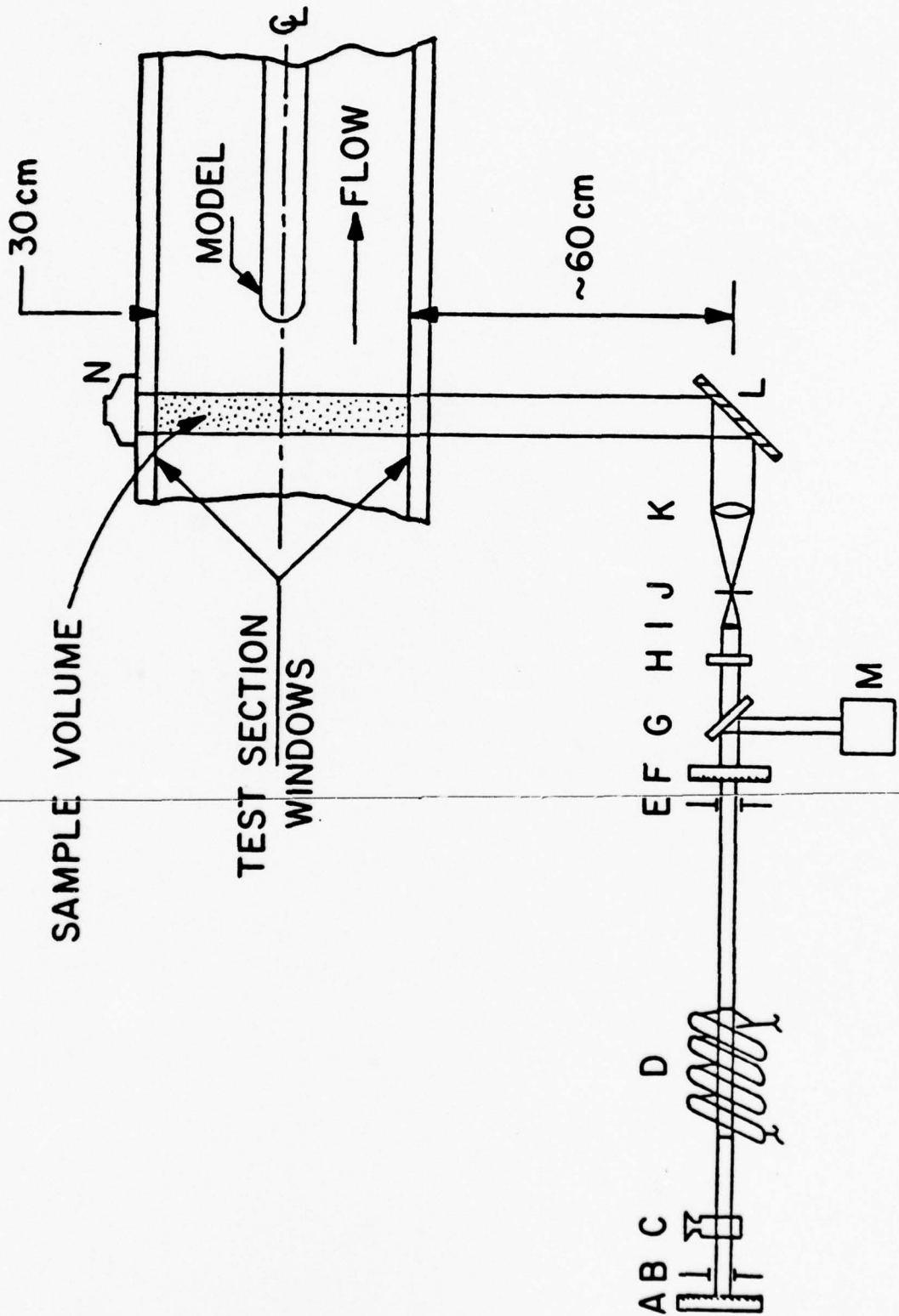


Fig. 6

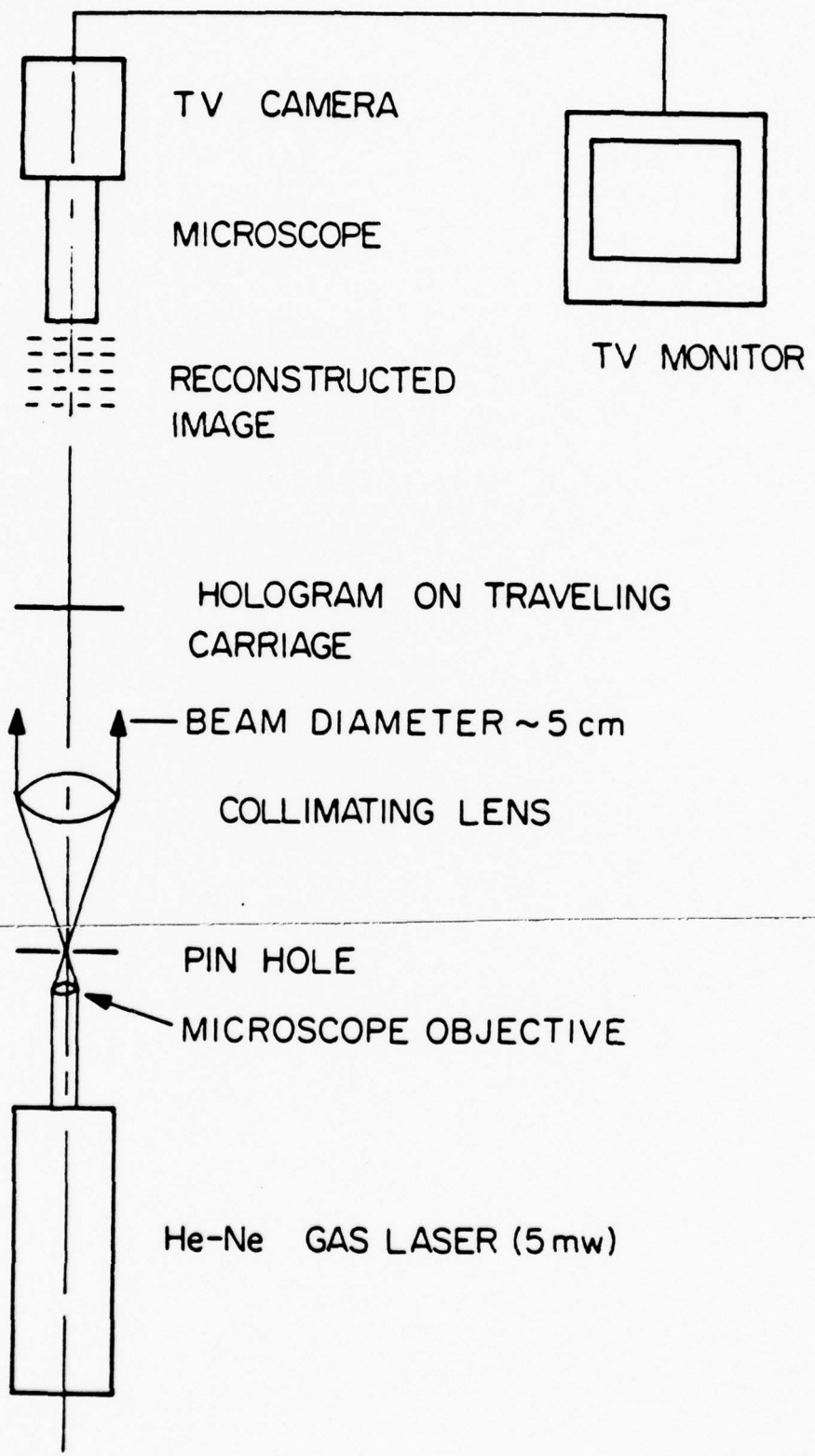


Fig. 7

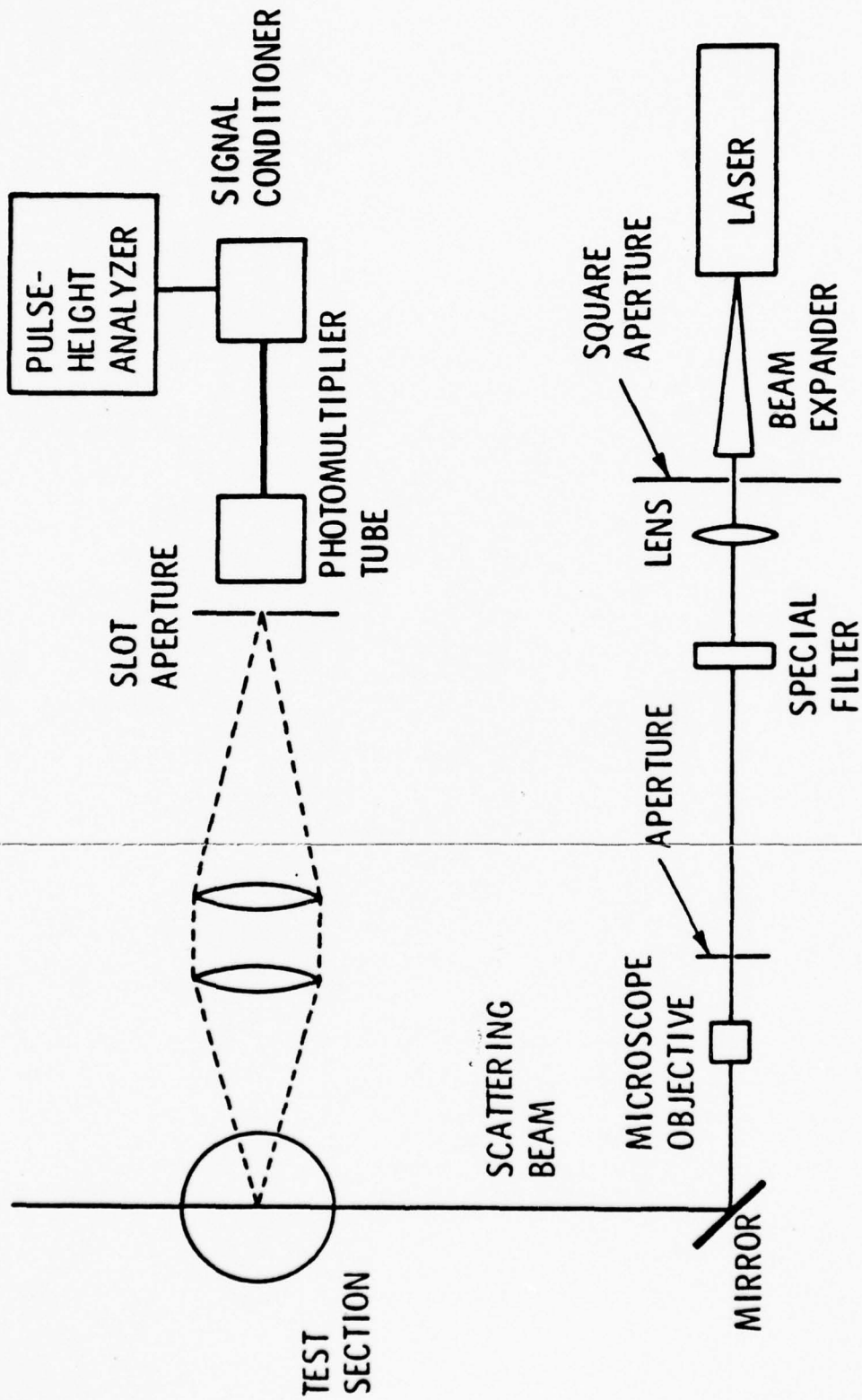


Fig. 8

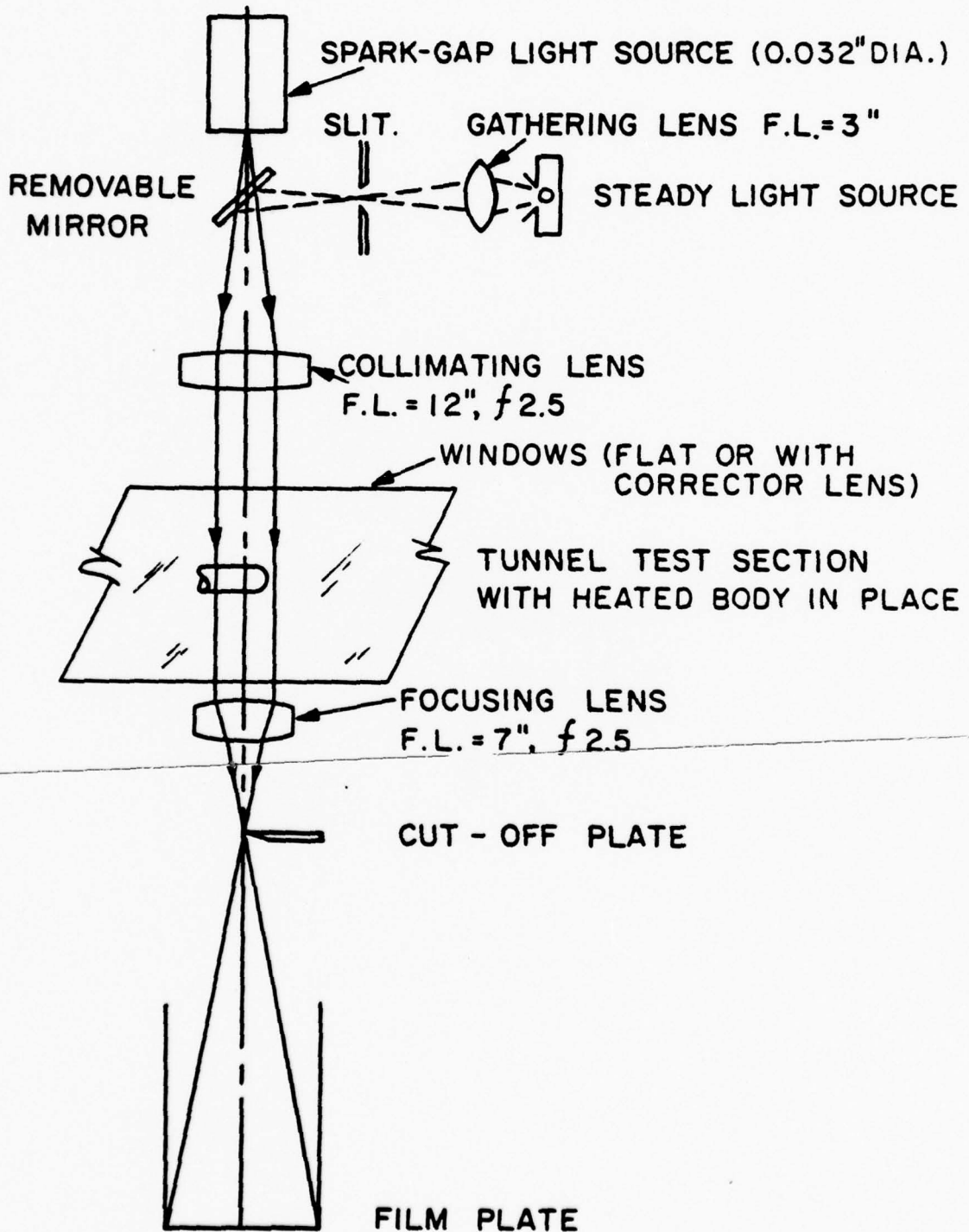


Fig. 9

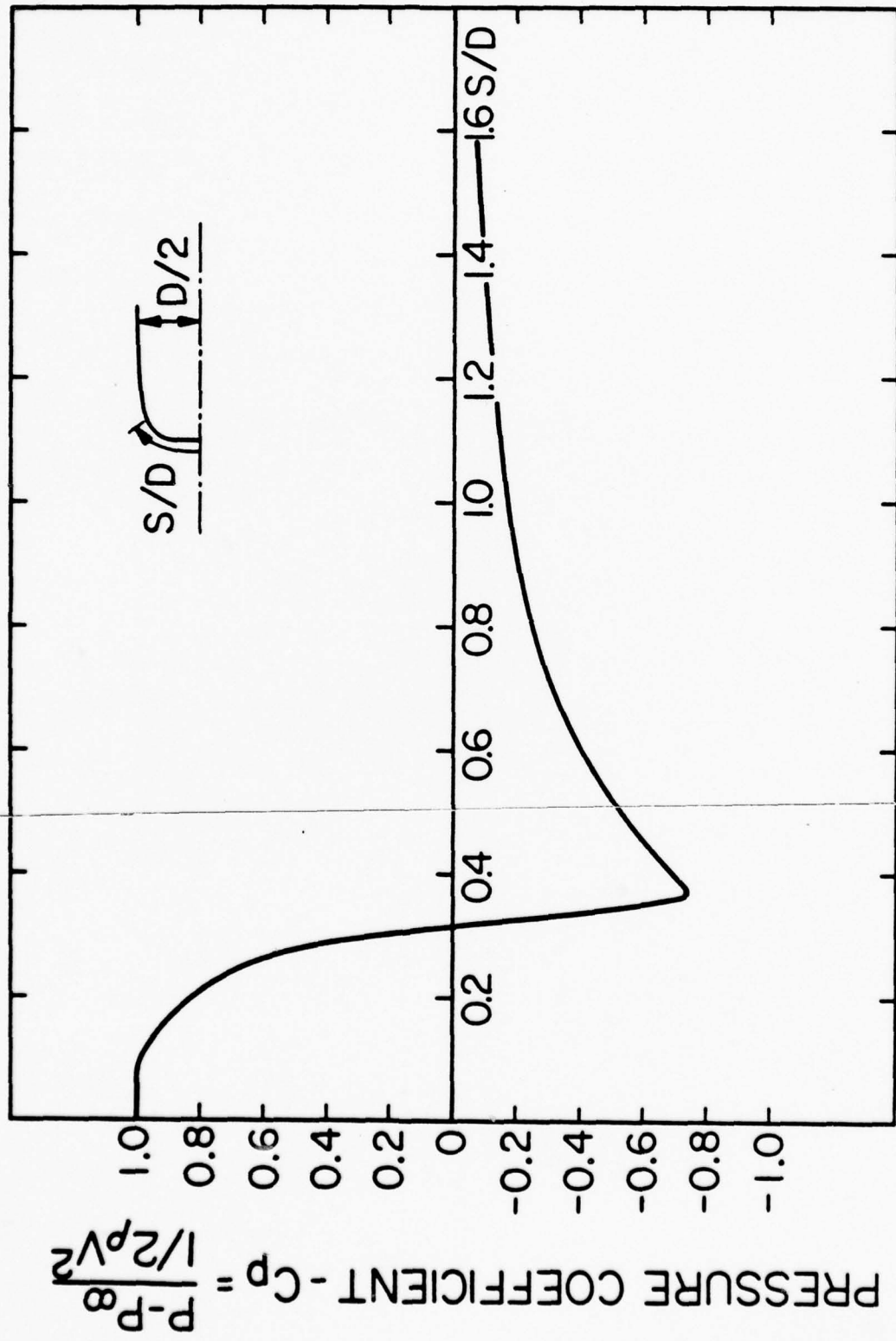


Fig. 10

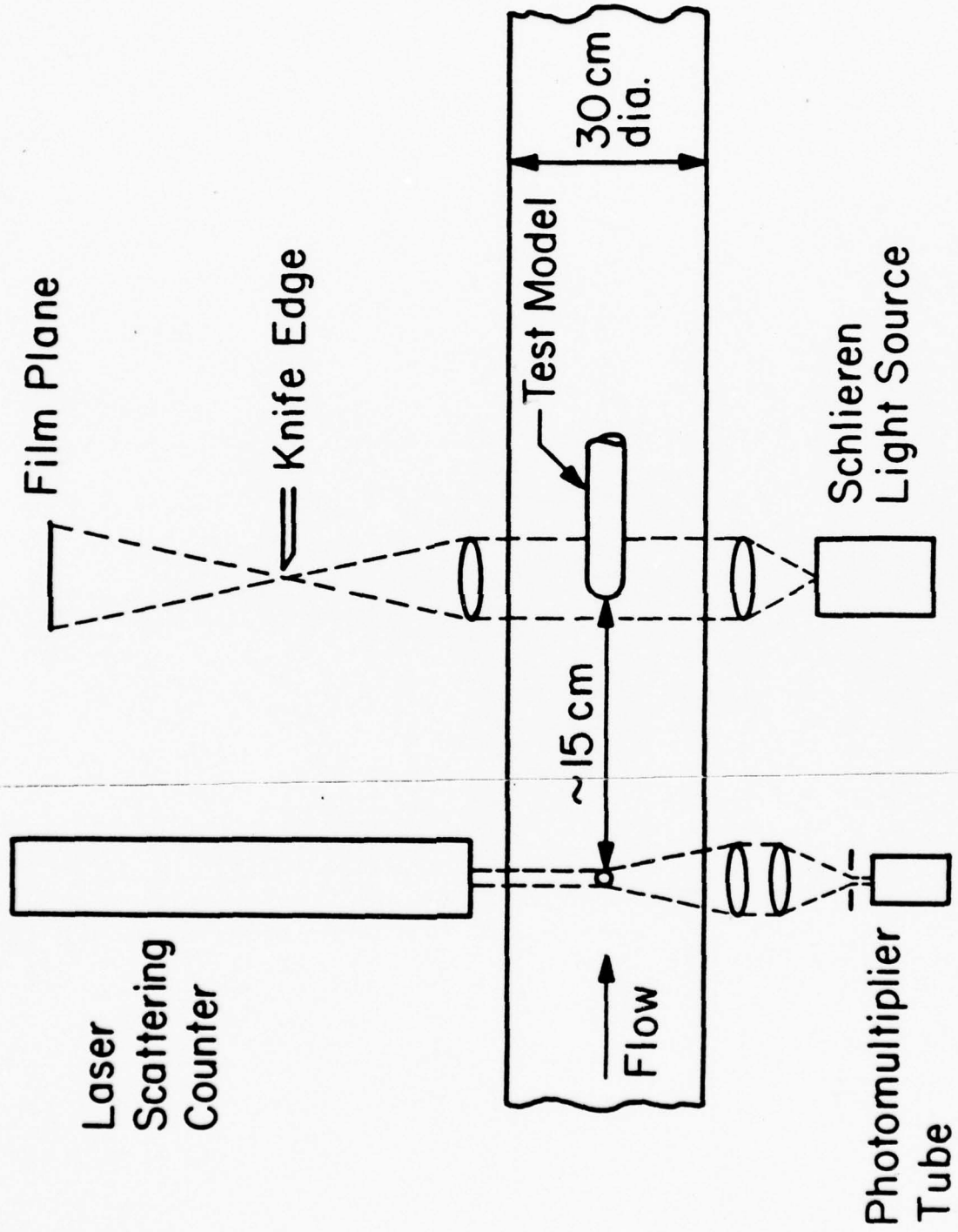
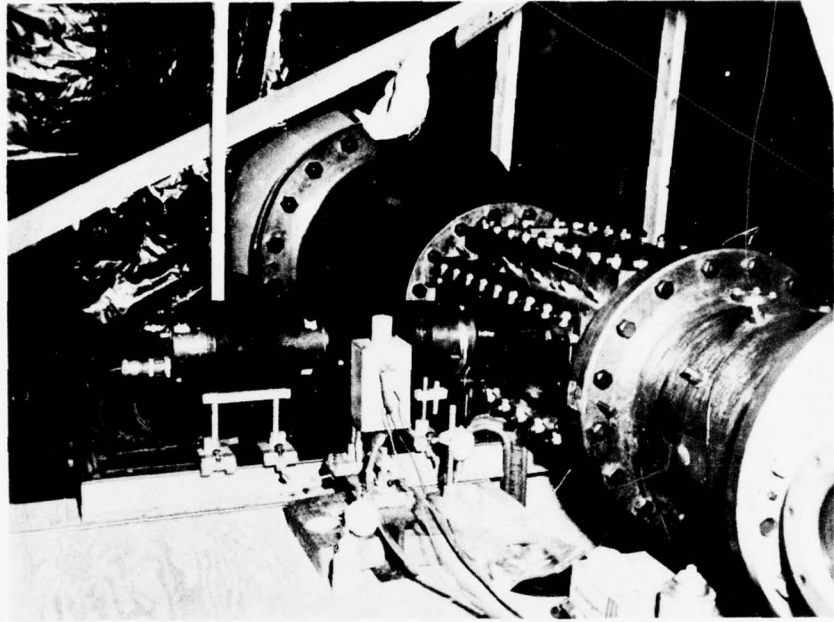
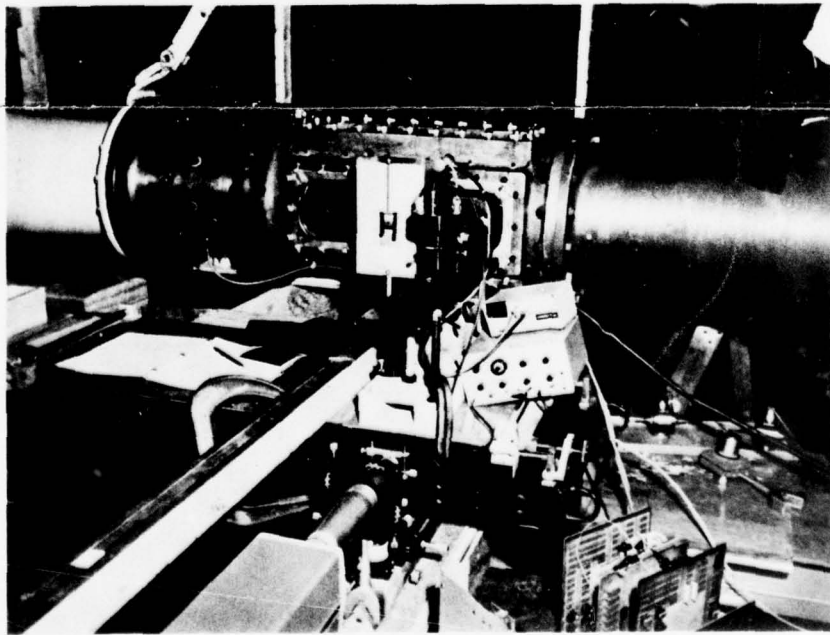


Fig. 11



(a)



(b)

Fig. 12

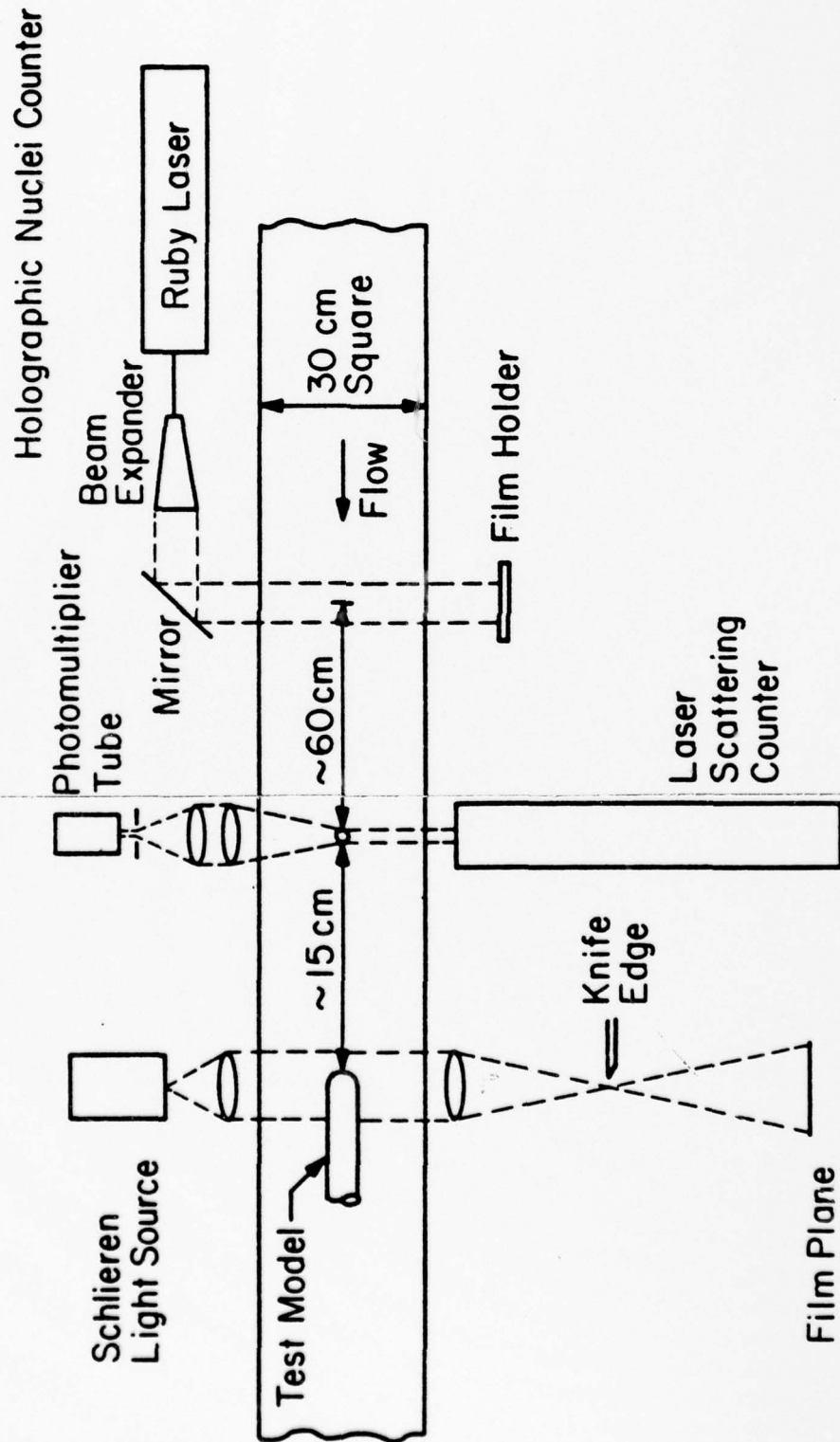


Fig. 13

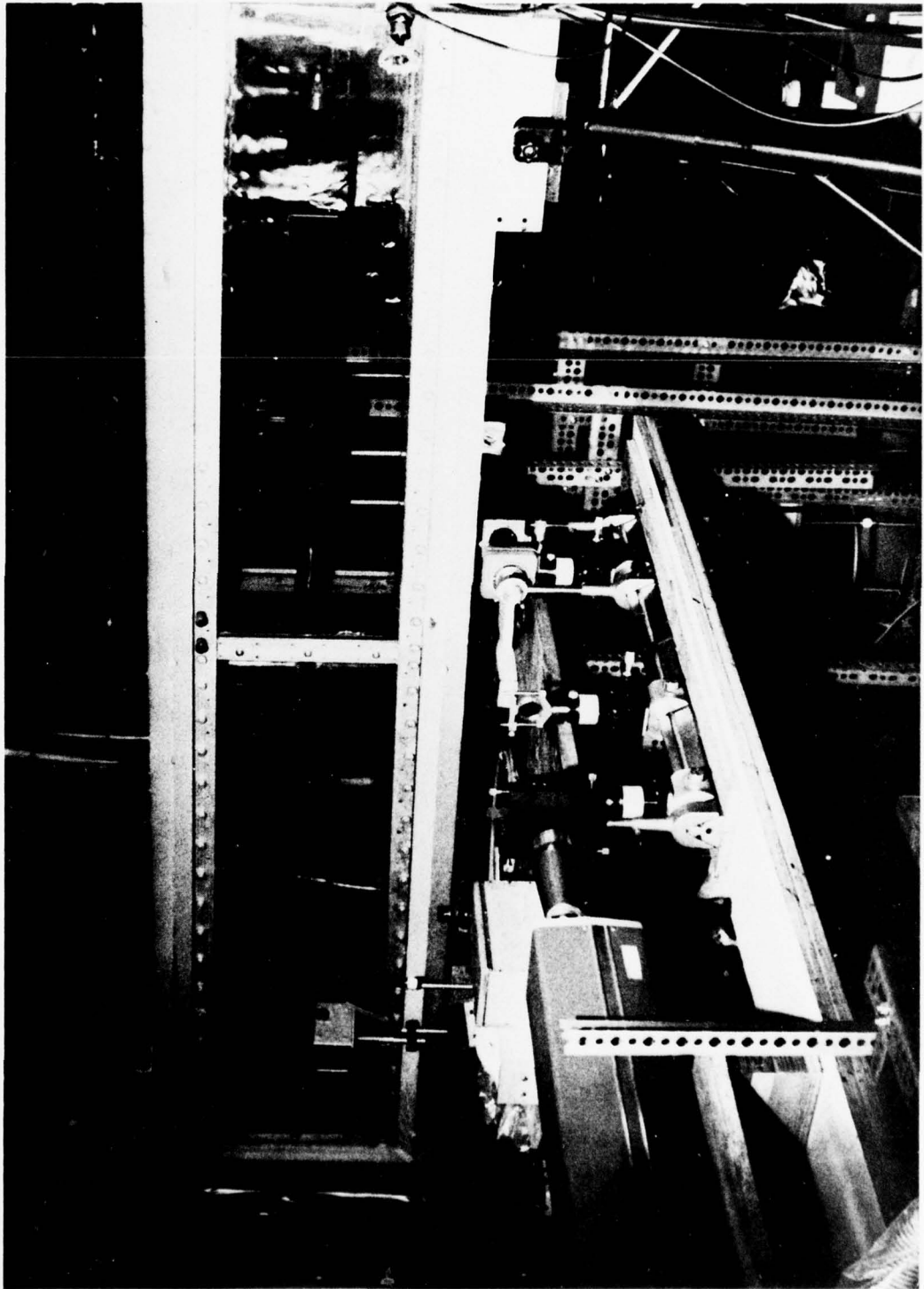


Fig. 14

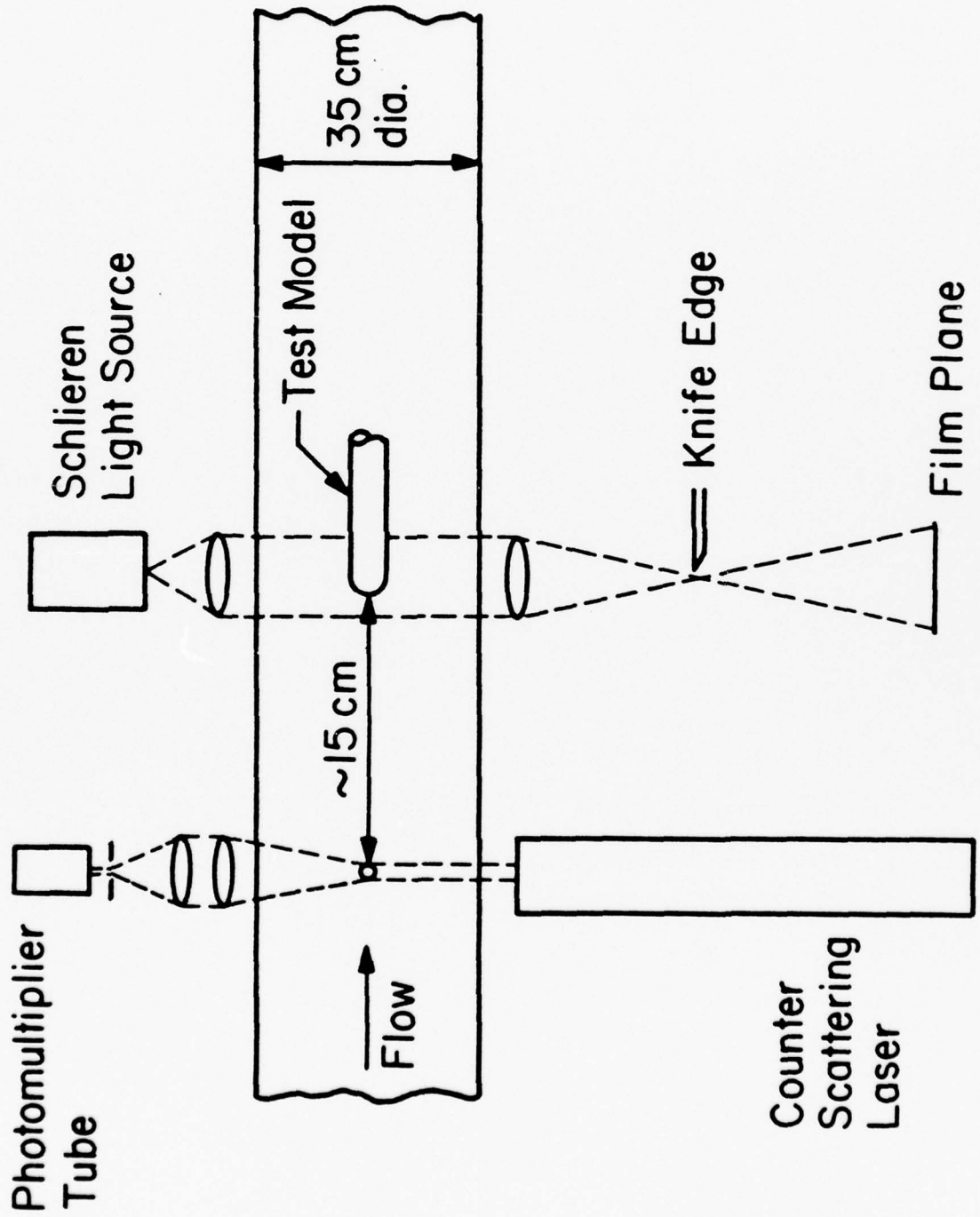


Fig. 15

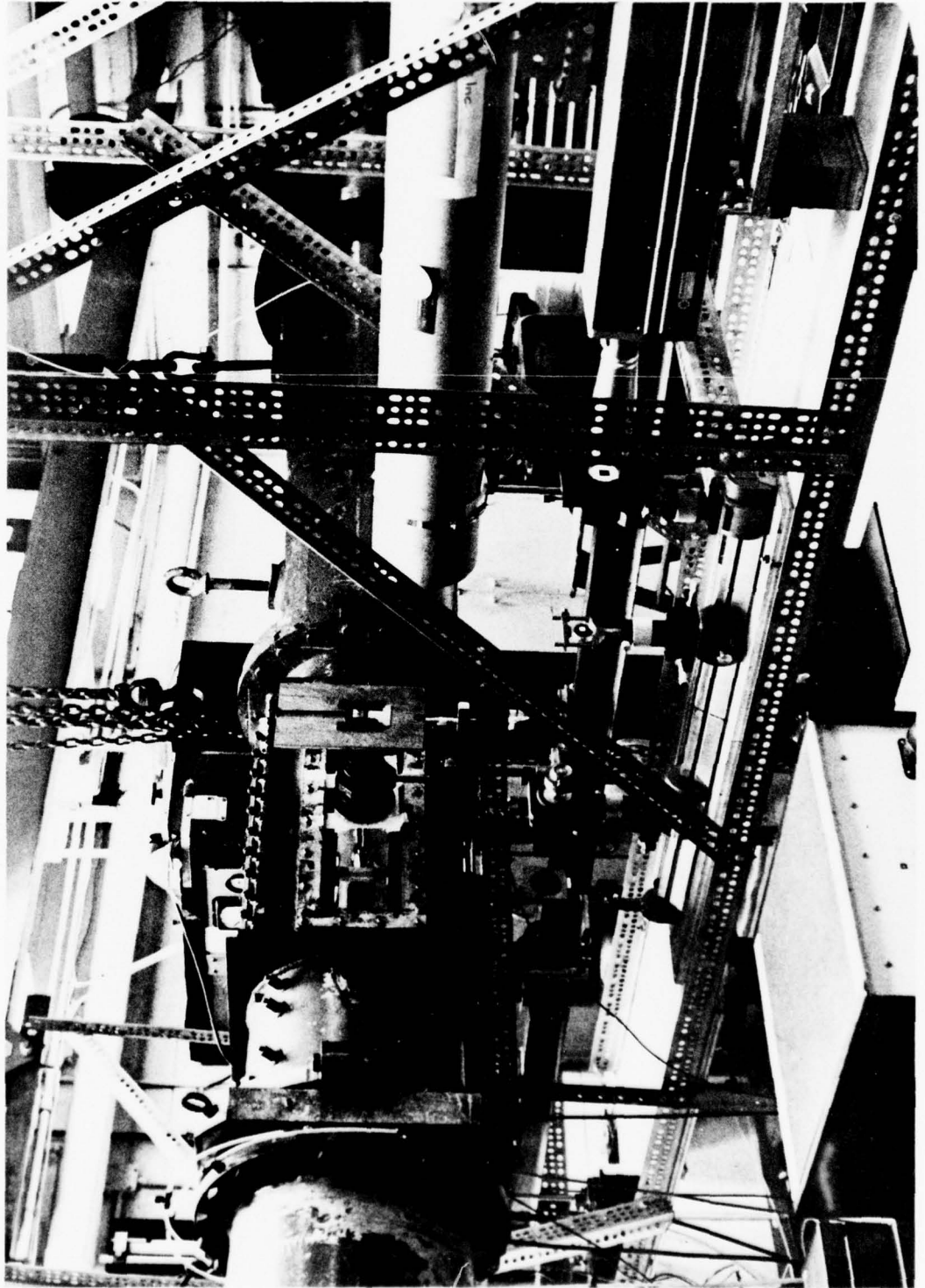
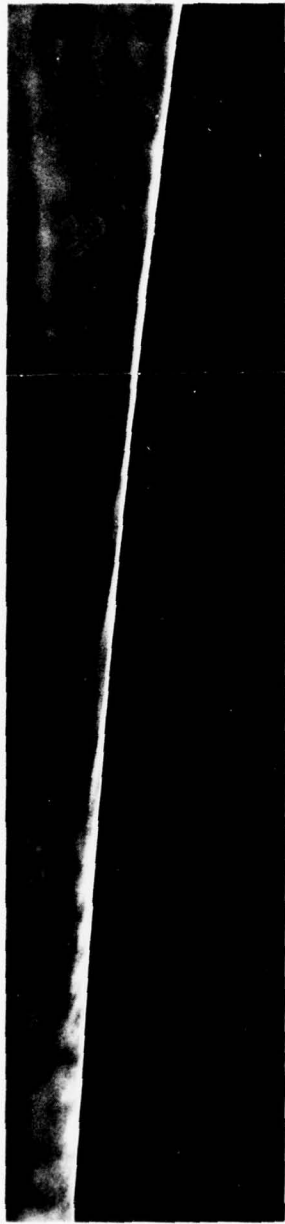


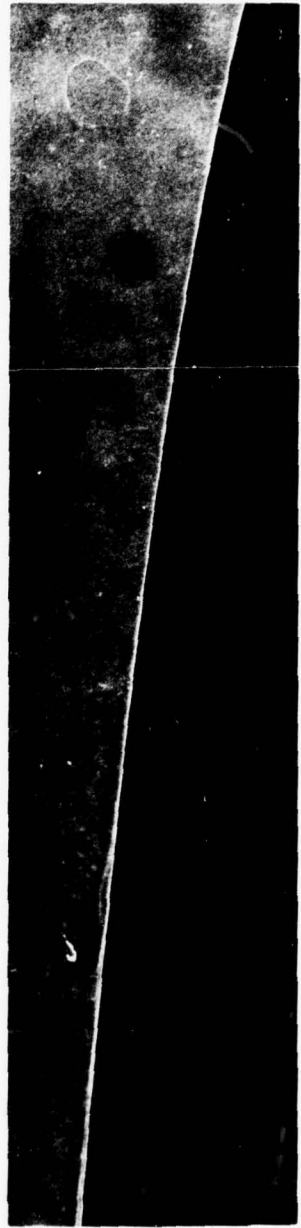
Fig. 16



(a)



(b)



(c)

Fig. 17

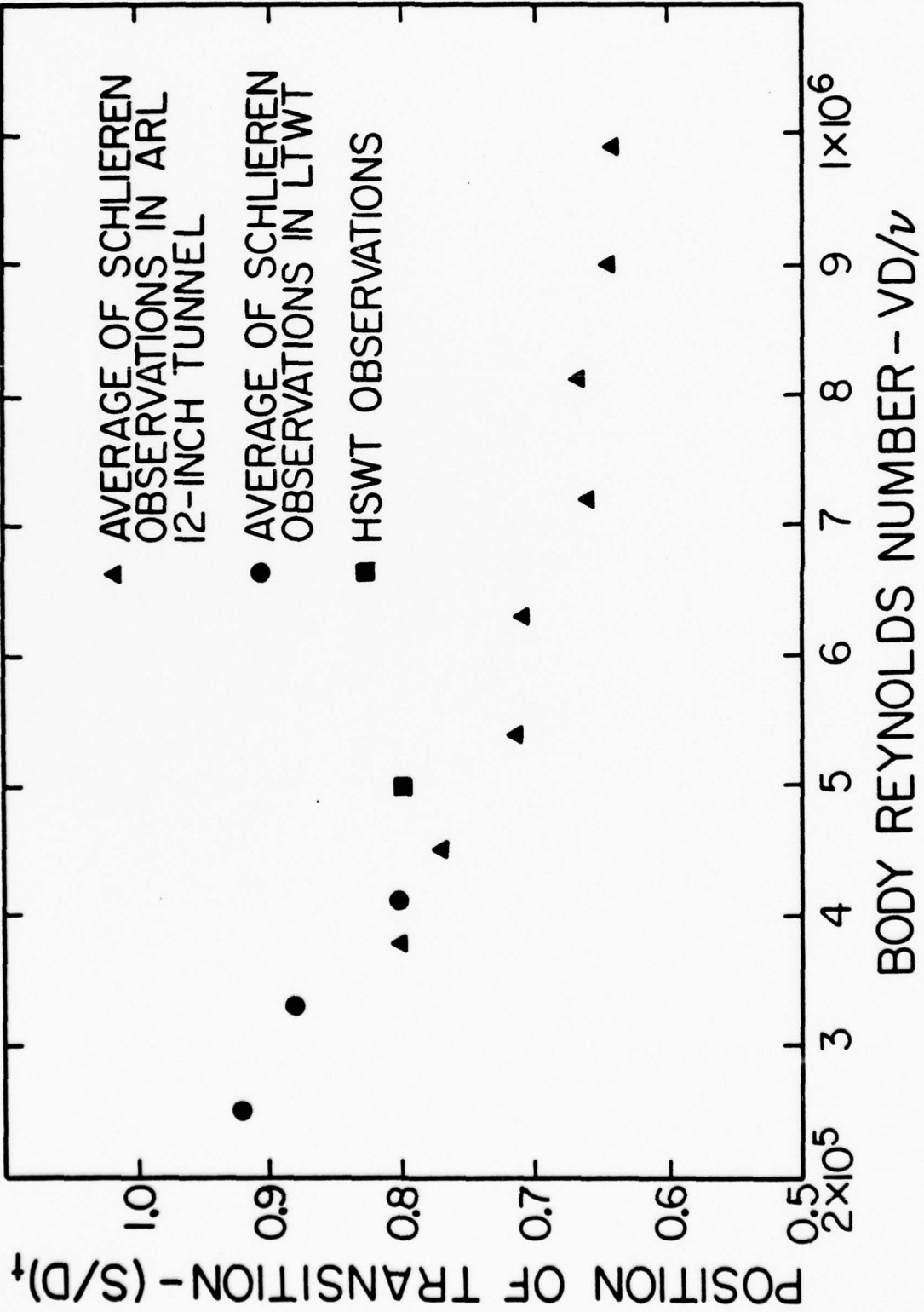


Fig. 18

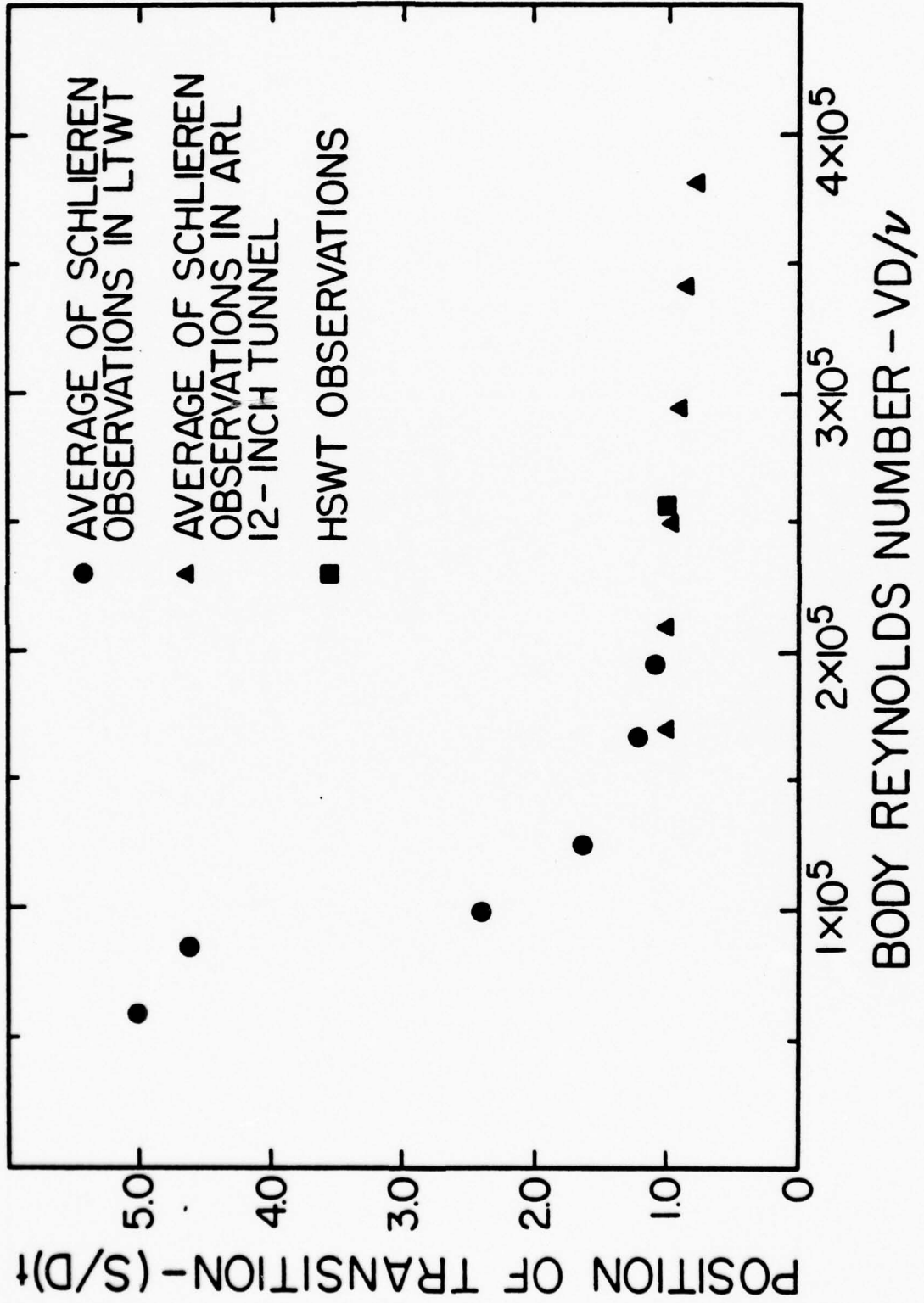


Fig. 19



(c)



(b)



(a)



(e)



(d)

Fig. 20

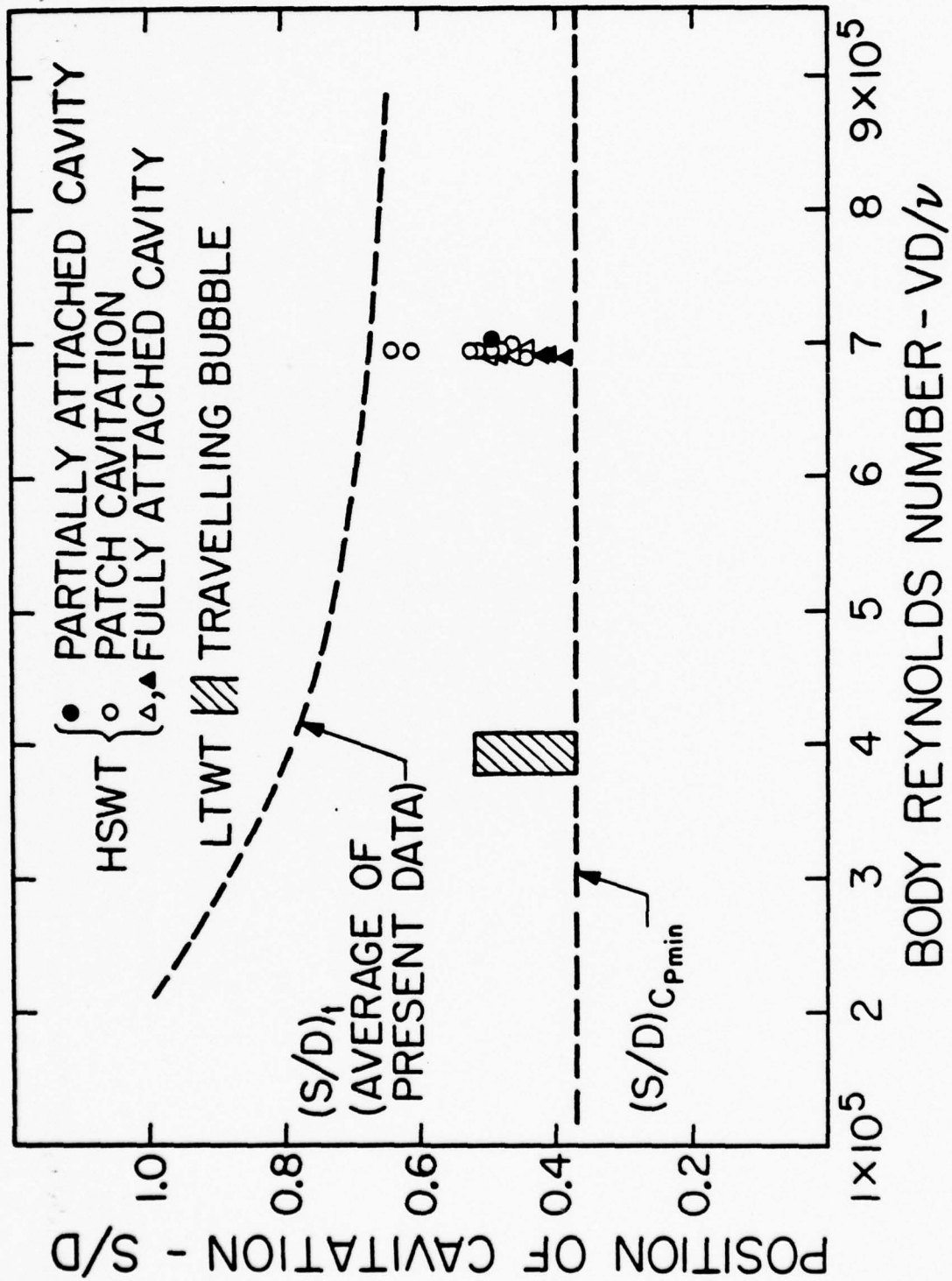


Fig. 21

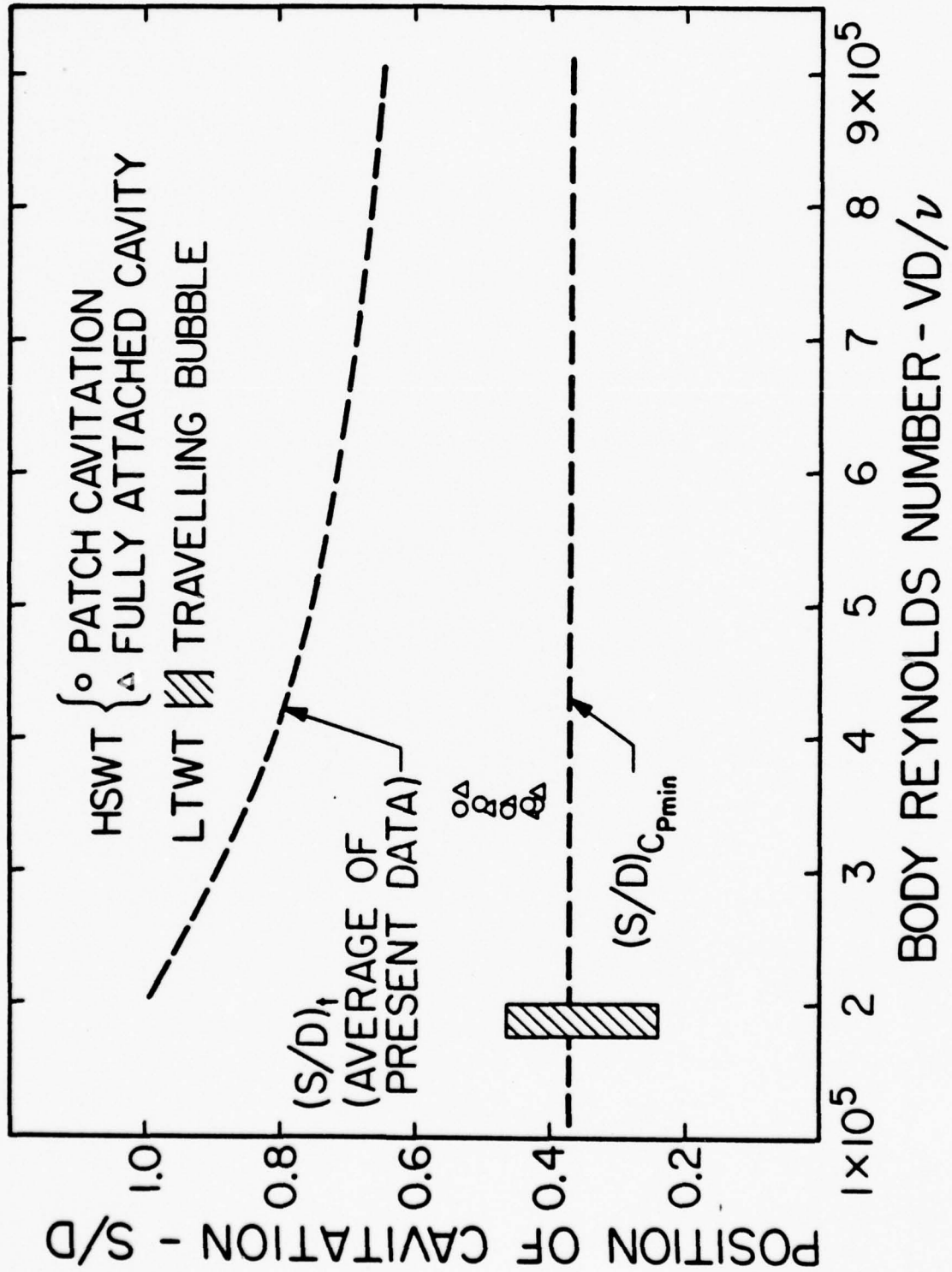


Fig. 22

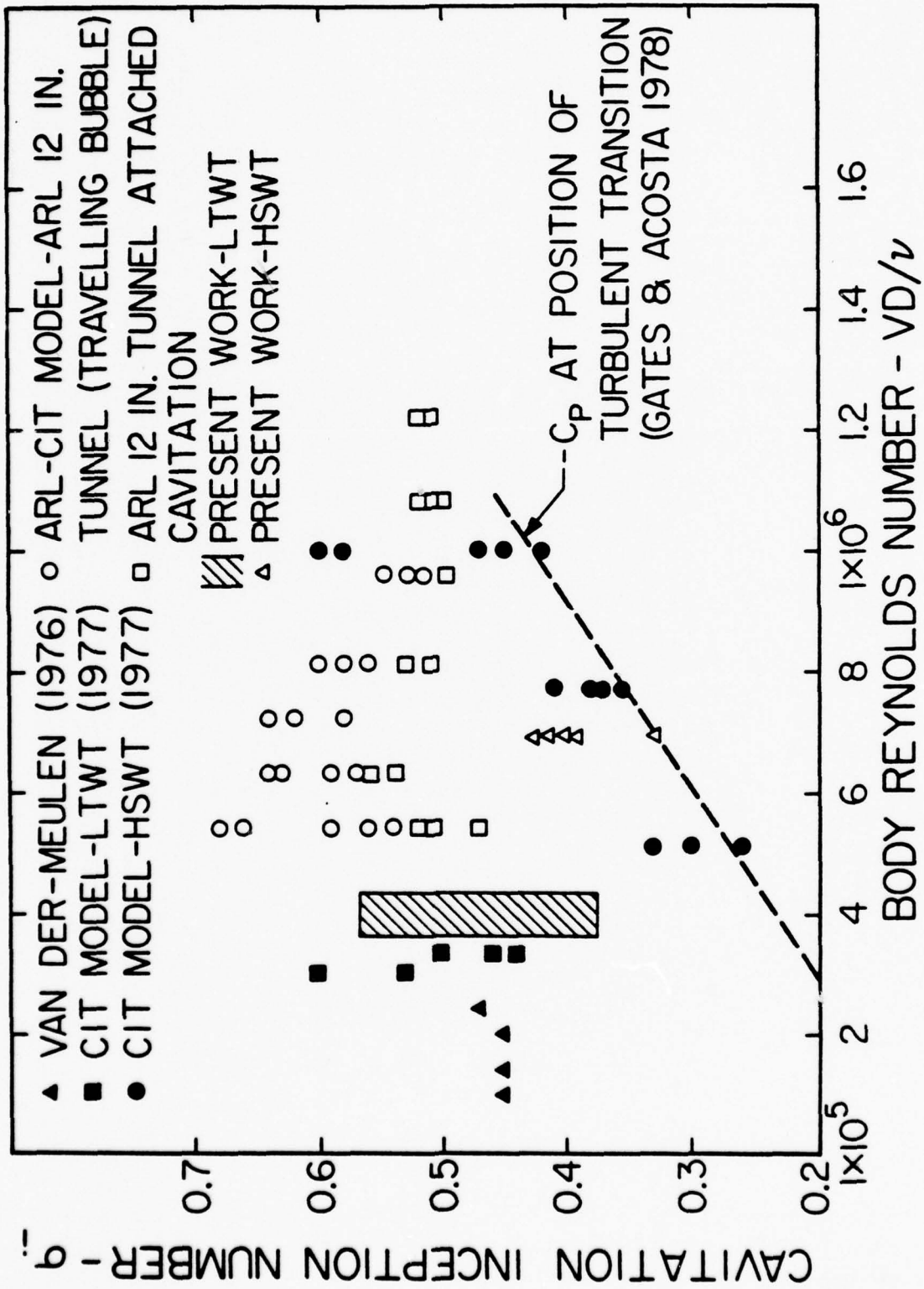


Fig. 23

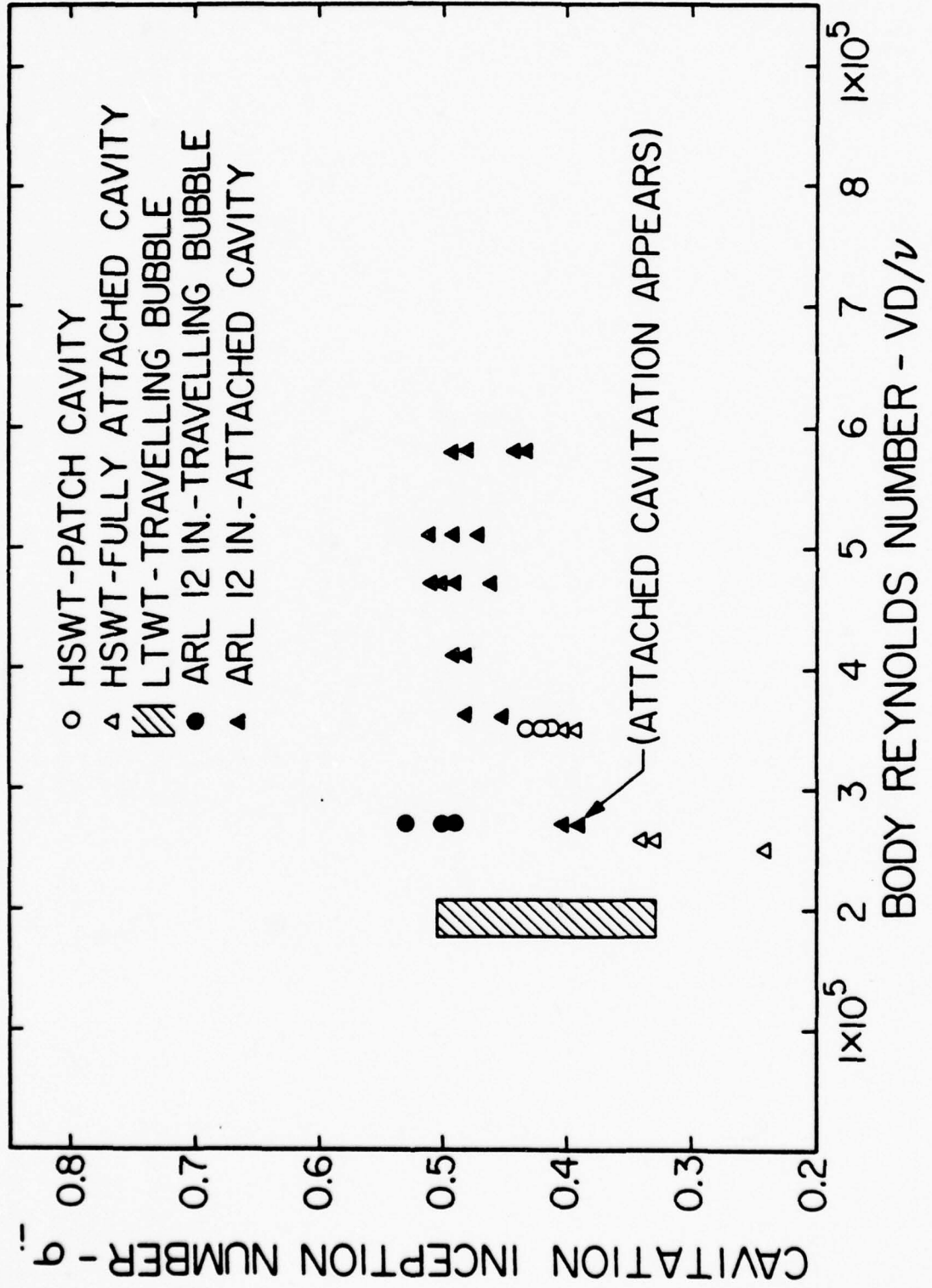
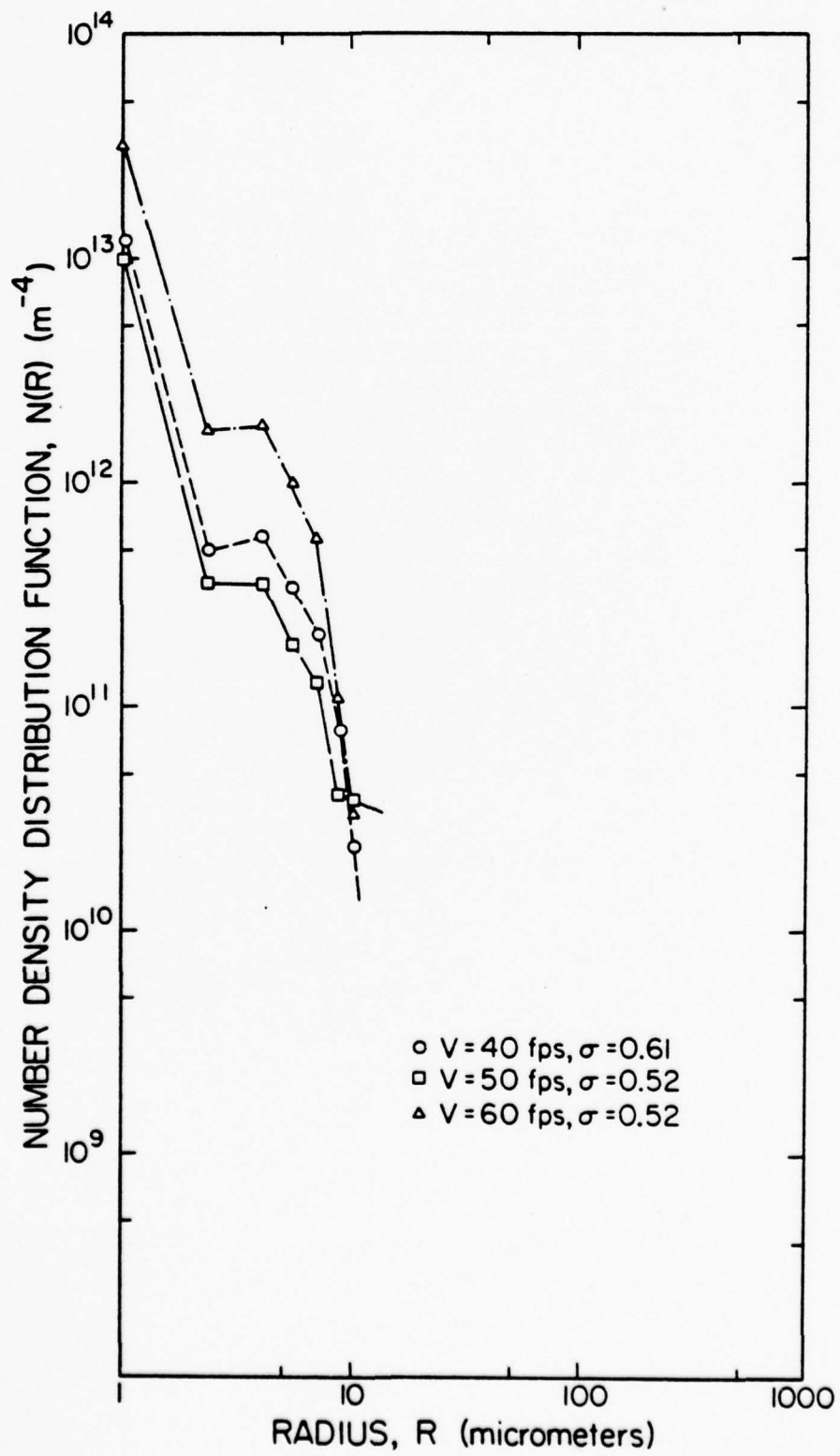


Fig. 24



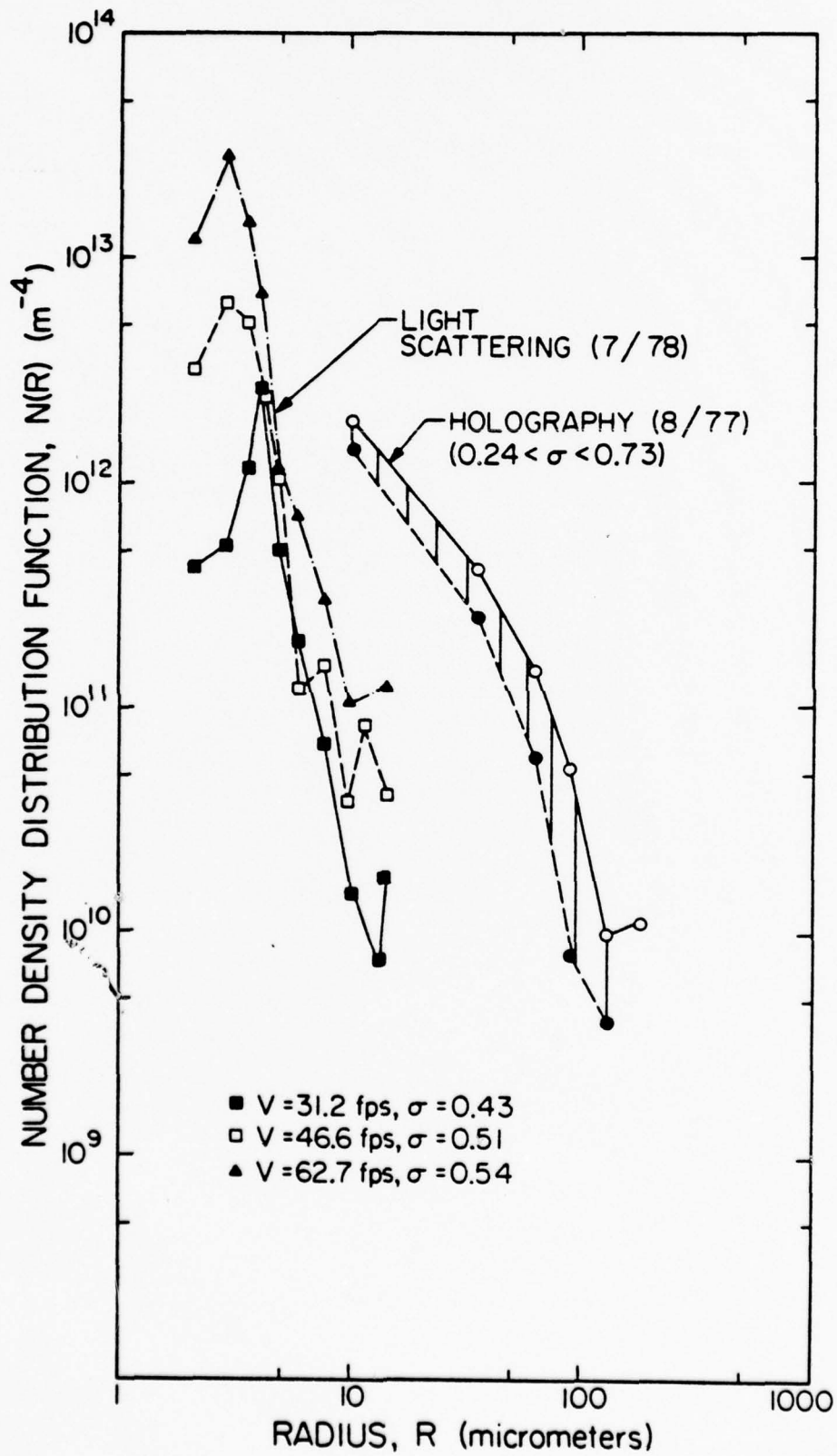


FIG. 26

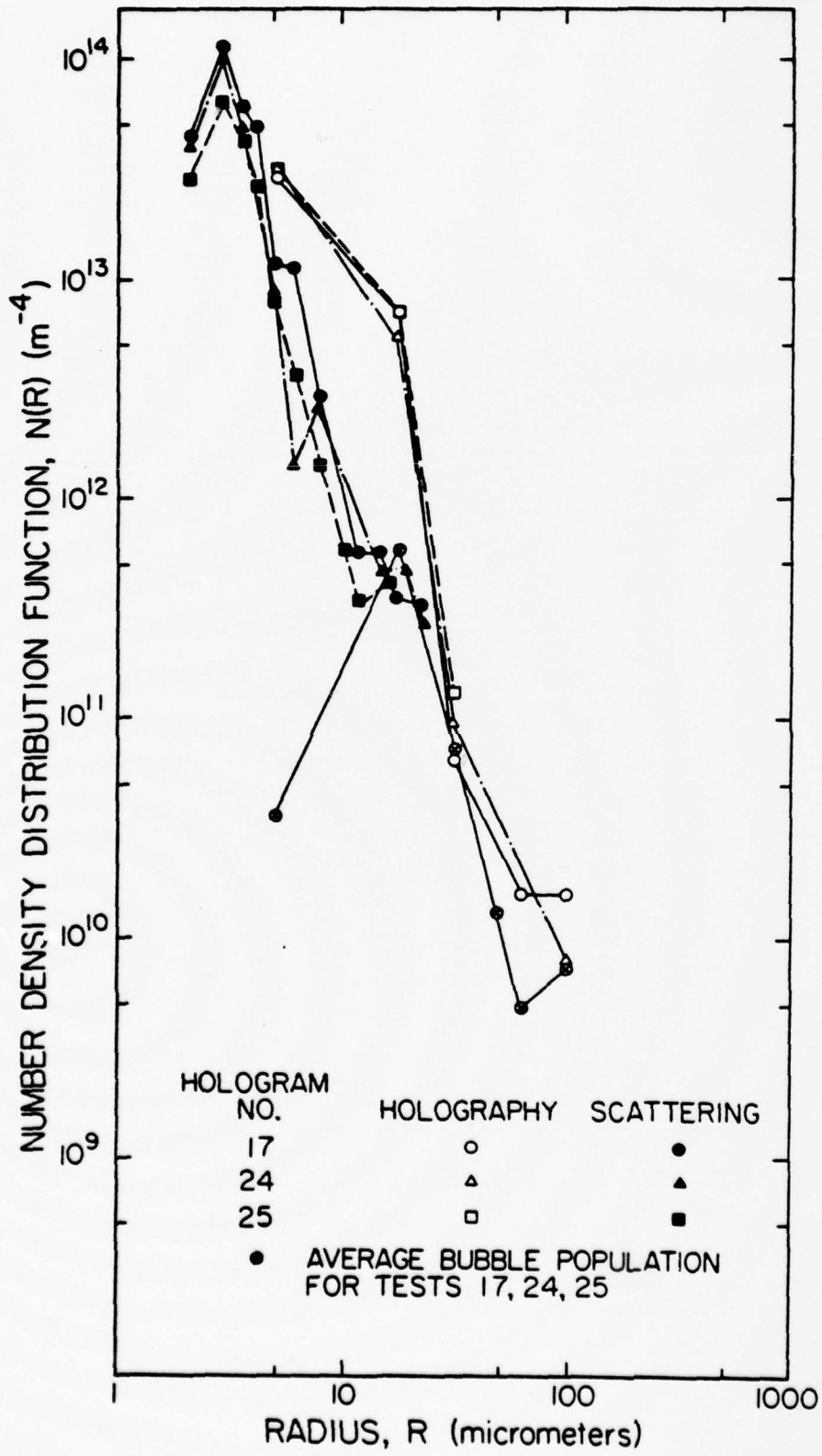


FIG. 27

APPENDIX I

COORDINATES OF THE SCHIEBE MODELS

The original non-dimensional coordinates for the $-C_{p_{min}} = 0.75$ Schiebe model were obtained from a report by Schiebe (1972). The number of coordinates was increased by using a spline routine. These coordinates were then substituted into a Douglas Neumann program to determine the pressure distribution. In the appendix we have summarized all this information by including a copy of the potential flow program output. The following symbols used in the program output will be of interest:

- x - coordinate measured along the axis of symmetry in inches.
- Y - coordinate measured perpendicular to the axis of symmetry in inches (i.e. local body radius)
- C_p - pressure coefficient,
- SUMDS - coordinate measured along the surface of the model from the stagnation point in inches.

Ignore all other outputs. The flow program output starts on Page 74.

APPENDIX II

CALIBRATION OF THE LIGHT SCATTERING NUCLEI COUNTER

The LSC is calibrated by injecting a solution containing polystyrene spheres of a known size into the sample volume of the counter. The intensity of the scattered light for each sphere diameter is recorded and a calibration of signal amplitude versus particle diameter is obtained. From this calibration then voltages corresponding to the desired ranges are determined and used to program the processor to size and sort detected particles into a series of 16 bins.

The calibration curve of signal amplitude versus particle size for the present LSC system is given in Fig. IIA and tabulated below are the present tests.

TABLE IIA
BIN SIZES FOR TESTS AT ARL*

<u>Channel</u>	<u>Particle Diameter (micrometers)</u>
1	1 - 3
2	3 - 6.5
3	6.5 - 10.0
4	10 - 12.5
5	12.5 - 16.0
6	16.0 - 19.0
7	19 - 21.5

* Information for channels 8 - 16 is not available. However since more than 95% of all particles were counted in the first 7 channels the loss of this information is not considered serious.

TABLE IIB

Bin Sizes for Tests at Caltech

<u>Channel</u>	<u>Particle Diameter (micrometers)</u>
1	- -
2	3.5 - 5.0
3	5.0 - 6.5
4	6.5 - 8.0
5	8.0 - 8.5
6	8.5 - 11
7	11 - 13
8	13 - 18
9	18 - 21.5
10	21.5 - 24.5
11	24.5 - 28
12	28 - 31
13	31 - 36
14	36 - 39
15	39 - 50
16	750

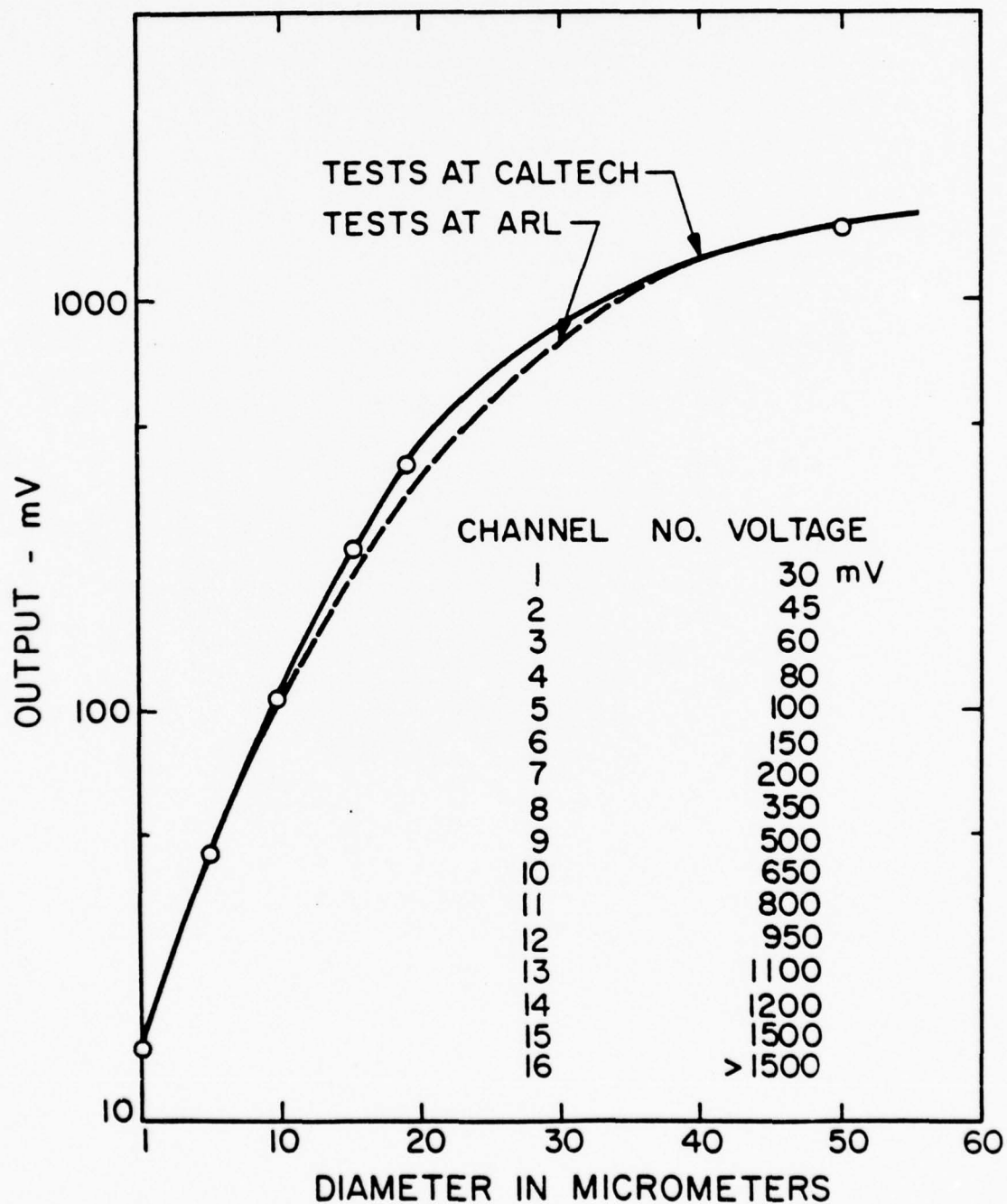


Fig II-A Calibration curve for the LSC showing output amplitude (voltage) versus particle diameter.

APPENDIX III

METHOD AND INSTRUMENTATION

Nuclei counting by holography consists of two processes. In the first one, a sample volume is illuminated by a collimated beam of coherent quasi-monochromatic light causing interference between the main coherent beam, and the light diffracted from the particles in the sample volume. The result is recorded on a high resolution film. In the second process, the photographic record is illuminated by another collimated beam of quasi-monochromatic light, producing a three dimensional image of the original volume. Using a TV vidicon and a monitor, it is possible to size and count the particle distribution.

Holocamera

The holocamera consists of a light source, a beam expander and a recording film. The coherent light source is a "Q Switched" pulsed ruby laser. A 3 inch long X 0.25 inch diameter ruby is excited by a helical Xenon Flashlamp, which is activated by discharging through it a 1000 Joule pulse in a period of 1.5 milliseconds. The ruby is located in an optical cavity created by 2 flat mirrors. The back mirror is 100% dielectric reflecting surface, while the front (output) one is a single layer Saphir Etalen (reflectivity - 60% in the red light wavelength) from which the output light is emitted.

When the lamp is flashed it excites the ruby rod, which then emits part of the energy absorbed by it. The emitted light oscillates in the cavity, bringing (together with the added energy from the flash lamp) the ruby to an increasingly "unstable state". When the ruby reaches a certain critical state, it emits a giant pulse, part of which is emitted outside of the cavity through the front mirror. Since the duration of one light pulse

is approximately 50 nano-seconds, the same process repeats itself several times during a single flash of the Xenon lamp. Therefore, needing only one single pulse, it is necessary to "Q switch" the laser. The present system is switched by inserting in the cavity a coated surface quartz bottle containing acetone and cryptocyanine. The material in the bottle absorbs part of the light oscillating in the cavity and thus reduces the gain due to these oscillations to a level where only one light pulse is emitted during the operation of the lamp.

The output light passes through a "beam splitter" in which part of the beam is transferred to a pin diode. The diode signal is then displayed on an oscilloscope. The rest of the beam (0.6943 micrometer wavelength) enters a beam expander-spatial filter (10 micrometer pin hole) and after being collimated it passes through the water tunnel to the recording film (Agfa-Gaevert 10E-75) located on the opposite side of the test section.

Reconstructing System

The reconstructing system uses a Spectra Physics 5 mw Helium Neon Laser as the illumination source. The beam is again expanded, passes through a spatial filter (pin hole) and is collimated by a collimating lens. The collimated beam (2.5 inch diameter) passes through the hologram, and creates a three dimensional image of the original sample volume. By positioning a microscope objective in the field of the reconstructed hologram the image is magnified and focused onto a silicon vidicon. The image is then displayed on a TV monitor. By changing the distance between the objective and the vidicon, one can control the magnification of the nuclei-image shown on the monitor. The hologram itself is mounted on a x-y-z Vernier carriage, making it possible (with the help of scales in all three dimensions) to count the particles in any desired volume.

By careful direct observation of the monitor screen, on which a calibrated reticle is placed, one can count the number and size the particles and bubbles recorded on the hologram. The magnification used is 220X. This magnification makes it possible to observe 10 μ particles, but the background noise of the system prevents sizing of smaller ones. Higher magnification is impossible due to significant decrease in resolution when the hologram is further magnified.

Since the accuracy of the result depends also on the quality of the hologram and the personal judgment of the one who counts the particles, several holograms were read by different people at different occasions. Since the results were almost equal, it seems that "human error" plays a minor role.

The volume studied is 2.5 cm X 1 cm X 1 cm starting 4 inches from the tunnel window. Since the TV screen covers an area of 1mm² at a time, it is necessary to observe 100 different squares, continuously varying the depth of each until the entire volume is covered.

By applying this technique it is possible to distinguish between a bubble and a solid particle. While the particle has got an arbitrary shape, the cross section of a bubble is circular (or at least almost circular). Therefore, distinction is possible only when the image is large enough to observe its shape — in the present magnification, when the size of the bubble/particle is above 20 micrometers.

Results

The holograms counted were obtained during experiments in the LTWT and HSWT at Caltech. The number of particles and bubbles, found on each hologram is presented in Tables II, V, VI and an approximated number density distribution function:

$$N\left(\frac{R_1+R_2}{2}\right) = \frac{\text{Number of nuclei within radii between } R_1 \text{ and } R_2 \text{ per unit volume}}{R_2 - R_1}$$

for each hologram is presented in Figs. 26 and 27.

The results are divided into two groups. The first one refers to the total number of solid particles and bubbles, and the second one refers only to bubbles. As noted before it is impossible to distinguish between bubbles and particles when their size is less than 20μ , therefore all nuclei found in that region are categorized as particles.

DOUGLAS AIRCRAFT COMPANY
LONG BEACH DIVISION

PROGRAM 500 -- AXISYMMETRIC AND CROSSFLOW

***** CASE CONTROL DATA *****

SHIELD BODY - 1.0145 INCH - - WITH WALLS CASE NO. 1

NGULIES = 2
NNU = 0
CHURU = 0.0
MACH NO. = 0.0
TCNST = 0.0

SURFACE OF REVOLUTION
OFF-BODY POINTS
UNIT CROSSFLOW UNIFORM FLOW SOLUTION

Douglas Aircraft Company
Long Beach Division

SCHEDULE BODY - 1.0125 INCH - WITH WALLS

IN = 102 MX = 0.0 MY = 0.0
 THETA = 0.0 ADDX = 0.0 ADDY = 0.0
 AE = 0.0 YL = 0.0

ON-BODY COORDINATE (UNTRANSFORMED)

BODY NO.	X	Y	SIN A	COS A	DELTA S	SUMDS	D ALPHA
1	0.0	0.0	1.0000000	0.0	0.0036400	0.0036400	0.0
2	0.0	0.0010200	1.0000000	0.0	0.0036400	0.0036400	0.0
3	0.0	0.0034500	1.0000000	0.0	0.0036400	0.0036400	0.0
4	0.0	0.0077000	1.0000000	0.0	0.0036400	0.0036400	0.0
5	0.0	0.0099500	1.0000000	0.0	0.0036400	0.0036400	0.0
6	0.0	0.0107200	1.0000000	0.0	0.0036400	0.0036400	0.0
7	0.0	0.0127000	1.0000000	0.0	0.0036400	0.0036400	0.0
8	0.0	0.0143000	1.0000000	0.0	0.0036400	0.0036400	0.0
9	0.0	0.0163750	1.0000000	0.0	0.0036400	0.0036400	0.0
10	0.0	0.0181900	0.9999858	0.0053704	0.0093101	0.0275001	-0.3077409
11	0.0004500	0.0229450	0.9999201	0.0139982	0.0100098	0.0375011	-0.4983063
12	0.0005000	0.0270000	0.9997992	0.0346521	0.0126976	0.0752072	-0.6411884
13	0.0006000	0.0320000	0.9993026	0.0734203	0.0123156	0.0875259	-0.4122153
14	0.0007000	0.0375000	0.9990683	0.0431558	0.0120170	0.1000375	-0.2703548
15	0.0008000	0.0420000	0.9988113	0.0487420	0.0125148	0.1125523	-0.1541422
16	0.0009000	0.0470000	0.9983026	0.0582473	0.0139671	0.1245192	-0.3336410
17	0.0010000	0.0520000	0.9979572	0.0636871	0.0099785	0.1375972	-0.3239148
18	0.0011000	0.0570000	0.9976013	0.0692214	0.0093235	0.1474219	-0.3062656
19	0.0012000	0.0620000	0.9969089	0.0785718	0.0162906	0.1637117	-0.5300226
20	0.0013000	0.0670000	0.9961381	0.0877919	0.0115043	0.1752160	-0.4460675
21	0.0014000	0.0720000	0.9954236	0.0955685	0.0125745	0.1877734	-0.5438567
22	0.0015000	0.0770000	0.9943709	0.1048028	0.0125755	0.2003441	-0.5465416
23	0.0016000	0.0820000	0.9932473	0.1160115	0.0125846	0.2129297	-0.6766257
24	0.0017000	0.0870000	0.9918083	0.1277324	0.0106475	0.2235761	-0.7523000

24	0.0137000	0.2307996	0.98997688	0.14122933	0.01455620	0.23016246	-0.97130746
	0.0147000	0.2370001	0.93744065	0.15799063	0.01265018	0.25042141	-1.07632633
25	0.0167000	0.2500000	0.98423684	0.17045544	0.01300498	0.26382637	-1.30360058
	0.0179000	0.2569999	0.97995800	0.17920433	0.01244551	0.27027587	-2.05102348
26	0.0200000	0.2639998	0.97220099	0.23414893	0.01637065	0.29284050	-2.22494698
	0.0230000	0.28305495	0.96237755	0.27171636	0.00923757	0.30204403	-2.72332973
27	0.0254000	0.29110998	0.94810343	0.21790235	0.01210036	0.31419235	-4.94161415
	0.0284000	0.3030001	0.91719013	0.23845043	0.01596183	0.33015416	-7.06552887
28	0.0310000	0.3149999	0.86121351	0.50824750	0.01249401	0.34264815	-6.7187130
	0.0340000	0.3300001	0.79516888	0.60638791	0.01040034	0.35313648	-4.84374037
29	0.0370000	0.3410000	0.74113137	0.67136002	0.00844959	0.35550606	-3.35695397
	0.0400000	0.34701000	0.70077121	0.71338906	0.00713499	0.36672103	-3.11137989
30	0.0430000	0.3520002	0.65813166	0.75290293	0.00759726	0.37431824	-3.02819394
	0.0460000	0.3550001	0.61743817	0.78001901	0.00809796	0.38291619	-2.74562767
31	0.0490000	0.3600000	0.57904673	0.81529444	0.00863487	0.39105105	-2.58811187
	0.0520000	0.3650000	0.54163063	0.84501676	0.00723137	0.40028238	-2.27002621
32	0.0550000	0.3700000	0.50790936	0.88141038	0.00934427	0.41012063	-2.14363556
	0.0580000	0.3750000	0.47472173	0.89013607	0.01053148	0.420665907	-2.04867363
33	0.0610000	0.3800000	0.44295460	0.89694404	0.01127813	0.43194087	-1.84857273
	0.0640000	0.3850000	0.41380328	0.91036624	0.01208302	0.44402987	-1.77314091
34	0.0670000	0.3900000	0.38543642	0.92273439	0.01297230	0.45700216	-1.21134839
	0.0700000	0.3950000	0.36583352	0.93068003	0.00885570	0.46383594	-0.64153390
35	0.0730000	0.4010000	0.35212517	0.93595308	0.00709974	0.47093952	-0.79310322
	0.0760000	0.4060000	0.33913457	0.94073790	0.00737187	0.47330737	-0.72531140
36	0.0790000	0.4120000	0.32719910	0.94495583	0.00764060	0.48594797	-0.75512171
	0.0820000	0.4170000	0.31471694	0.94918573	0.00794304	0.49369160	-0.72059147
37	0.0850000	0.4230000	0.30275500	0.95306873	0.00825749	0.50214905	-0.72619247
	0.0880000	0.4280000	0.29065138	0.95682895	0.00860136	0.51075035	-0.68793660
38	0.0910000	0.4340000	0.27914220	0.96024906	0.00895103	0.51970631	-0.65197503
	0.0940000	0.4400000	0.26819754	0.96336401	0.00932148	0.52902770	-0.60553723
39	0.0970000	0.4460000	0.2580000	0.9660000	0.00970000	0.5380000	
40	0.1000000	0.4520000	0.2480000	0.9680000	0.0100000	0.5470000	
41	0.1030000	0.4580000	0.2380000	0.9700000	0.0103000	0.5560000	
42	0.1060000	0.4640000	0.2280000	0.9720000	0.0106000	0.5650000	
43	0.1090000	0.4700000	0.2180000	0.9740000	0.0109000	0.5740000	
44	0.1120000	0.4760000	0.2080000	0.9760000	0.0112000	0.5830000	
45	0.1150000	0.4820000	0.1980000	0.9780000	0.0115000	0.5920000	
46	0.1180000	0.4880000	0.1880000	0.9800000	0.0118000	0.6010000	
47	0.1210000	0.4940000	0.1780000	0.9820000	0.0121000	0.6100000	
48	0.1240000	0.5000000	0.1680000	0.9840000	0.0124000	0.6190000	
49	0.1270000	0.5060000	0.1580000	0.9860000	0.0127000	0.6280000	
50	0.1300000	0.5120000	0.1480000	0.9880000	0.0130000	0.6370000	
51	0.1330000	0.5180000	0.1380000	0.9900000	0.0133000	0.6460000	
52	0.1360000	0.5240000	0.1280000	0.9920000	0.0136000	0.6550000	
53	0.1390000	0.5300000	0.1180000	0.9940000	0.0139000	0.6640000	
54	0.1420000	0.5360000	0.1080000	0.9960000	0.0142000	0.6730000	
55	0.1450000	0.5420000	0.0980000	0.9980000	0.0145000	0.6820000	
56	0.1480000	0.5480000	0.0880000	0.9990000	0.0148000	0.6910000	
57	0.1510000	0.5540000	0.0780000	1.0000000	0.0151000	0.7000000	
58	0.1540000	0.5600000	0.0680000	1.0000000	0.0154000	0.7090000	
59	0.1570000	0.5660000	0.0580000	1.0000000	0.0157000	0.7180000	
60	0.1600000	0.5720000	0.0480000	1.0000000	0.0160000	0.7270000	
61	0.1630000	0.5780000	0.0380000	1.0000000	0.0163000	0.7360000	
62	0.1660000	0.5840000	0.0280000	1.0000000	0.0166000	0.7450000	
63	0.1690000	0.5900000	0.0180000	1.0000000	0.0169000	0.7540000	
64	0.1720000	0.5960000	0.0080000	1.0000000	0.0172000	0.7630000	
65	0.1750000	0.6020000	0.0000000	1.0000000	0.0175000	0.7720000	
66	0.1780000	0.6080000	0.0000000	1.0000000	0.0178000	0.7810000	
67	0.1810000	0.6140000	0.0000000	1.0000000	0.0181000	0.7900000	
68	0.1840000	0.6200000	0.0000000	1.0000000	0.0184000	0.7990000	
69	0.1870000	0.6260000	0.0000000	1.0000000	0.0187000	0.8080000	
70	0.1900000	0.6320000	0.0000000	1.0000000	0.0190000	0.8170000	
71	0.1930000	0.6380000	0.0000000	1.0000000	0.0193000	0.8260000	
72	0.1960000	0.6440000	0.0000000	1.0000000	0.0196000	0.8350000	
73	0.1990000	0.6500000	0.0000000	1.0000000	0.0199000	0.8440000	
74	0.2020000	0.6560000	0.0000000	1.0000000	0.0202000	0.8530000	
75	0.2050000	0.6620000	0.0000000	1.0000000	0.0205000	0.8620000	
76	0.2080000	0.6680000	0.0000000	1.0000000	0.0208000	0.8710000	
77	0.2110000	0.6740000	0.0000000	1.0000000	0.0211000	0.8800000	
78	0.2140000	0.6800000	0.0000000	1.0000000	0.0214000	0.8890000	
79	0.2170000	0.6860000	0.0000000	1.0000000	0.0217000	0.8980000	
80	0.2200000	0.6920000	0.0000000	1.0000000	0.0220000	0.9070000	
81	0.2230000	0.6980000	0.0000000	1.0000000	0.0223000	0.9160000	
82	0.2260000	0.7040000	0.0000000	1.0000000	0.0226000	0.9250000	
83	0.2290000	0.7100000	0.0000000	1.0000000	0.0229000	0.9340000	
84	0.2320000	0.7160000	0.0000000	1.0000000	0.0232000	0.9430000	
85	0.2350000	0.7220000	0.0000000	1.0000000	0.0235000	0.9520000	
86	0.2380000	0.7280000	0.0000000	1.0000000	0.0238000	0.9610000	
87	0.2410000	0.7340000	0.0000000	1.0000000	0.0241000	0.9700000	
88	0.2440000	0.7400000	0.0000000	1.0000000	0.0244000	0.9790000	
89	0.2470000	0.7460000	0.0000000	1.0000000	0.0247000	0.9880000	
90	0.2500000	0.7520000	0.0000000	1.0000000	0.0250000	0.9970000	
91	0.2530000	0.7580000	0.0000000	1.0000000	0.0253000	1.0060000	
92	0.2560000	0.7640000	0.0000000	1.0000000	0.0256000	1.0150000	
93	0.2590000	0.7700000	0.0000000	1.0000000	0.0259000	1.0240000	
94	0.2620000	0.7760000	0.0000000	1.0000000	0.0262000	1.0330000	
95	0.2650000	0.7820000	0.0000000	1.0000000	0.0265000	1.0420000	
96	0.2680000	0.7880000	0.0000000	1.0000000	0.0268000	1.0510000	
97	0.2710000	0.7940000	0.0000000	1.0000000	0.0271000	1.0600000	
98	0.2740000	0.8000000	0.0000000	1.0000000	0.0274000	1.0690000	
99	0.2770000	0.8060000	0.0000000	1.0000000	0.0277000	1.0780000	
100	0.2800000	0.8120000	0.0000000	1.0000000	0.0280000	1.0870000	

54	0.21109998	0.42374398	0.25702220	0.50640169	0.20872077	0.53875382	-0.21030956
	0.21579959	0.42500001	0.23571304	0.56902843	0.01013022	0.54866773	-0.65300067
55	0.22501997	0.42750001	0.23565257	0.57103740	0.01006083	0.55949052	-0.01520047
	0.23077500	0.43000001	0.22512237	0.57433025	0.01110503	0.57000152	-0.600943037
56	0.24135998	0.43124998	0.21474683	0.57666085	0.01104100	0.58224308	-0.59411371
	0.24075000	0.43200000	0.20446084	0.57884393	0.01221846	0.59496150	-0.50115660
57	0.25242997	0.43374997	0.19401858	0.58067907	0.01284502	0.60730708	-0.50487700
	0.25014000	0.43500000	0.10500268	0.98273796	0.01351330	0.62082034	-0.50115660
58	0.26040996	0.43624997	0.17530513	0.98451430	0.01426083	0.63508117	-0.50487700
	0.26000000	0.43700000	0.16612256	0.98610520	0.01504911	0.65013027	-0.50115660
59	0.27007997	0.43874997	0.15705313	0.98758972	0.01591755	0.66609781	-0.50487700
	0.27037994	0.43950000	0.14318514	0.98969591	0.02451578	0.70096755	-0.50115660
60	0.28267998	0.44100000	0.12561119	0.99207556	0.03940532	0.74077284	-0.50487700
	0.28293999	0.44174999	0.10868955	0.99407578	0.04006252	0.78677535	-0.50115660
61	0.29319999	0.44249999	0.09667021	0.99531645	0.02586109	0.81263644	-0.50487700
	0.29590001	0.44374999	0.08661989	0.99609562	0.02921101	0.84084743	-0.50115660
62	0.30290000	0.44449999	0.080069450	0.99673897	0.03098100	0.87182844	-0.50487700
	0.30290000	0.44524999	0.07324558	0.99731404	0.03413171	0.90590014	-0.50487700
63	0.31740001	0.44624999	0.06592381	0.99782479	0.03792250	0.94388258	-0.50487700
	0.31740001	0.44700000	0.05935257	0.99829508	0.04294297	0.98672551	-0.50487700
64	0.32700001	0.44774999	0.05104756	0.99869627	0.04697387	1.03560809	-0.50487700
	0.32700001	0.44850000	0.04441632	0.99901407	0.05628559	1.09198190	-0.50487700
65	0.33780001	0.44924999	0.03823929	0.99926972	0.06537771	1.15730103	-0.50487700
	0.33780001	0.45000000	0.03141122	0.99950641	0.07950931	1.23694992	-0.50487700
66	0.34750001	0.45074999	0.02496973	0.99968663	0.10012114	1.33707047	-0.50487700
	0.34750001	0.45149998	0.01946065	0.99981070	0.12846422	1.46553421	-0.50487700
67	0.35720001	0.45224999	0.01341601	0.99991012	0.24150157	1.70704506	-0.50487700
	0.35720001	0.45300000	0.00862190	0.99996227	0.20248795	1.90952301	-0.50487700
68	0.36700001	0.45374999	0.0	1.00000000	0.21776011	2.12730312	0.0
	0.36700001	0.45449999	0.0	1.00000000	0.25000000	2.37730312	0.0
69	0.37680001	0.45524999	0.0	1.00000000	0.25000000	2.37730312	0.0
	0.37680001	0.45600000	0.0	1.00000000	0.25000000	2.37730312	0.0
70	0.38660001	0.45674999	0.0	1.00000000	0.25000000	2.37730312	0.0
	0.38660001	0.45749999	0.0	1.00000000	0.25000000	2.37730312	0.0
71	0.39640001	0.45824999	0.0	1.00000000	0.25000000	2.37730312	0.0
	0.39640001	0.45900000	0.0	1.00000000	0.25000000	2.37730312	0.0
72	0.40620001	0.45974999	0.0	1.00000000	0.25000000	2.37730312	0.0
	0.40620001	0.46049999	0.0	1.00000000	0.25000000	2.37730312	0.0
73	0.41600001	0.46124999	0.0	1.00000000	0.25000000	2.37730312	0.0
	0.41600001	0.46200000	0.0	1.00000000	0.25000000	2.37730312	0.0
74	0.42580001	0.46274999	0.0	1.00000000	0.25000000	2.37730312	0.0
	0.42580001	0.46349999	0.0	1.00000000	0.25000000	2.37730312	0.0
75	0.43560001	0.46424999	0.0	1.00000000	0.25000000	2.37730312	0.0
	0.43560001	0.46500000	0.0	1.00000000	0.25000000	2.37730312	0.0
76	0.44540001	0.46574999	0.0	1.00000000	0.25000000	2.37730312	0.0
	0.44540001	0.46649999	0.0	1.00000000	0.25000000	2.37730312	0.0
77	0.45520001	0.46724999	0.0	1.00000000	0.25000000	2.37730312	0.0
	0.45520001	0.46800000	0.0	1.00000000	0.25000000	2.37730312	0.0
78	0.46500001	0.46874999	0.0	1.00000000	0.25000000	2.37730312	0.0
	0.46500001	0.46949999	0.0	1.00000000	0.25000000	2.37730312	0.0
79	0.47480001	0.47024999	0.0	1.00000000	0.25000000	2.37730312	0.0
	0.47480001	0.47100000	0.0	1.00000000	0.25000000	2.37730312	0.0
80	0.48460001	0.47174999	0.0	1.00000000	0.25000000	2.37730312	0.0
	0.48460001	0.47249999	0.0	1.00000000	0.25000000	2.37730312	0.0
81	0.49440001	0.47324999	0.0	1.00000000	0.25000000	2.37730312	0.0
	0.49440001	0.47400000	0.0	1.00000000	0.25000000	2.37730312	0.0
82	0.50420001	0.47474999	0.0	1.00000000	0.25000000	2.37730312	0.0
	0.50420001	0.47549999	0.0	1.00000000	0.25000000	2.37730312	0.0
83	0.51400001	0.47624999	0.0	1.00000000	0.25000000	2.37730312	0.0
	0.51400001	0.47700000	0.0	1.00000000	0.25000000	2.37730312	0.0

84	4.999981	0.50000000	0.0	1.00000000	0.30000013	2.67730230	0.0
	4.999999	0.50000000	0.0	1.00000000	0.34999943	3.02730179	0.0
85	4.999992	0.50000000	0.0	1.00000000	0.40000057	3.42730236	0.0
	4.999999	0.50000000	0.0	1.00000000	0.39999962	3.82730198	0.0
86	4.999999	0.50000000	0.0	1.00000000	0.50000000	4.32730198	0.0
	4.999999	0.50000000	0.0	1.00000000	0.50000000	4.82730198	0.0
87	4.999999	0.50000000	0.0	1.00000000	0.50000000	5.32730198	14.03617764
	4.999999	0.50000000	0.24253452	0.97014278	0.05153909	5.37884049	0.0
88	4.999999	0.50000000	0.24253452	0.97014278	0.05153909	5.43037891	0.00032102
	4.999999	0.50000000	0.24253452	0.97014278	0.05153909	5.48191643	0.0
89	4.999999	0.50000000	0.24253452	0.97014278	0.05153909	5.53345385	0.00010587
	4.999999	0.50000000	0.24253452	0.97014278	0.05153909	5.58499132	-0.00004440
90	4.999999	0.50000000	0.24253452	0.97014278	0.05153909	5.63652879	0.0
	4.999999	0.50000000	0.24253452	0.97014278	0.05153909	5.68806626	0.0
91	4.999999	0.50000000	0.24253452	0.97014278	0.05153909	5.73960373	0.0
	4.999999	0.50000000	0.24253452	0.97014278	0.05153909	5.79114120	0.0
92	4.999999	0.50000000	0.24253452	0.97014278	0.05153909	5.84267867	0.0
	4.999999	0.50000000	0.24253452	0.97014278	0.05153909	5.89421614	0.0
93	4.999999	0.50000000	0.24253452	0.97014278	0.05153909	5.94575361	0.0
	4.999999	0.50000000	0.24253452	0.97014278	0.05153909	6.00000000	0.0
94	4.999999	0.50000000	0.24253452	0.97014278	0.05153909	6.05424647	0.0
	4.999999	0.50000000	0.24253452	0.97014278	0.05153909	6.10849294	0.0
95	4.999999	0.50000000	0.24253452	0.97014278	0.05153909	6.16273941	0.0
	4.999999	0.50000000	0.24253452	0.97014278	0.05153909	6.21698588	0.0
96	4.999999	0.50000000	0.24253452	0.97014278	0.05153909	6.27123235	0.0
	4.999999	0.50000000	0.24253452	0.97014278	0.05153909	6.32547882	0.0
97	4.999999	0.50000000	0.24253452	0.97014278	0.05153909	6.37972529	0.0
	4.999999	0.50000000	0.24253452	0.97014278	0.05153909	6.43397176	0.0
98	4.999999	0.50000000	0.24253452	0.97014278	0.05153909	6.48821823	0.0
	4.999999	0.50000000	0.24253452	0.97014278	0.05153909	6.54246470	0.0
99	4.999999	0.50000000	0.24253452	0.97014278	0.05153909	6.59671117	0.0
	4.999999	0.50000000	0.24253452	0.97014278	0.05153909	6.65095764	0.0
100	4.999999	0.50000000	0.24253452	0.97014278	0.05153909	6.70520411	0.0
	4.999999	0.50000000	0.24253452	0.97014278	0.05153909	6.75945058	0.0
101	4.999999	0.50000000	0.24253452	0.97014278	0.05153909	6.81369705	0.0
	4.999999	0.50000000	0.24253452	0.97014278	0.05153909	6.86794352	0.0
102	4.999999	0.50000000	0.24253452	0.97014278	0.05153909	6.92219000	0.0
	4.999999	0.50000000	0.24253452	0.97014278	0.05153909	6.97643647	0.0

DUUGLAS AIRCRAFT COMPANY
LONG BEACH DIVISION

SCHIEBE BODY - 1.0125 INCH - WITH WALLS

NN = 41 MX = 0.0 MY = 0.0
THETA = 0.0 ALDX = 0.0 ADCY = 0.0
XE = 3.0 YE = 0.0

ORIG BODY COORDINATES (UNTRANSFORMED)

BODY NO.	X	Y	SIN A	COS A	DELTA S	SUMMS	D ALPHA
1	20.00000000	6.00000000	0.0	-1.00000000	1.00000000	1.00000000	0.0
2	19.50000000	6.00000000	0.0	-1.00000000	1.00000000	2.00000000	0.0
3	19.00000000	6.00000000	0.0	-1.00000000	1.00000000	3.00000000	0.0
4	18.50000000	6.00000000	0.0	-1.00000000	1.00000000	4.00000000	0.0
5	18.00000000	6.00000000	0.0	-1.00000000	1.00000000	5.00000000	0.0
6	17.50000000	6.00000000	0.0	-1.00000000	1.00000000	6.00000000	0.0
7	17.00000000	6.00000000	0.0	-1.00000000	1.00000000	7.00000000	0.0
8	16.50000000	6.00000000	0.0	-1.00000000	1.00000000	8.00000000	0.0
9	16.00000000	6.00000000	0.0	-1.00000000	1.00000000	9.00000000	0.0
10	15.50000000	6.00000000	0.0	-1.00000000	1.00000000	10.00000000	0.0
11	15.00000000	6.00000000	0.0	-1.00000000	1.00000000	11.00000000	0.0
12	14.50000000	6.00000000	0.0	-1.00000000	1.00000000	12.00000000	0.0
13	14.00000000	6.00000000	0.0	-1.00000000	1.00000000	13.00000000	0.0
14	13.50000000	6.00000000	0.0	-1.00000000	1.00000000	14.00000000	0.0
15	13.00000000	6.00000000	0.0	-1.00000000	1.00000000	15.00000000	0.0
16	12.50000000	6.00000000	0.0	-1.00000000	1.00000000	16.00000000	0.0
17	12.00000000	6.00000000	0.0	-1.00000000	1.00000000	17.00000000	0.0
18	11.50000000	6.00000000	0.0	-1.00000000	1.00000000	18.00000000	0.0
19	11.00000000	6.00000000	0.0	-1.00000000	1.00000000	19.00000000	0.0
20	10.50000000	6.00000000	0.0	-1.00000000	1.00000000	20.00000000	0.0
21	10.00000000	6.00000000	0.0	-1.00000000	1.00000000	21.00000000	0.0
22	9.50000000	6.00000000	0.0	-1.00000000	1.00000000	22.00000000	0.0
23	9.00000000	6.00000000	0.0	-1.00000000	1.00000000	23.00000000	0.0
24	8.50000000	6.00000000	0.0	-1.00000000	1.00000000	24.00000000	0.0

26	6.00000000	0.0	-1.00000000	1.00000000	23.00000000	0.0
27	6.00000000	0.0	-1.00000000	1.00000000	24.00000000	0.0
28	6.00000000	0.0	-1.00000000	1.00000000	25.00000000	0.0
29	6.00000000	0.0	-1.00000000	1.00000000	26.00000000	0.0
30	6.00000000	0.0	-1.00000000	1.00000000	27.00000000	0.0
31	6.00000000	0.0	-1.00000000	1.00000000	28.00000000	0.0
32	6.00000000	0.0	-1.00000000	1.00000000	29.00000000	0.0
33	6.00000000	0.0	-1.00000000	1.00000000	30.00000000	0.0
34	6.00000000	0.0	-1.00000000	1.00000000	31.00000000	0.0
35	6.00000000	0.0	-1.00000000	1.00000000	32.00000000	0.0
36	6.00000000	0.0	-1.00000000	1.00000000	33.00000000	0.0
37	6.00000000	0.0	-1.00000000	1.00000000	34.00000000	0.0
38	6.00000000	0.0	-1.00000000	1.00000000	35.00000000	0.0
39	6.00000000	0.0	-1.00000000	1.00000000	36.00000000	0.0
40	6.00000000	0.0	-1.00000000	1.00000000	37.00000000	0.0
41	6.00000000	0.0	-1.00000000	1.00000000	38.00000000	0.0
42	6.00000000	0.0	-1.00000000	1.00000000	39.00000000	0.0
43	6.00000000	0.0	-1.00000000	1.00000000	40.00000000	0.0

DOUGLAS AIRCRAFT COMPANY
LUNG BEACH DIVISION

SCHIEDE BODY - 1.0123 INCH - WITH WALLS

NN = 0
 THETA = 0.0
 AC = 0.0
 MX = 0.0
 ADX = 0.0
 YE = 0.0
 MY = 0.0
 ADY = 0.0

OFF-BODY COORDINATES (UNTRANSFORMED)

	X-UFF	Y-UFF
1	-1.00000000	0.0
2	-2.00000000	0.0
3	-3.00000000	0.0
4	-4.00000000	0.0
5	-5.00000000	0.0
6	-6.00000000	0.0

DUNLAP AIRCRAFT COMPANY
 LONG BEACH DIVISION

SCHIELE BODY - 1.0125 INCH - WITH MILLS CASE NO. 1

ON-BODY UNIFORM AXI-SYMMETRIC FLOW
 TRANSFORMED COORDINATES

	X	Y	PHI	TI	CP	SIN A	COS A	SIGMA	N
1	0.0	0.0	-0.79476649	0.00312422	0.99999228	1.00000	C.C.	-0.14276296	-0.00003844
2	0.0	0.00364000	-0.79474354	0.00934899	0.99991267	1.00000	C.C.	-0.14277765	-0.00004131
3	0.0	0.00728000	-0.79469788	0.01558086	0.99975729	1.00000	0.0	-0.14257681	-0.00003940
4	0.0	0.01092000	-0.79462886	0.02174437	0.99952722	1.00000	C.C.	-0.14235383	-0.00003940
5	0.0	0.01456000	-0.79453719	0.02706580	0.99926728	1.00000	C.C.	-0.14191985	-0.00004035
6	0.0	0.01819000	-0.79434001	0.03916776	0.99846590	0.99999	C.C.	-0.14155352	-0.00003928
7	0.0	0.02183000	-0.79395545	0.05861199	0.99656469	0.99990	0.01400	-0.14112324	-0.00003791
8	0.0	0.02547000	-0.79338276	0.08014953	0.99357611	0.99975	0.02237	-0.14114904	-0.00003922
9	0.0	0.02911000	-0.79256386	0.10352212	0.98926320	0.99956	0.02959	-0.14128011	-0.00003904
10	0.0	0.03275000	-0.79152459	0.12656826	0.98395648	0.99940	0.03465	-0.14148253	-0.00003785
11	0.0	0.03639000	-0.79025406	0.14849269	0.97794998	0.99930	0.03734	-0.14146745	-0.00003639
12	0.0	0.04003000	-0.78875083	0.17312425	0.97002661	0.99907	0.04316	-0.14114594	-0.00003612
13	0.0	0.04367000	-0.78699952	0.19742280	0.96102428	0.99881	0.04874	-0.14084136	-0.00003624
14	0.0	0.04731000	-0.78472984	0.22422887	0.94791162	0.99830	0.05824	-0.14057022	-0.00003601
15	0.0	0.05095000	-0.78246027	0.25433977	0.93532658	0.99796	0.06389	-0.14010405	-0.00003624
16	0.0	0.05459000	-0.78058042	0.27432686	0.92474478	0.99760	0.06922	-0.13974160	-0.00003334
17	0.0	0.05823000	-0.77777290	0.30472694	0.90714520	0.99691	0.07857	-0.13946718	-0.00003290
18	0.0	0.06187000	-0.77448029	0.33877385	0.88523233	0.99614	0.08779	-0.13874453	-0.00003397
19	0.0	0.06551000	-0.77128392	0.36822408	0.86441064	0.99542	0.09556	-0.13825673	-0.00003241
20	0.0	0.06915000	-0.76769418	0.40256327	0.83794884	0.99439	0.10560	-0.13748902	-0.00003074
21	0.0	0.07279000	-0.76378751	0.43838823	0.80741931	0.99325	0.11601	-0.13664174	-0.00002841
22	0.0	0.07643000	-0.75987792	0.47494984	0.77442271	0.99181	0.12773	-0.13547719	-0.00002607

DOUGLAS AIRCRAFT COMPANY
LUNG LEACH DIVISION

SMIEBE BODY - 1.0125 INCH - WITH WALLS CASE NO. 1

UN-BODY UNIFORM AXISYMMETRIC FLOW
TRANSFORMED COORDINATES

	X	Y	PHI	TI	CP	SIN A	COS A	SIGMA	N
23	0.0127000	0.22306001	-0.75531358	0.51608908	0.73305211	0.98998	0.14123	-0.13452077	-0.00002098
24	0.01375000	0.23027998	-0.74993491	0.56743014	0.67802304	0.98744	0.15799	-0.13273001	-0.00002617
25	0.01470000	0.23506000	-0.74443269	0.62035447	0.61516035	0.98424	0.17686	-0.13078487	-0.00002569
26	0.01565000	0.23799999	-0.73850471	0.67996633	0.53764576	0.97996	0.19920	-0.12812388	-0.00002748
27	0.02150000	0.27499999	-0.73116869	0.75619165	0.42514545	0.97220	0.23415	-0.12465471	-0.00002575
28	0.02584000	0.29110998	-0.72394878	0.84923410	0.27860144	0.96238	0.27172	-0.11869067	-0.00002623
29	0.02792000	0.30000001	-0.71756804	0.92433500	0.14566465	0.94810	0.31796	-0.11312658	-0.00002766
30	0.03160000	0.30574000	-0.70867079	1.03788635	-0.07674272	0.91719	0.39845	-0.10333031	-0.00002664
31	0.03413000	0.31499999	-0.69898826	1.17403793	-0.37836450	0.86121	0.50824	-0.08615690	-0.00002706
32	0.04768997	0.34105003	-0.69113755	1.25581169	-0.57766261	0.79517	0.66639	-0.07018477	-0.00002903
33	0.05067000	0.34522003	-0.68556595	1.29819489	-0.68520941	0.74113	0.67136	-0.05866688	-0.00001311
34	0.05520000	0.35000002	-0.68138510	1.30376148	-0.69979382	0.70077	0.71339	-0.05241866	-0.00001193
35	0.06270000	0.35560002	-0.67710209	1.30861664	-0.71247673	0.65813	0.75290	-0.04604441	-0.00001174
36	0.06601000	0.36000001	-0.67282122	1.30762482	-0.70981178	0.61744	0.78662	-0.04067139	-0.00001134
37	0.07236001	0.36500001	-0.66859156	1.30364132	-0.67798606	0.57905	0.81529	-0.03613896	-0.00001097
38	0.07941997	0.37000000	-0.66428173	1.29731369	-0.68302450	0.54163	0.84062	-0.03196974	-0.00001079
39	0.08716002	0.37500000	-0.66002625	1.28948116	-0.68276073	0.50791	0.86141	-0.02874366	-0.00001019
40	0.09141999	0.37700000	-0.65575951	1.28168959	-0.68262486	0.47472	0.88014	-0.02561389	-0.00001037
41	0.10494995	0.38299999	-0.65147990	1.27245522	-0.68191456	0.44295	0.89654	-0.02280044	-0.00000948
42	0.11505002	0.38999999	-0.64719260	1.26280689	-0.68168079	0.41380	0.91037	-0.02051805	-0.00000904
43	0.12584995	0.39899999	-0.64288133	1.25315762	-0.68168079	0.38544	0.92273	-0.01834344	-0.00000844
44	0.13619998	0.39999999	-0.63964576	1.24349606	-0.68168079	0.36583	0.93069	-0.01683160	-0.00000842

103

DOUGLAS AIRCRAFT COMPANY
LONG BEACH DIVISION

SCHEIBE BODY - 1.015 INCH - WITH WALLS CASE NO. 1

ON-BODY UNIFORM AXISYMMETRIC FLOW
TRANSFORMED COORDINATES

	X	Y	PHI	TI	CP	SIN A	COS A	SIGMA	N
45	0.14437997	0.40249997	-0.63745993	1.20307346	-0.54523087	0.35213	0.93995	-0.01586213	-0.00000823
46	0.14776246	0.40374994	-0.63526678	1.23751545	-0.53144360	0.33913	0.94074	-0.01490392	-0.00000440
47	0.15449250	0.40625000	-0.63306803	1.23237419	-0.51874142	0.32720	0.94496	-0.01426047	-0.00000811
48	0.16051603	0.41000003	-0.63085479	1.22756195	-0.50690746	0.31472	0.94819	-0.01342769	-0.00000717
49	0.16695002	0.41250002	-0.62862813	1.22258854	-0.49472237	0.30275	0.95307	-0.01267901	-0.00000787
50	0.17302697	0.41500002	-0.62638426	1.21748429	-0.48227692	0.29065	0.95643	-0.01188456	-0.00000757
51	0.17880000	0.41750002	-0.62412685	1.21213436	-0.47026880	0.27914	0.96025	-0.01119955	-0.00000703
52	0.18442000	0.42000002	-0.62185585	1.20700932	-0.45847103	0.26820	0.96336	-0.01060363	-0.00000715
53	0.18999998	0.42250001	-0.61956596	1.20192528	-0.44682395	0.25702	0.96641	-0.00994347	-0.00000650
54	0.19579998	0.42500001	-0.61725891	1.19700901	-0.43532396	0.24671	0.96909	-0.00943518	-0.00000668
55	0.20170000	0.42750001	-0.61492461	1.19218445	-0.424130375	0.23565	0.97184	-0.008976335	-0.00000620
56	0.20775000	0.42874998	-0.61256582	1.18700693	-0.41349814	0.22512	0.97433	-0.00861425	-0.00000602
57	0.21399998	0.43250000	-0.61018169	1.18179512	-0.40366387	0.21475	0.97667	-0.008362070	-0.00000622
58	0.22024997	0.43500000	-0.60777050	1.17652035	-0.39420010	0.20461	0.97894	-0.008203907	-0.00000608
59	0.22700997	0.43730000	-0.60533100	1.17115974	-0.38516146	0.19462	0.98088	-0.008157257	-0.00000596
60	0.23426998	0.44000000	-0.60286355	1.16581154	-0.37691163	0.18500	0.98274	-0.008111241	-0.00000542
61	0.24200001	0.44250000	-0.60036206	1.16039467	-0.36951566	0.17531	0.98451	-0.008066377	-0.00000513
62	0.25000000	0.44499999	-0.59782875	1.15493470	-0.36348329	0.16612	0.98611	-0.008021747	-0.00000442
63	0.25826001	0.44749999	-0.59525943	1.14976406	-0.35716663	0.15706	0.98759	-0.008041605	-0.00000519
64	0.26690002	0.44999999	-0.59249999	1.14404921	-0.35084661	0.14819	0.98899	-0.008041965	-0.00000447
65	0.27590000	0.45249999	-0.58958653	1.13915140	-0.34450705	0.13961	0.99029	-0.008034741	-0.00000352
66	0.28524998	0.45499998	-0.58624460	1.13453358	-0.33816205	0.13169	0.99148	-0.008023839	-0.00000324

THIS PAGE IS BEST QUALITY AVAILABLE
FROM THE UNIVERSITY OF ALBERTA

DUNLAP AIRCRAFT COMPANY
LONG BEACH DIVISION

HIEB WUDY - I L25 CH - ITH LLS CASE NO. 1

UN-BODY UNIFORM ASYMMETRIC FLOW
TRANSFORMED COORDINATES

	X	Y	PHI	T1	CP	SIN A	COS A	SIGMA	N
67	0.46034002	0.46455997	-0.57525468	1.10943985	-0.23085594	0.09667	0.99532	-0.00226903	-0.00000334
68	0.47320998	0.46625594	0.46755997	1.10318655	-0.21692240	0.08862	0.99607	-0.00196601	-0.00000328
69	0.50012970	0.46875000	-0.57295460	1.09672832	-0.20281219	0.08069	0.99674	-0.00167373	-0.00000334
70	0.52961969	0.47125000	-0.56987977	1.09025002	-0.18804441	0.07325	0.99731	-0.00145090	-0.00000304
71	0.56207991	0.47375000	-0.56673229	1.08385754	-0.17478651	0.06592	0.99782	-0.00123528	-0.00000268
72	0.59301960	0.47624999	-0.56350017	1.07722282	-0.16096697	0.05835	0.99830	-0.00096721	-0.00000209
73	0.63832474	0.47874999	-0.56015635	1.07012081	-0.14515781	0.05105	0.99870	-0.00073563	-0.00000206
74	0.68410500	0.48124999	-0.55669284	1.06287384	-0.12970060	0.04442	0.99901	-0.00059986	-0.00000072
75	0.72480002	0.48374999	-0.55312884	1.05588513	-0.11490154	0.03924	0.99927	-0.00051403	-0.00000061
76	0.7751492	0.48624998	-0.54946578	1.04862499	-0.09901414	0.03141	0.99951	-0.00030663	-0.00000053
77	0.83017999	0.48874999	-0.54561722	1.04062080	-0.08285146	0.02497	0.99969	-0.00015283	-0.00000041
78	0.88973002	0.49124999	-0.54156333	1.03243256	-0.06591606	0.01946	0.99981	-0.00011865	-0.00000039
79	1.00981928	0.49374999	-0.53737748	1.02291679	-0.04635611	0.01342	0.99991	-0.00006955	-0.00000029
80	1.07403946	0.49560000	-0.53228980	1.01600833	-0.03227234	0.00869	0.99996	-0.00006487	-0.00000021
81	1.13825982	0.49662000	-0.52804339	1.00918674	-0.01845741	0.0	1.00000	0.000077310	-0.00000000
82	1.20979982	0.49732999	-0.52504778	1.00185585	-0.00371456	0.0	1.00000	0.000049355	0.00000004
83	1.28222000	0.49799999	-0.52394754	0.99670935	0.00657652	0.0	1.00000	0.000034423	0.00000004
84	1.35822000	0.50000000	-0.52424294	0.99203539	0.01586580	0.0	1.00000	0.00027976	0.00000003
85	1.43822000	0.50000000	-0.52612323	0.98701066	0.02581000	0.0	1.00000	0.00028342	0.00000004
86	1.52000000	0.50000000	-0.53004527	0.98087353	0.03788716	0.0	1.00000	0.00036171	0.00000004
87	1.60000000	0.50000000	-0.53637868	0.97406267	0.05766267	0.0	1.00000	0.00059431	0.00000005
88	1.70000000	0.50000000	-0.54695022	0.96944030	0.09856313	0.0	1.00000	0.00133201	0.00000004

Douglas Aircraft Company
 Long Beach Division

HELD BODY - 1 125 CH - 1TH LLS CASE No. 1

ON-BODY UNIFORM AXISYMMETRIC FLOW
 TRANSFORMED COORDINATES

	X	Y	PHI	TI	C _p	SIN A	COS A	SIGMA	N
89	4.50000000	0.50000000	-0.60166193	0.88636637	0.21435409	0.0	1.00000	0.00371471	-0.00000002
90	4.75000000	0.50000000	-0.65161675	0.74755784	0.44115753	0.24253	0.97014	-0.024481159	-0.000000232
91	5.00000000	0.51245921	-0.66094023	0.61495726	0.3354470	0.24253	0.97014	-0.02395494	-0.000000276
92	5.10000000	0.52499949	-0.66805989	0.54610057	0.28411388	0.24254	0.97014	-0.02331039	-0.000000276
93	5.14999902	0.53750002	-0.67646748	0.47277615	0.23426142	0.24253	0.97014	-0.02262504	-0.000000203
94	5.25000000	0.55000000	-0.68511903	0.40632672	0.19059491	0.24253	0.97014	-0.02205983	-0.000000244
95	5.35000000	0.56249931	-0.69324607	0.351571009	0.16147506	0.24254	0.97014	-0.02170225	-0.000000215
96	5.45000000	0.57500000	-0.70199877	0.31821049	0.11976111	0.24254	0.97014	-0.02161396	-0.000000232
97	5.55000000	0.58750000	-0.70742613	0.29047825	0.07748157	0.24254	0.97014	-0.02201345	-0.000000244
98	5.65000000	0.60000000	-0.70749285	0.26816104	0.03530120	0.24254	0.97014	-0.02281950	-0.000000203
99	5.75000000	0.61250000	-0.70192051	1.00603390	-0.01210403	0.24254	0.97014	-0.02401191	-0.000000203
100	5.85000000	0.62500000	-0.68919259	1.04017639	-0.04104640	0.24254	0.97014	-0.02567354	-0.000000197
101	5.95000000	0.63750000	-0.66440731	1.11193943	-0.02640519	0.24254	0.97014	-0.02811430	-0.000000263
102	6.05000000	0.65000000	-0.28312689	-1.02042254	-0.0412763	0.0	-1.00000	-0.00124471	-0.000000002
103	6.15000000	0.66250000	-0.30293405	-1.01396000	-0.03427658	0.0	-1.00000	-0.00150414	-0.000000002
104	6.25000000	0.67500000	-0.32193029	-1.01851540	-0.03738117	0.0	-1.00000	-0.00171251	-0.000000002
105	6.35000000	0.68750000	-0.34062707	-1.01831341	-0.02696156	0.0	-1.00000	-0.00192179	-0.000000002
106	6.45000000	0.70000000	-0.35916924	-1.01818180	-0.03059357	0.0	-1.00000	-0.00212587	-0.000000002
107	6.55000000	0.71250000	-0.37752733	-1.01825496	-0.03364313	0.0	-1.00000	-0.00232573	-0.000000001
108	6.65000000	0.72500000	-0.39589544	-1.01788235	-0.03606418	0.0	-1.00000	-0.00252517	-0.000000001
109	6.75000000	0.73750000	-0.41399449	-1.01760387	-0.03851674	0.0	-1.00000	-0.00272494	0.000000000
110	6.85000000	0.75000000							
111	6.95000000	0.76250000							
112	7.05000000	0.77500000							

THIS PAGE IS BEST QUALITY AVAILABLE
 FROM COPY FURNISHED TO DDC

DOUGLAS AIRCRAFT COMPANY
LUNG BEACH DIVISION

HIED LUDY - 1 125 CH - - 1TH LLS CASE NO. 1

UN-BODY UNIFORM AXISYMMETRIC FLOW
TRANSFORMED COORDINATES

	X	Y	PHI	TI	CP	SIN A	COS A	SIGMA	N
111	12.00000000	0.00000000	-0.443175018	-1.01712950	-0.03455257	0.0	-1.00000	-0.00310408	0.00000001
112	11.50000000	0.00000000	-0.44890428	-1.01632404	-0.03291416	0.0	-1.00000	-0.00338452	0.00000002
113	10.50000000	0.00000000	-0.46503025	-1.01500797	-0.03024101	0.0	-1.00000	-0.00367965	0.00000002
114	9.50000000	0.00000000	-0.47949374	-1.01299477	-0.02615233	0.0	-1.00000	-0.00396450	0.00000000
115	8.50000000	0.00000000	-0.49149448	-1.01020145	-0.02050686	0.0	-1.00000	-0.00420697	-0.00000000
116	7.50000000	0.00000000	-0.50025207	-1.00679207	-0.01362991	0.0	-1.00000	-0.00436664	-0.00000007
117	6.50000000	0.00000000	-0.50530928	-1.00318909	-0.00638771	0.0	-1.00000	-0.00441894	-0.00000010
118	5.50000000	0.00000000	-0.50673521	-0.99987829	0.0024343	0.0	-1.00000	-0.00437246	-0.00000006
119	4.50000000	0.00000000	-0.50503600	-0.99713987	0.00571209	0.0	-1.00000	-0.00426142	-0.00000003
120	3.50000000	0.00000000	-0.50085360	-0.99496913	0.01003647	0.0	-1.00000	-0.00412139	-0.00000001
121	2.50000000	0.00000000	-0.49470359	-0.99319685	0.01356006	0.0	-1.00000	-0.00397161	-0.00000001
122	1.50000000	0.00000000	-0.48690099	-0.99166657	0.01659467	0.0	-1.00000	-0.00381402	-0.00000000
123	0.0	0.00000000	-0.47764730	-0.989033231	0.01924193	0.0	-1.00000	-0.00364372	0.00000001
124	-1.00000000	0.00000000	-0.46715218	-0.984923111	0.02142185	0.0	-1.00000	-0.00346501	0.00000001
125	-2.00000000	0.00000000	-0.45568025	-0.98440213	0.02306128	0.0	-1.00000	-0.00326916	-0.00000001
126	-3.00000000	0.00000000	-0.44351536	-0.98783356	0.02418489	0.0	-1.00000	-0.00307486	0.00000000
127	-4.00000000	0.00000000	-0.43090129	-0.98747158	0.02499990	0.0	-1.00000	-0.00289530	0.00000001
128	-5.00000000	0.00000000	-0.41801655	-0.98725265	0.02533221	0.0	-1.00000	-0.00272705	0.00000001
129	-6.00000000	0.00000000	-0.40497607	-0.98712403	0.02558119	0.0	-1.00000	-0.00256605	0.00000000
130	-7.00000000	0.00000000	-0.39184844	-0.98704922	0.02573389	0.0	-1.00000	-0.00241406	0.00000000
131	-8.00000000	0.00000000	-0.37867355	-0.98700535	0.02582643	0.0	-1.00000	-0.00226951	0.00000001
132	-9.00000000	0.00000000	-0.36547250	-0.98697907	0.02587235	0.0	-1.00000	-0.00213088	0.00000000

DOUGLAS AIRCRAFT COMPANY
LONG BEACH DIVISION

HIER BODY - 1 125 CH - - ITH LLS CASE NO. 1

ON-BODY UNIFORM AXISYMMETRIC FLOW
TRANSFORMED COORDINATES

X	Y	PHI	TI	CP	SIN A	COS A	SIGMA	N
133	-10.00000000	0.00000000	-0.35225689	0.02590507	0.0	-1.00000	-0.00199089	-0.00000000
134	-10.50000000	0.00000000	-0.33903293	0.02592814	0.0	-1.00000	-0.00199089	-0.00000000
135	-11.00000000	0.00000000	-0.32580143	0.02594791	0.0	-1.00000	-0.00199089	-0.00000000
136	-11.50000000	0.00000000	-0.31256251	0.02596951	0.0	-1.00000	-0.00199089	-0.00000000
137	-12.00000000	0.00000000	-0.29931200	0.02600211	0.0	-1.00000	-0.00199089	-0.00000000
138	-12.50000000	0.00000000	-0.28604043	0.02603939	0.0	-1.00000	-0.00199089	-0.00000000
139	-13.00000000	0.00000000	-0.27272749	0.02617073	0.0	-1.00000	-0.00199089	-0.00000000
140	-13.50000000	0.00000000	-0.25933027	0.02640551	0.0	-1.00000	-0.00199089	-0.00000000
141	-14.00000000	0.00000000	-0.24574232	0.02664966	0.0	-1.00000	-0.00199089	-0.00000000
142	-14.50000000	0.00000000	-0.23161829	0.02687619	0.0	-1.00000	-0.00199089	-0.00000000
143	-15.00000000	0.00000000						

88

*****WARNING*****QUIPUI FIELD WITH TOO SMALL CONDITION OCCURRED DURING A FORMATED WRITE ON FORTRAN UNIT 6 WHICH IS ATTACHED TO
SINK. THE WRITE IS SEQUENTIAL AT RECORD NUMBER 733. FOR THIS AND ALL FUTURE OCCURRENCES OF THIS CONDITION, A
FIELD OF *'S WILL BE WRITTEN.

ADDED MASS = 2.15955257 VOLUME =*****

DOUGLAS AIRCRAFT COMPANY
LONG BEACH DIVISION

PROGRAM 50D -- AXISYMMETRIC AND CROSSFLOW

***** CASE CONTROL DATA *****

SCHIEBE BODY 2.025 INCH - WITH WALLS

CASE NO. 1

12" DIA Test section.

BODIES = 2
NNU = 0
CHORD = 0.0
MACH NO. = 0.0
ICNST = 0.0

SURFACE OF REVOLUTION
OFF-BODY POINTS
OMIT_CROSSELOW UNIFORM FLOW SOLUTION
DOUGLAS AIRCRAFT COMPANY
LONG BEACH DIVISION

SCHIEBE BODY 2.025 INCH - WITH WALLS

NN = 87 MX = 0.0 MY = 0.0
THETA = 0.0 ADDX = 0.0 ADDY = 0.0
XF = 0.0 YF = 0.0

ON-BODY COORDINATES (UNTRANSFORMED)

BODY NO. 1

X	Y	SIN A	COS A	DELTA S	SUMDS	D ALPHA
1	0.0	0.0	0.0	0.00728000	0.00728000	0.0
2	0.0	0.00364000	0.0	0.00728000	0.01455000	0.0
3	0.0	0.00728000	0.0	0.00728000	0.02183000	0.0
4	0.0	0.01091500	0.0	0.00728000	0.02911000	0.0
5	0.0	0.01455000	0.0	0.00728000	0.03638000	0.0
6	0.0	0.01819000	0.0	0.01862026	0.05500026	-0.30774099
7	0.0	0.02183000	0.0	0.02000194	0.07500219	-0.49439633
8	0.0	0.02547000	0.0	0.02500624	0.10000843	-0.48111844
9	0.0	0.02911000	0.0	0.02500624	0.12501907	-0.38932073
10	0.0	0.0327497	0.0	0.02500624	0.15041423	-0.31325972
11	0.0	0.03638000	0.0	0.02500624	0.17505211	-0.20069826
12	0.0	0.03998599	0.0	0.02500624	0.20007497	-0.26424628
13	0.0	0.04363800	0.0	0.02500624	0.22510517	-0.36593419

2

14	0.00579000	0.22499996	0.99833864	0.05762048	0.03193307	0.25703824	-0.48652798
15	0.00671000	0.24073997	0.99833864	0.05762048	0.03193307	0.25703824	-0.39123321
16	0.00763000	0.25687999	0.99792206	0.05443548	0.01815772	0.27519596	-0.30593777
17	0.00880000	0.27499998	0.99756384	0.06976306	0.01963786	0.29483378	-0.50483286
18	0.01017000	0.29459000	0.99691027	0.07855016	0.03259065	0.32742441	-0.50658143
19	0.01145000	0.31083454	0.99617672	0.08736092	0.02300798	0.35043234	-0.47177476
20	0.01273000	0.32707995	0.99542356	0.09556049	0.02511497	0.37554729	-0.58985507
21	0.01373500	0.34599996	0.99438721	0.10580295	0.02514109	0.40068835	-0.50854365
22	0.01474000	0.36249995	0.99324811	0.11601138	0.02516992	0.42585826	-0.67318338
23	0.01594000	0.37500000	0.99181652	0.12767339	0.02130437	0.44716263	-0.76716679
24	0.01714000	0.38749999	0.99001819	0.14054120	0.02916107	0.47632366	-0.98791850
25	0.01847000	0.39999998	0.98744071	0.15799028	0.02531601	0.50164163	-1.11807442
26	0.01980000	0.41249996	0.98469990	0.17722780	0.02601172	0.52765334	-1.30467510
27	0.02126000	0.42499995	0.97987974	0.19959021	0.02490101	0.55255431	-1.99485207
28	0.02272000	0.43556494	0.97333796	0.23357826	0.03313663	0.58569092	-2.28844070
29	0.02440000	0.44612598	0.96223563	0.27221835	0.01647781	0.60416871	-2.72092819
30	0.02540000	0.45656497	0.94822812	0.31758994	0.02421359	0.62838227	-4.96412563
31	0.02640000	0.46056497	0.91718978	0.39845085	0.03192361	0.66030586	-7.08525467
32	0.02749500	0.47499996	0.86103892	0.50853968	0.02499308	0.68529892	-6.77871227
33	0.02895000	0.48749995	0.79499382	0.60661781	0.02096870	0.70626760	-4.76403618
34	0.03035000	0.50000000	0.74186629	0.67054808	0.01289990	0.71916747	-3.42983341
35	0.03155000	0.51279974	0.70042074	0.711373010	0.01427712	0.73344457	-3.30334654
36	0.03279996	0.70999998	0.65813023	0.75290424	0.01519455	0.74863911	-3.00619411
37	0.03402000	0.71499968	0.61773926	0.78638297	0.01618804	0.76482713	-2.78693485
38	0.03528500	0.72499990	0.57877320	0.81548887	0.01727791	0.78210503	-2.55248928
39	0.03657500	0.73499966	0.54188144	0.84045511	0.01845431	0.80055934	-2.31678963
40	0.03783993	0.75499964	0.50746357	0.86167359	0.01970583	0.82026511	-2.14085007
41	0.03913296	0.75999999	0.47492051	0.88002908	0.02105613	0.84132123	-2.05028248
42	0.04046497	0.76499987	0.44313204	0.89645684	0.02256661	0.86388779	-1.86978054
43	0.04184995	0.76999998	0.41364640	0.91043782	0.02417521	0.88806295	-1.75472927
44	0.04320999	0.78499995	0.38557380	0.92267728	0.02593534	0.91399825	-1.25115395
45	0.04460649	0.78999996	0.36533511	0.93087602	0.01368605	0.92768425	
46	0.04602994	0.79499960					
47	0.04749995	0.79999995					
48	0.04899995	0.80249977					

6
1

3

45	0.28876996	0.80499995	0.35235769	0.93586534	0.01419011	0.94187433	-0.79662198
46	0.29540998	0.80749789	0.33934784	0.94066101	0.01473431	0.95650859	-0.79444653
47	0.30897999	0.81249952	0.32699764	0.94502503	0.01529061	0.97189915	-0.75049084
48	0.31590998	0.81500000	0.31490529	0.94912314	0.01587777	0.98777688	-0.73155415
49	0.32313496	0.81749964	0.30257910	0.95312464	0.01652459	1.00430107	-0.74252343
50	0.33036000	0.81999999	0.29065251	0.95662919	0.01720265	1.02150345	-0.71555787
51	0.33763995	0.82249975	0.27914226	0.96025008	0.01791199	1.03941536	-0.68800145
52	0.34542996	0.82499999	0.26805812	0.96340322	0.01865265	1.05806732	-0.66028112
53	0.35330492	0.82749987	0.25727826	0.96633774	0.01943419	1.07750130	-0.64011842
54	0.36117995	0.82999998	0.24647713	0.96914881	0.02028584	1.09778690	-0.63947642
55	0.36940992	0.83249958	0.23576140	0.97181118	0.02120786	1.11899471	-0.63263255
56	0.37763995	0.83499998	0.22512233	0.97433066	0.02221012	1.14120483	-0.62643415
57	0.38623995	0.83749966	0.21474743	0.97666997	0.02328314	1.16448784	-0.60936892
58	0.39483994	0.83999997	0.20461005	0.97884387	0.02443699	1.18892479	-0.59403515
59	0.40382493	0.84249973	0.19469261	0.98086458	0.02568148	1.21460533	-0.57990688
60	0.41280997	0.84499997	0.18493623	0.98275077	0.02703632	1.24164104	-0.56934744
61	0.42199996	0.84749985	0.17536539	0.98450357	0.02851186	1.27015209	-0.55749708
62	0.43158996	0.84999996	0.16612291	0.98610514	0.03009816	1.30025005	-0.53744364
63	0.44141996	0.85249996	0.15696162	0.98760492	0.03185489	1.33210468	-0.53189749
64	0.45124996	0.85499996	0.14322579	0.98949078	0.06981975	1.40192413	-0.79603118
65	0.46155494	0.85749960	0.12559569	0.99209194	0.07962048	1.48154449	-1.01939201
66	0.47189999	0.85999995	0.10368961	0.99407613	0.09200501	1.57354927	-0.97537482
67	0.48267996	0.86249971	0.09665149	0.99531829	0.05117320	1.625228133	-0.69339734
68	0.49346999	0.86499999	0.08361899	0.99606556	0.05642189	1.69170261	-0.46221590
69	0.50489999	0.86749959	0.08069450	0.99673891	0.06196201	1.74366379	-0.45567942
70	0.51623994	0.86999995	0.07324576	0.99731499	0.06826323	1.81192684	-0.42805475
71	0.52819967	0.87249994	0.06593317	0.99782437	0.07583427	1.88776112	-0.41999853
72	0.54015994	0.87499985	0.05835203	0.99829644	0.08568674	1.97344780	-0.43520701
73	0.55275488	0.87749959	0.05105294	0.998869633	0.09793746	2.07138443	-0.41983546
74	0.56535000	0.88000000	0.04441253	0.99901360	0.11258072	2.18396473	-0.38090146
75	0.57863474	0.88249969	0.03872999	0.99999997	0.13074977	2.31000000	-0.35400695
76	0.59191996	0.88499999	0.03307192	0.99999997	0.15000000	2.44000000	-0.32000000
77	0.60595465	0.88749981	0.02800000	0.99999997	0.17000000	2.57000000	-0.28000000
78	0.61998999	0.88999999	0.02400000	0.99999997	0.19000000	2.70000000	-0.24000000
79	0.63482952	0.89249992	0.02100000	0.99999997	0.21000000	2.83000000	-0.20000000
80	0.64966999	0.89499998	0.01900000	0.99999997	0.23000000	2.96000000	-0.16000000
81	0.66539955	0.89749956	0.01700000	0.99999997	0.25000000	3.09000000	-0.12000000
82	0.68112999	0.89999998	0.01600000	0.99999997	0.27000000	3.22000000	-0.08000000
83	0.697157965	0.90499973	0.01500000	0.99999997	0.29000000	3.35000000	-0.04000000
84	0.71567995	0.90999997	0.01400000	0.99999997	0.31000000	3.48000000	-0.00000000
85	0.73972483	0.91499996	0.01300000	0.99999997	0.33000000	3.61000000	0.04000000
86	0.82927000	0.91999996	0.01200000	0.99999997	0.35000000	3.74000000	0.08000000
87	0.87494993	0.92499971	0.01100000	0.99999997	0.37000000	3.87000000	0.12000000
88	0.92067999	0.92999995	0.01000000	0.99999997	0.39000000	4.00000000	0.16000000
89	0.94542456	0.93249989	0.00900000	0.99999997	0.41000000	4.13000000	0.20000000
90	0.97217000	0.93499994	0.00800000	0.99999997	0.43000000	4.26000000	0.24000000
91	1.03026989	0.93749952	0.00700000	0.99999997	0.45000000	4.39000000	0.28000000
92	1.02836990	0.94000000	0.00600000	0.99999997	0.47000000	4.52000000	0.32000000
93	1.05924988	0.94249964	0.00500000	0.99999997	0.49000000	4.65000000	0.36000000
94	1.09012985	0.94499999	0.00400000	0.99999997	0.51000000	4.78000000	0.40000000
95	1.12416935	0.94749975	0.00300000	0.99999997	0.53000000	4.91000000	0.44000000
96	1.15820990	0.94999999	0.00200000	0.99999997	0.55000000	5.04000000	0.48000000
97	1.19604397	0.95249987	0.00100000	0.99999997	0.57000000	5.17000000	0.52000000
98	1.23387909	0.95499998	0.00000000	0.99999997	0.59000000	5.30000000	0.56000000
99	1.27664948	0.95749998	0.00000000	0.99999997	0.61000000	5.43000000	0.60000000
100	1.31941986	0.95999998	0.00000000	0.99999997	0.63000000	5.56000000	0.64000000
101	1.36832428	0.96249962	0.00000000	0.99999997	0.65000000	5.69000000	0.68000000
102	1.41722965	0.96499997	0.00000000	0.99999997	0.67000000	5.82000000	0.72000000
103	1.47346401	0.96749973	0.00000000	0.99999997	0.69000000	5.95000000	0.76000000
104	1.52969933	0.96999997	0.00000000	0.99999997	0.71000000	6.08000000	0.80000000
105	1.59502888	0.97249998	0.00000000	0.99999997	0.73000000	6.21000000	0.84000000

(4)

76	1.66035938	0.97499956	0.03141113	0.99950647	0.15917909	2.47389889	-0.39145857
77	1.73990917	0.97749996	0.02496852	0.99969833	0.20025200	2.67415047	-0.36928242
78	1.81945992	0.97999996	0.01946138	0.99981111	0.25691879	2.93106842	-0.31561404
79	1.91955471	0.98499995	0.01339567	0.99991024	0.48299354	3.41406155	-0.34758633
80	2.01964951	0.98749971	0.00871644	0.99996215	0.40498453	3.81904602	-0.26811671
81	2.27651978	0.98999995	0.00000000	1.00000000	0.43556023	4.25460625	-0.49942166
82	2.51799488	0.99323463	0.00000000	1.00000000	0.50000000	4.75460625	0.00
83	2.75946999	0.99646997	0.00000000	1.00000000	0.60000038	5.35460663	0.00
84	2.96195412	1.00000000	0.00000000	1.00000000	0.69999981	6.05460644	0.00
85	3.16443920	1.00000000	0.00000000	1.00000000	0.80000019	6.85460663	0.00
86	3.38221931	1.00000000	0.00000000	1.00000000	0.80000019	7.65460682	0.00
87	3.59999943	1.00000000	0.00000000	1.00000000			
88	3.84999943	1.00000000					
89	4.09999943	1.00000000					
90	4.39999962	1.00000000					
91	4.69999981	1.00000000					
92	5.04999924	1.00000000					
93	5.39999962	1.00000000					
94	5.79999924	1.00000000					
95	6.19999981	1.00000000					
96	6.59999943	1.00000000					
97	7.00000000	1.00000000					

DOUGLAS AIRCRAFT COMPANY
LONG BEACH DIVISION

SCHIEBE BODY 2.025 INCH - WITH WALLS

MX = 0.0 MY = 0.0
 THETA = 0.0 ADDX = 0.0
 XE = 0.0 YE = 0.0
 ON-BODY COORDINATES (UNTRANSFORMED)

BODY NO.	X	Y	SIN A	COS A	DELTA S	SUMDS	D ALPHA
1	20.00000000	6.00000000	0.0	-1.00000000	1.00000000	1.00000000	0.0
2	19.50000000	6.00000000	0.0	-1.00000000	1.00000000	2.00000000	0.0
3	18.50000000	6.00000000	0.0	-1.00000000	1.00000000	3.00000000	0.0
4	17.50000000	6.00000000	0.0	-1.00000000	1.00000000	4.00000000	0.0
5	16.50000000	6.00000000	0.0	-1.00000000	1.00000000	5.00000000	0.0
6	15.50000000	6.00000000	0.0	-1.00000000	1.00000000	6.00000000	0.0
7	14.50000000	6.00000000	0.0	-1.00000000	1.00000000	7.00000000	0.0
8	13.50000000	6.00000000	0.0	-1.00000000	1.00000000	8.00000000	0.0
9	12.50000000	6.00000000	0.0	-1.00000000	1.00000000	9.00000000	0.0
10	11.50000000	6.00000000	0.0	-1.00000000	1.00000000	10.00000000	0.0
11	10.50000000	6.00000000	0.0	-1.00000000	1.00000000	11.00000000	0.0
12	9.50000000	6.00000000	0.0	-1.00000000	1.00000000	12.00000000	0.0
13	8.50000000	6.00000000	0.0	-1.00000000	1.00000000		0.0

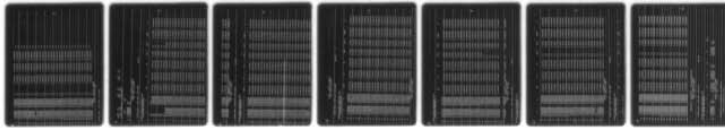
AD-A077 633

PENNSYLVANIA STATE UNIV UNIVERSITY PARK APPLIED RESE--ETC F/G 20/4
CAVITATION INCEPTION AND NUCLEI DISTRIBUTIONS JOINT ARL/CIT EXP--ETC(U)
SEP 79 E M GATES , M L BILLET , J KATZ N00014-79-C-6043

UNCLASSIFIED

NL

2 OF 2
ADA
077633



END
DATE
FILMED
1 -80
DDC

5

14	7.50000000	6.00000000	0.0	-1.00000000	1.00000000	13.00000000	0.0
15	7.00000000	6.00000000	0.0	-1.00000000	1.00000000	14.00000000	0.0
16	6.50000000	6.00000000	0.0	-1.00000000	1.00000000	15.00000000	0.0
17	6.00000000	6.00000000	0.0	-1.00000000	1.00000000	16.00000000	0.0
18	5.50000000	6.00000000	0.0	-1.00000000	1.00000000	17.00000000	0.0
19	5.00000000	6.00000000	0.0	-1.00000000	1.00000000	18.00000000	0.0
20	4.50000000	6.00000000	0.0	-1.00000000	1.00000000	19.00000000	0.0
21	4.00000000	6.00000000	0.0	-1.00000000	1.00000000	20.00000000	0.0
22	3.50000000	6.00000000	0.0	-1.00000000	1.00000000	21.00000000	0.0
23	3.00000000	6.00000000	0.0	-1.00000000	1.00000000	22.00000000	0.0
24	2.50000000	6.00000000	0.0	-1.00000000	1.00000000	23.00000000	0.0
25	2.00000000	6.00000000	0.0	-1.00000000	1.00000000	24.00000000	0.0
26	1.50000000	6.00000000	0.0	-1.00000000	1.00000000	25.00000000	0.0
27	1.00000000	6.00000000	0.0	-1.00000000	1.00000000	26.00000000	0.0
28	0.50000000	6.00000000	0.0	-1.00000000	1.00000000	27.00000000	0.0
29	0.0	6.00000000	0.0	-1.00000000	1.00000000	28.00000000	0.0
30	-0.50000000	6.00000000	0.0	-1.00000000	1.00000000	29.00000000	0.0
31	-1.00000000	6.00000000	0.0	-1.00000000	1.00000000	30.00000000	0.0
32	-1.50000000	6.00000000	0.0	-1.00000000	1.00000000	31.00000000	0.0
33	-2.00000000	6.00000000	0.0	-1.00000000	1.00000000	32.00000000	0.0
34	-2.50000000	6.00000000	0.0	-1.00000000	1.00000000	33.00000000	0.0
35	-3.00000000	6.00000000	0.0	-1.00000000	1.00000000	34.00000000	0.0
36	-3.50000000	6.00000000	0.0	-1.00000000	1.00000000	35.00000000	0.0
37	-4.00000000	6.00000000	0.0	-1.00000000	1.00000000	36.00000000	0.0
38	-4.50000000	6.00000000	0.0	-1.00000000	1.00000000	37.00000000	0.0
39	-5.00000000	6.00000000	0.0	-1.00000000	1.00000000	38.00000000	0.0
40	-5.50000000	6.00000000	0.0	-1.00000000	1.00000000	39.00000000	0.0
41	-6.00000000	6.00000000	0.0	-1.00000000	1.00000000	40.00000000	0.0

DOUGLAS AIRCRAFT COMPANY
LONG BEACH DIVISION

NX = 3 MX = 0.0 MY = 0.0
 THETA = 0.0 ADDX = 0.0 ADDY = 0.0
 XE = 0.0 YE = 0.0
 DEF-BODY COORDINATES (UNTRANSFORMED)

X-OFF Y-OFF

1 -2.00000000 0.0
 2 -4.00000000 0.0
 3 -6.00000000 0.0

DOUGLAS AIRCRAFT COMPANY
LONG BEACH DIVISION

SCHIEBE BODY 2.025 INCH - WITH WALLS

CASE NO. 1

ON-BODY UNIFORM AXISYMMETRIC FLOW
TRANSFORMED COORDINATES

	X	Y	PHI	T1	CP	SIN A	COS A	SIGMA	N
1	0.0	0.0	-1.07514954	0.00312923	0.99999022	1.00000	0.0	-0.14428157	-0.00004274
2	0.0	0.00364000	-1.07510281	0.00944209	0.99991089	1.00000	0.0	-0.14422148	-0.00004664
3	0.0	0.01091500	-1.07501030	0.01574836	0.99975204	1.00000	0.0	-0.14409387	-0.00004178
4	0.0	0.01819000	-1.07487106	0.02194327	0.99951851	1.00000	0.0	-0.14386898	-0.00004274
5	0.0	0.02547000	-1.07468700	0.02733194	0.99925297	1.00000	0.0	-0.14343065	-0.00004274
6	0.0	0.03274497	-1.07428837	0.03954294	0.99843639	0.99999	0.00537	-0.14306045	-0.00004303
7	0.00050000	0.04568997	-1.07351112	0.05914108	0.99650234	0.99990	0.01400	-0.14262742	-0.00004232
8	0.00100000	0.05500000	-1.07235050	0.08092928	0.99345046	0.99975	0.02239	-0.14266235	-0.00003821
9	0.00250000	0.07499999	-1.07069016	0.10426188	0.98912948	0.99957	0.02919	-0.14278024	-0.00003541
10	0.00500000	0.11249995	-1.06857872	0.12775695	0.98367816	0.99940	0.03665	-0.14293545	-0.00003654
11	0.00750000	0.13768995	-1.06600952	0.15044558	0.97736615	0.99927	0.03815	-0.14295352	-0.00003737
12	0.01000000	0.16268992	-1.06297207	0.17434335	0.96960443	0.99909	0.04276	-0.14272124	-0.00003606
13	0.01250000	0.18749994	-1.05942535	0.19568200	0.96012712	0.99879	0.04914	-0.14234239	-0.00003308
14	0.01500000	0.21249998	-1.05482769	0.22993308	0.94713080	0.99834	0.05762	-0.14208210	-0.00003290
15	0.01750000	0.23687999	-1.05021954	0.25724757	0.93382370	0.99792	0.06444	-0.14152145	-0.00003356
16	0.02000000	0.25939995	-1.04643250	0.27717596	0.92317349	0.99756	0.06976	-0.14122152	-0.00003338
17	0.02250000	0.28479499	-1.04074287	0.30750793	0.90543890	0.99691	0.07855	-0.14089901	-0.00003129
18	0.02500000	0.31093494	-1.03398991	0.34169185	0.88324672	0.99618	0.08736	-0.14025772	-0.00002927
19	0.02750000	0.33853996	-1.02759361	0.37185293	0.86172545	0.99542	0.09556	-0.13971728	-0.00002897
20	0.03000000	0.36249995	-1.02171400	0.37500000					

2

0.01847000 0.38749999 -1.02031898 0.40644211 0.83480483 0.99439 0.10580 -0.13894343 -C.00002927
 21 0.01980000 0.39999998 0.01240000 0.41249996 -1.01240444 0.44259208 0.80411226 0.99325 0.11601 -0.13810199 -0.000002903
 22 0.02272000 0.42499995 -1.00448227 0.47954732 0.77003437 0.99182 0.12767 -0.13693804 -0.00002474
 0.02408000 0.43556494 DOUGLAS AIRCRAFT COMPANY
 LONG BEACH DIVISION

SCHIEBE BODY 2.025 INCH - WITH WALLS CASE NO. 1

ON-BODY UNIFORM AXISYMMETRIC FLOW TRANSFORMED COORDINATES

	X	Y	PHI	II	CP	SIN A	COS A	SIGMA	N
23	0.02544000	0.44612998	-0.99523491	0.52096581	0.72859465	0.99002	0.14094	-0.13597041	-0.000002700
24	0.02955000	0.47499996	-0.98434001	0.57306486	0.67159671	0.58744	0.15799	-0.134411510	-0.000002253
25	0.03355000	0.50000000	-0.97319907	0.62665033	0.60730940	0.98417	0.17723	-0.13213193	-0.000002331
26	0.03816000	0.52559996	-0.96119899	0.68668121	0.52846897	0.97988	0.19959	-0.12948674	-0.000002331
27	0.04313000	0.54999995	-0.94631803	0.76520497	0.41446137	0.97234	0.23358	-0.12606847	-0.000002283
28	0.05087000	0.58221996	-0.93169200	0.85813057	0.26361197	0.96224	0.27222	-0.11988455	-0.000002259
29	0.05974498	0.61147976	-0.91873473	0.93325377	0.12903744	0.94823	0.31759	-0.11440748	-0.000002193
30	0.06358999	0.62295997	-0.90063703	1.04822350	-0.09877205	0.91719	0.39845	-0.10443568	-0.000002480
31	0.07630998	0.65223998	-0.88095081	1.18599796	-0.40659046	0.86104	0.50854	-0.08704203	-0.000002313
32	0.08901995	0.67376000	-0.86497611	1.26827335	-0.60851669	0.79499	0.60662	-0.07094264	-0.000002545
33	0.10173994	0.65042999	-0.85363668	1.31106663	-0.71889496	0.74187	0.67055	-0.05957862	-0.000001198
34	0.11038995	0.69999999	-0.84506840	1.31752872	-0.73588181	0.70042	0.71373	-0.05291888	-0.000001019
35	0.12057996	0.70999998	-0.83630013	1.32182407	-0.74721813	0.65813	0.75290	-0.04666688	-0.000001007
36	0.13202000	0.71999997	-0.82753360	1.32113266	-0.74535089	0.61774	0.78638	-0.04124753	-0.000001001
37	0.14475000	0.72999996	-0.81875318	1.31728554	-0.73524094	0.57877	0.81549	-0.03651353	-0.000000966
39	0.15883994	0.73999995	-0.80997592	1.31082344	-0.71825790	0.54188	0.84046	-0.03244713	-0.000000930
39	0.17434996	0.75000000	-0.80119461	1.30305426	-0.65781971	0.50746	0.86167	-0.02902633	-0.000000894
40	0.19132956	0.75999999	-0.79239422	1.25485512	-0.67664909	0.47492	0.88003	-0.02602444	-0.000000817
41	0.20985997	0.76999998	-0.78354049	1.28599930	-0.65379333	0.44313	0.89646	-0.02316998	-0.000000817
42	0.23008996	0.77999997	-0.77466451	1.27632236	-0.62899876	0.41365	0.91044	-0.02079210	-0.000000757
43	0.25209999	0.78999996	-0.76568443	1.26662827	-0.60434628	0.38557	0.92268	-0.01866246	-0.000000793
44	0.26406497	0.79999995	-0.75894496	1.26193047	-0.59246826	0.36534	0.93088	-0.01705372	-0.000000733

DOUGLAS AIRCRAFT COMPANY
LONG BEACH DIVISION

SCHIEBE BODY 2.025 INCH - WITH WALLS

CASE NO. 1

ON-BODY UNIFORM AXISYMMETRIC FLOW
TRANSFORMED COORDINATES

	X	Y	PHI	TI	CP	SIN A	COS A	SIGMA	N
45	0.28876996	0.80499995	-0.75439119	1.25624371	-0.57814789	0.35236	0.93587	-0.01618297	-0.00000715
46	0.29540998	0.80749998	-0.75439119	1.25624371	-0.57814789	0.35236	0.93587	-0.01618297	-0.00000715
46	0.30204999	0.80999994	-0.74981201	1.25105572	-0.56513977	0.33935	0.94066	-0.01527132	-0.00000697
47	0.30897999	0.81249952	-0.74520838	1.24587917	-0.55221462	0.32700	0.94503	-0.01447648	-0.00000703
47	0.31590998	0.81500000	-0.74520838	1.24587917	-0.55221462	0.32700	0.94503	-0.01447648	-0.00000703
48	0.32313496	0.81749964	-0.74057388	1.24101353	-0.54011440	0.31491	0.94912	-0.01371105	-0.00000644
48	0.33036000	0.81999999	-0.73589790	1.23610210	-0.52794838	0.30258	0.95312	-0.01288001	-0.00000656
49	0.33789498	0.82249975	-0.73118407	1.23088074	-0.51506710	0.29065	0.95683	-0.01211775	-0.00000626
49	0.34542996	0.82499999	-0.72643256	1.22586594	-0.50206089	0.27914	0.96025	-0.01142377	-0.00000554
50	0.35330492	0.82749987	-0.72164315	1.22037125	-0.48930550	0.26806	0.96340	-0.01079564	-0.00000572
50	0.36117995	0.82999998	-0.71681058	1.21537876	-0.47714520	0.25728	0.96634	-0.01020734	-0.00000536
51	0.36940992	0.83249998	-0.71192479	1.21051025	-0.46533489	0.24648	0.96915	-0.00959615	-0.00000536
51	0.37763995	0.83499998	-0.70697927	1.20558453	-0.45343399	0.23576	0.97181	-0.00898720	-0.00000501
52	0.38623995	0.83749962	-0.70196855	1.20051289	-0.44123077	0.22512	0.97433	-0.00837996	-0.00000507
52	0.39483994	0.83999997	-0.69689274	1.19529915	-0.42873955	0.21475	0.97667	-0.00781133	-0.00000477
53	0.40382493	0.84249973	-0.69174808	1.19002628	-0.41616249	0.20461	0.97884	-0.00727487	-0.00000530
53	0.41280997	0.84499997	-0.68653131	1.18472672	-0.40357685	0.19469	0.98086	-0.00676685	-0.00000507
54	0.42219996	0.84749985	-0.68123585	1.17939377	-0.39096928	0.18494	0.98275	-0.00627554	-0.00000489
54	0.43158996	0.84999996	-0.67585677	1.17398548	-0.37824154	0.17537	0.98450	-0.00580623	-0.00000447
55	0.44141996	0.85249996	-0.67039049	1.16861153	-0.36565208	0.16612	0.98611	-0.00538427	-0.00000423
55	0.45124996	0.85499996	-0.66482456	1.16340733	-0.35351658	0.15696	0.98760	-0.00496143	-0.00000405
56	0.46155494	0.85749960	-0.65916387	1.158191681	-0.34191681	0.14323	0.98969	-0.00435580	-0.00000381
56	0.47185999	0.85999995	-0.654431471	1.15300060	-0.330644989	0.12560	0.99208	-0.00357304	-0.00000292
57	0.48267996	0.86249971	-0.63188225	1.143136864	-0.27999496	0.10869	0.99408	-0.00288084	-0.00000292
57	0.49349999	0.86499995	-0.61823585	1.13136864	-0.27999496	0.10869	0.99408	-0.00288084	-0.00000292
58	0.50486994	0.86749983	-0.6051289	1.119529915	-0.42873955	0.21475	0.97667	-0.00781133	-0.00000477
58	0.51623994	0.86999995	-0.59249994	1.108123585	-0.41616249	0.20461	0.97884	-0.00727487	-0.00000530
59	0.52819967	0.87249994	-0.58123585	1.09749994	-0.40357685	0.19469	0.98086	-0.00676685	-0.00000507
59	0.54015994	0.87500000	-0.57039049	1.08749994	-0.39096928	0.18494	0.98275	-0.00627554	-0.00000489
60	0.55275488	0.87749958	-0.56039049	1.07819994	-0.37824154	0.17537	0.98450	-0.00580623	-0.00000447
60	0.56535000	0.88000000	-0.55039049	1.06939049	-0.36565208	0.16612	0.98611	-0.00538427	-0.00000423
61	0.57863474	0.88249969	-0.54039049	1.06112999	-0.35351658	0.15696	0.98760	-0.00496143	-0.00000405
61	0.59191996	0.88499999	-0.53039049	1.05300060	-0.34191681	0.14323	0.98969	-0.00435580	-0.00000381
62	0.60595465	0.88749981	-0.52039049	1.04500060	-0.330644989	0.12560	0.99208	-0.00357304	-0.00000292
62	0.61998999	0.88999999	-0.51039049	1.03700060	-0.320644989	0.10869	0.99408	-0.00288084	-0.00000292
63	0.63482952	0.89249992	-0.50039049	1.02900060	-0.310644989	0.09208	0.99611	-0.00238427	-0.00000243
63	0.64966995	0.89499998	-0.49039049	1.02100060	-0.300644989	0.07560	0.99869	-0.00196143	-0.00000195
64	0.66539955	0.89749956	-0.48039049	1.01300060	-0.290644989	0.05912	0.99912	-0.00154105	-0.00000147
64	0.68112999	0.89999998	-0.47039049	1.00500060	-0.280644989	0.04260	0.99969	-0.00112105	-0.00000100
65	0.71567965	0.90499973	-0.46039049	0.99700060	-0.270644989	0.02610	0.99999	-0.00070105	-0.00000053
65	0.75022995	0.90999997	-0.45039049	0.98900060	-0.260644989	0.00960	0.99999	-0.00028105	-0.00000006
66	0.78972483	0.91499996	-0.44039049	0.98100060	-0.250644989	0.00310	0.99999	-0.00006105	-0.00000000
66	0.82922000	0.91999996	-0.43039049	0.97300060	-0.240644989	0.00060	0.99999	-0.00000105	-0.00000000
66	0.87494993	0.92499971	-0.42039049	0.96500060	-0.230644989	0.00010	0.99999	-0.00000005	-0.00000000

ON-BODY UNIFORM AXISYMMETRIC FLOW
TRANSFORMED COORDINATES

	X	Y	PHI	TI	CP	SIN A	COS A	SIGMA	N
67	0.92067999	0.92999999	-0.62229693	1.12366458	-0.26221715	0.09665	0.99532	-0.00240287	-0.00000262
68	0.94642496	0.93249989	-0.61553675	1.11729186	-0.24822903	0.08862	0.99607	-0.00209989	-0.00000262
69	1.00026989	0.93749952	-0.60854954	1.11051900	-0.23414040	0.08069	0.99674	-0.00180441	-0.00000226
70	1.05924998	0.94249964	-0.60132593	1.10454750	-0.22002506	0.07325	0.99731	-0.00151907	-0.00000226
71	1.1216935	0.94749975	-0.59382802	1.09828377	-0.20622635	0.06593	0.99782	-0.00136245	-0.00000197
72	1.19604397	0.95249987	-0.58596790	1.09179401	-0.19201374	0.05835	0.99830	-0.00108936	-0.00000068
73	1.27664948	0.95749958	-0.57769626	1.08485889	-0.17691803	0.05105	0.99870	-0.00085592	-0.00000061
74	1.31941986	0.95999998	-0.56900561	1.07780838	-0.16167068	0.04441	0.99901	-0.00071708	-0.00000054
75	1.36932428	0.96249962	-0.55984730	1.07106304	-0.14717579	0.03824	0.99927	-0.00063106	-0.00000047
76	1.41722965	0.96499997	-0.54992735	1.06410217	-0.13231277	0.03141	0.99951	-0.000542108	-0.00000041
77	1.47346401	0.96749973	-0.53900105	1.05648041	-0.11614990	0.02497	0.99969	-0.00046545	-0.00000034
78	1.52969933	0.96999997	-0.52694654	1.04880810	-0.09999752	0.01946	0.99981	-0.00032311	-0.00000027
79	1.59502888	0.97249985	-0.51055074	1.04017258	-0.08195877	0.01340	0.99991	-0.00021196	-0.00000020
80	1.66035938	0.97499996	-0.49415272	1.03442574	-0.07003593	0.00872	0.99996	-0.00021018	-0.00000013
81	1.73990917	0.97749996	-0.48016697	1.02875710	-0.05834103	0.0	1.00000	0.00066418	-0.00000002
82	1.81945992	0.97999996	-0.46851462	1.02276897	-0.04605579	0.0	1.00000	0.00037055	0.00000001
83	1.91955471	0.98249960	-0.45713049	1.01943398	-0.03524561	0.0	1.00000	0.00020264	-0.00000001
84	2.0164951	0.98499995	-0.44535345	1.0172772	-0.03485394	0.0	1.00000	0.00010794	-0.00000002
85	2.14808464	0.98749971	-0.43301016	1.01591396	-0.03208065	0.0	1.00000	0.00005702	-0.00000001
86	2.27651978	0.98999995	-0.42066389	1.01509190	-0.03041077	0.0	1.00000	0.00003225	-0.00000000
87	2.51799488	0.99323463							
88	2.75946999	0.99646997							
89	2.96195412	0.99823475							
90	3.16443920	1.00000000							
91	3.38221931	1.00000000							
92	3.59999943	1.00000000							
93	3.84999943	1.00000000							
94	4.03999943	1.00000000							
95	4.39999962	1.00000000							
96	4.69999981	1.00000000							
97	5.04999924	1.00000000							
98	5.39999962	1.00000000							
99	5.79999924	1.00000000							
100	6.19999981	1.00000000							
101	6.59999943	1.00000000							
102	7.00000000	1.00000000							
103	20.00000000	6.00000000	-0.23474425	-1.01561260	-0.03146839	0.0	-1.00000	-0.00093964	-0.00000001
104	19.50000000	6.00000000							

SCHIEBE BODY 2.025 INCH - MITTEL WALLS CASE NO. 1

ON-BODY UNIFORM AXISYMMETRIC FLOW
TRANSFORMED COORDINATES

DOUGLAS AIRCRAFT COMPANY
LONG BEACH DIVISION

10

	X	Y	PHI	TL	CP	SIN A	COS A	SIGMA	N
89	19.00000000	6.00000000	-0.24989933	-1.01454639	-0.02930355	0.0	-1.00000	-0.00109105	-0.00000002
90	18.50000000	6.00000000	-0.26446462	-1.01423359	-0.02866936	0.0	-1.00000	-0.00123500	-0.00000001
91	17.50000000	6.00000000	-0.27882051	-1.01410103	-0.02843042	0.0	-1.00000	-0.00137682	-0.00000002
92	16.00000000	6.00000000	-0.29308283	-1.01403713	-0.02827072	0.0	-1.00000	-0.00151846	-0.00000001
93	15.00000000	6.00000000	-0.30729926	-1.01400280	-0.02820110	0.0	-1.00000	-0.00166115	-0.00000002
94	14.00000000	6.00000000	-0.32149112	-1.01397991	-0.02815437	0.0	-1.00000	-0.00180593	-0.00000001
95	13.00000000	6.00000000	-0.33566779	-1.01396179	-0.02811813	0.0	-1.00000	-0.00195388	-0.00000001
96	12.00000000	6.00000000	-0.34983146	-1.01394081	-0.02807522	0.0	-1.00000	-0.00210625	-0.00000002
97	11.50000000	6.00000000	-0.36397898	-1.01391220	-0.02801704	0.0	-1.00000	-0.00226460	-0.00000001
98	10.50000000	6.00000000	-0.37810022	-1.01386452	-0.02792072	0.0	-1.00000	-0.00243086	-0.00000001
99	9.50000000	6.00000000	-0.39217371	-1.01378441	-0.02775860	0.0	-1.00000	-0.00260756	-0.00000001
100	8.00000000	6.00000000	-0.40615731	-1.01364040	-0.02746677	0.0	-1.00000	-0.00279792	-0.00000000
101	7.00000000	6.00000000	-0.41996932	-1.01338196	-0.02694225	0.0	-1.00000	-0.00300526	0.00000001
102	6.00000000	6.00000000	-0.43345767	-1.01291656	-0.02599907	0.0	-1.00000	-0.00323313	0.00000001
103	5.00000000	6.00000000	-0.44634658	-1.01209450	-0.02433491	0.0	-1.00000	-0.00348192	0.00000001
104	4.00000000	6.00000000	-0.45817244	-1.01171072	-0.02153587	0.0	-1.00000	-0.00374464	-0.00000001
105	3.00000000	6.00000000	-0.46823102	-1.00854492	-0.01716232	0.0	-1.00000	-0.00400024	-0.00000002
106	2.50000000	6.00000000	-0.47561347	-1.00548458	-0.01099873	0.0	-1.00000	-0.00420965	-0.00000002
107	1.00000000	6.00000000	-0.47940964	-1.00169468	-0.00392222	0.0	-1.00000	-0.00432427	-0.00000005
108	0.0	6.00000000	-0.47906506	-0.99766684	0.00466090	0.0	-1.00000	-0.00431085	-0.00000001
109	-1.00000000	6.00000000	-0.47465944	-0.99401343	0.01193732	0.0	-1.00000	-0.00417469	-0.00000006
110	-2.00000000	6.00000000	-0.4685916	-0.99114960	0.01762247	0.0	-1.00000	-0.00395543	0.00000001

CASE NO. 1

SCHIEBE BODY 2.025 INCH - WITH WALLS

ON-BODY UNIFORM AXISYMMETRIC FLOW TRANSFORMED COORDINATES

X	Y	PHI	TL	CP	SIN A	COS A	SIGMA	N
-1.00000000	6.00000000							

111 -1.00000000 6.00000000

112	-3.50000000	6.00000000	-0.45658743	-0.98915714	0.02150818	0.0	-1.00000	-0.00370032	-0.00000001
113	-4.00000000	6.00000000	-0.44470066	-0.98788732	0.02407867	0.0	-1.00000	-0.00344335	0.00000001
114	-5.00000000	6.00000000	-0.43183661	-0.98712415	0.02558595	0.0	-1.00000	-0.00320128	0.00000000
115	-6.00000000	6.00000000	-0.41841096	-0.98668128	0.02646005	0.0	-1.00000	-0.00297906	-0.00000000
116	-7.00000000	6.00000000	-0.40467244	-0.98642868	0.02695847	0.0	-1.00000	-0.00277580	0.00000000
117	-8.00000000	6.00000000	-0.39076334	-0.98628509	0.02724177	0.0	-1.00000	-0.00258855	-0.00000000
118	-9.00000000	6.00000000	-0.37676173	-0.98620260	0.02740449	0.0	-1.00000	-0.00241409	0.00000000
119	-10.00000000	6.00000000	-0.36271006	-0.98615402	0.02750027	0.0	-1.00000	-0.00224958	-0.00000001
120	-11.00000000	6.00000000	-0.34863031	-0.98612374	0.02756000	0.0	-1.00000	-0.00209271	0.00000000
121	-12.00000000	6.00000000	-0.33453351	-0.98610246	0.02760196	0.0	-1.00000	-0.00194162	-0.00000001
122	-13.00000000	6.00000000	-0.32042331	-0.98608387	0.02763861	0.0	-1.00000	-0.00179483	0.00000000
123	-14.00000000	6.00000000	-0.30629742	-0.98606175	0.02768224	0.0	-1.00000	-0.00165113	-0.00000001
124	-15.00000000	6.00000000	-0.29214698	-0.98602718	0.02775043	0.0	-1.00000	-0.00150945	-0.00000000
125	-16.00000000	6.00000000	-0.27795082	-0.98596358	0.02787584	0.0	-1.00000	-0.00136877	-0.00000001
126	-17.00000000	6.00000000	-0.26366174	-0.98583210	0.02813512	0.0	-1.00000	-0.00122788	-0.00000000
127	-18.00000000	6.00000000	-0.24916440	-0.98552096	0.02874845	0.0	-1.00000	-0.00108484	0.00000000
128	-19.00000000	6.00000000	-0.23408026	-0.98446006	0.03083843	0.0	-1.00000	-0.00093437	-0.00000000
128	-20.00000000	6.00000000							

188

ADDED MASS = 2.61260223 VOLUME *****
DOUGLAS AIRCRAFT COMPANY
LONG BEACH DIVISION

SCHIERE BODY 2.025 INCH - WITH WALLS CASE NO. 1

OFF-BODY UNIFORM AXISYMMETRIC FLOW
TRANSFORMED COORDINATES

X Y PHI VX VY VI THETA

1	-2.00000000	0.0	-0.53236061	0.94296962	0.0	0.94296962	0.0
2	-6.00000000	0.0	-0.46526188	0.97831184	0.0	0.97831184	0.0
3	-6.00000000	0.0	-0.42903548	0.98405230	0.0	0.98405230	0.0

DOUGLAS AIRCRAFT COMPANY
LONG BEACH DIVISION

PROGRAM 500 - AXISYMMETRIC AND CROSSELOW

***** CASE CONTROL DATA *****